2017

Coordination Chemistry Of Carboranes And Furan Ligands On Transition Metal Cluster Complexes

Emmanuel Joseph Kiprotich
University of South Carolina

COORDINATION CHEMISTRY OF CARBORANES AND FURAN LIGANDS ON TRANSITION METAL CLUSTER COMPLEXES

by

Emmanuel Joseph Kiprotich

Bachelor of Science
Jacobs University Bremen, 2010

Master of Science
Jacobs University Bremen, 2012

Submitted in Partial Fulfillment of the Requirements

For the Degree of Doctor of Philosophy in

Chemistry

College of Arts and Sciences

University of South Carolina

2017

Accepted by:

Richard D. Adams, Major Professor

Dmitry V. Peryshkov, Committee Member

Linda S. Shimizu, Committee Member

Timir Datta, Committee Member

Cheryl L. Addy, Vice Provost and Dean of the Graduate School

ACKNOWLEDGEMENTS

I express a deep sense of gratitude and sincere thankfulness to my adviser Prof. Richard Adams for allowing me to undertake my Ph.D. work in his lab and for his invaluable guidance and constant encouragement throughout my work. I have greatly benefited from his vast knowledge and practical experience. His passion and love for chemistry inspired me to think, work harder and strive to learn more and for this, I will always be grateful to him.

I would also like to thank members of my research committee: Professors Dmitry Peryshkov, Linda Shimizu and Timir Datta for accepting to review my work and for taking the time to be there for all my comprehensive exams and dissertation defense. I am especially grateful for the wonderful collaboration with Dmitry's group when I started working on carborane chemistry

I wish to acknowledge help and support from former members and current members in the Adams group: Dr. Qiang Zhang and Dr. Mingwei Chen for helping me get settled and started in the lab, Dr. Gaya, Elpitiya for training me in crystal structure solving, Jonathan Tedder, Poonam Dhull, Humaiara Akter, Zhongwen Luo, Nutan Wakdikar and Morteza Maleki for your wonderful friendship and the time we spent together in the lab, you all made it enjoyable to be in the lab and I wish you the best in your future endeavors. Special recognition goes to Dr. Mark D. Smith for his help with crystals that were difficult to handle, Dr. Perry J. Pellechia for his assistance with VT-NMR and ^{11}B NMR and Dr. Mike Walla for excellent technical support with mass spec.

I express my affectionate gratitude to my family for their constant motivation and intensive support, thoughts, and prayers throughout my study. To my Mom, thank you for always believing in me and encouraging me to pursue my dreams. Thanks to Dr. Mark Olander for always being an encouragement to me and for always making time to check on my wellbeing. Special thanks to my wife Elizabeth for her endless patience, support and for being my number one fan. Thank you for your willingness to come second to chemistry especially in this past year. Finally, I thank God for making everything possible and for making everything come together even when it seemed impossible. Thank You for the giving me the patience and perseverance.

I acknowledge the facilities and the financial support from Department of Chemistry and Biochemistry at the University of South Carolina and funding from the National Science Foundation.

.

ABSTRACT

Chapter 1 presents the most relevant literature in the field of carborane chemistry. The focus is on icosahedral carboranes and the different methods of boron or carbon atoms substitution and functionalization. The direct addition of transition metal to boron atoms is covered in detail as well as strategies for cage opening of icosahedral carboranes.

Chapter 2 reports the preparation of some of the first polynuclear metal carbonyl cluster complexes where the closo-carborane cage: *o*-$C_2B_{10}H_{12}$ serves as a ligand on the face of one ($Os_3(CO)_9(\mu_3$-4,5,9-$C_2B_{10}H_{10})(\mu$-$H)_2$, **2.1**) and two triosmium clusters ($Os_3(CO)_9(\mu$-$H)_2(\mu_3$-4,5,9-μ_3-7,11,12-$C_2B_{10}H_7)Os_3(CO)_9(\mu$-$H)_3$, **2.3**), and the resulting opening of the cage in the presence of two metal clusters to form $Os_3(CO)_9(\mu$-$H)(\mu_3$-3,4,8-μ_3-7,11,12-$C_2B_{10}H_6)Os_3(CO)_9(\mu$-H), **2.4**.

Chapter 3 reports on a further investigation of the reaction of closo-carboranes with trimetallic clusters. The thiolate substituted derivative of *o*-$C_2B_{10}H_{12}$, closo-*o*-(1-$SCH_3)C_2B10H_{11}$ also reacts with $Os_3(CO)_{10}(NCMe)_2$. As with *o*-$C_2B_{10}H_{12}$, it is possible to add one and two $Os_3(CO)_9$ cluster units to the surface of the carborane and in the latter case, the carborane cage is also opened, but more importantly, in this case the opening occurs in a stepwise process that provides new insight into the mechanism of the cage opening process.

Chapter 4 presents the coordination chemistry of thioether-carboranes on dirhenium carbonyl cluster complexes. To follow up on our studies of the reaction and cage opening of closo-*o*-(1-SCH_3)C_2B10H_{11} and *o*-$C_2B_{10}H_{12}$ on triosmium clusters, we investigated the reaction of closo-*o*-(1-SCH_3)$C_2B_{10}H_{11}$ and closo-[o-1,2-$(SCH_3)_2$]$C_2B_{10}H_{10}$ with dirhenium complex $Re_2(CO)_8$[μ-η^2-C(H)C(H)Bu^n](μ-H). Two isomers were obtained from the reaction with closo-*o*-(1-SCH_3)C_2B10H_{11}, $Re_2(CO)_8$[μ-η^2-1,3-$C_2B_{10}H_{10}$(1-SCH_3)](μ-H), **4.1** and $Re_2(CO)_8$[μ-η^2-1,4-$C_2B_{10}H_{10}$(1-SCH_3)](μ–H), **4.2** and one product $Re_2(CO)_7$[μ-η^3-$C_2B_{10}H_9$(1,2-$SCH_3)_2$](μ–H), **4.3** from the reaction with [o-1,2-$(SCH_3)_2$]$C_2B_{10}H_{10}$. The synthesis, characterization and reactions are discussed.

Chapter 5 introduces the chemistry furan ligands on transition metal cluster complexes. Furans are products from the processing of biomass and intermediates in the production of biofuels. We have activated multiple C-H bonds of a furan ligand using transition metal clusters and obtained several new sandwich furyl and furyne cluster compounds. Starting with the furyl complex $Os_3(CO)_{10}$(μ,η^2-C_4H_3O) (μ-H), **5.1** and furyne (μ-H)$_2Os_3(CO)_9$(μ_3,η^2-C_4H_2O), **5.2** and reacting them with a dirhenium carbonyl cluster complexes, we have obtained two new sandwich structures, (μ-H)$Os_3(CO)_{10}$(μ-η^2-2,3,μ-η^2-4,5-C_4H_2O)$Re_2(CO)_8$(μ-H), **5.3** and (μ-H)$_2Os_3(CO)_9$(μ_3-η^2-2,3-,μ-η^2-4,5-C_4HO)$Re_2(CO)_8$(μ-H), **5.4** respectively. Compound **5.2** also reacts with a second triosmium cluster to form a new "Os_6" furyne sandwich cluster, (μ-H)$_2Os_3(CO)_9$(μ_3-η^2-2,3-,μ-η^2-4,5-C_4HO)$Os_3(CO)_{10}$(μ-H), **5.5**. Such sandwich furan structures formed by multiple C-H bond activations by different transition metals have not yet been reported.

TABLE OF CONTENTS

LIST OF TABLES

LIST OF FIGURES

CHAPTER 1

INTRODUCTION

Carboranes are a class of boron hydride compounds in which one or more of the BH vertices have been replaced by CH units. Icosahedral carboranes were first reported in 1963 and are one of the most extensively studied of the carborane family.[1] They are stabilized by electron delocalized covalent bonding resulting in highly stable three-dimensional molecular structures.[2] As a consequence of their high stability, polyhedral carboranes can undergo substitution reactions at both the cage boron and cage carbon atoms without cage degradation. This has resulted in the preparation of wide range of C- and B-substituted derivatives. Their unique structural and physicochemical properties have led to diverse structures resulting in practical applications in fields such as catalysis[3], luminescent materials[4], imaging materials for malignant tumors[5], delivery agents for boron neutron capture therapy (BNCT)[6], immunostimulants[7], biomolecule receptor agents[8] and supramolecular chemistry.[9] The *o*-dicarba-carborane is obtained by the reaction of decaborane with acetylene (Scheme 1.1).[1a, 10] It exhibits extraordinary resistance to degradation in the presence of oxidizing agents, alcohols and strong acids and phenomenal thermal stability up to 400^{o}C, which can limit its derivatization.[11] Under an inert atmosphere, *o*-carborane (1, 2) undergoes a thermal rearrangement to the *meta* (1, 7) and *para* (1, 12) carboranes based on the location of the carbon atoms in the clusters,[2] (Scheme 1.2) but the mechanism for these isomerizations still remains only partially understood.[2]

Transition metals have recently attracted considerable attention in carborane chemistry because of their ability to mediate/catalyze the functionalization of carboranes resulting in unique derivatives that cannot be attained by other conventional methods.[11] For example, copper (I) has been used to mediate the coupling reactions of carborane cage carbon atoms and alkenyl, alkynyl and aryl groups in carboranes[12], while nickel and palladium have been used to catalyze coupling reactions of iodocarboranes and with Grignard reagents.[13]

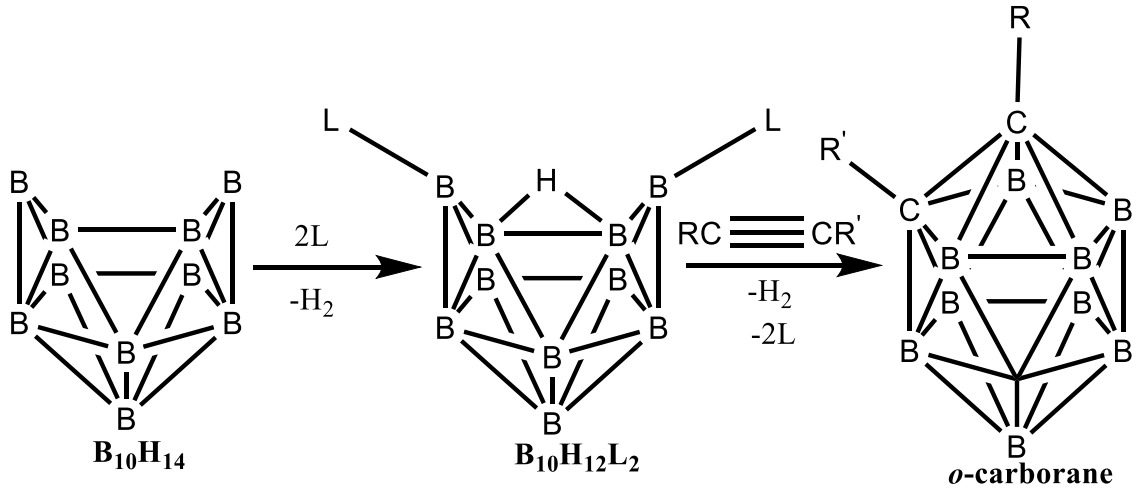

Scheme 1.1. Synthesis of *o*-carborane

1.1 Functionalization at Cage Carbon and Boron Atoms in *o*-Carborane

Cage carbon substitution can be accomplished in two ways: the reaction of substituted acetylenes with decaborane and electrophilic substitutions of carboranes metallated with alkali or alkaline earth metals.[2] The latter approach is more versatile and preferred. It exploits the high acidity of C-H bonds in the cage which is a result of the high polarity induced by the electronegative carbon atoms. The 1,2 carborane has the

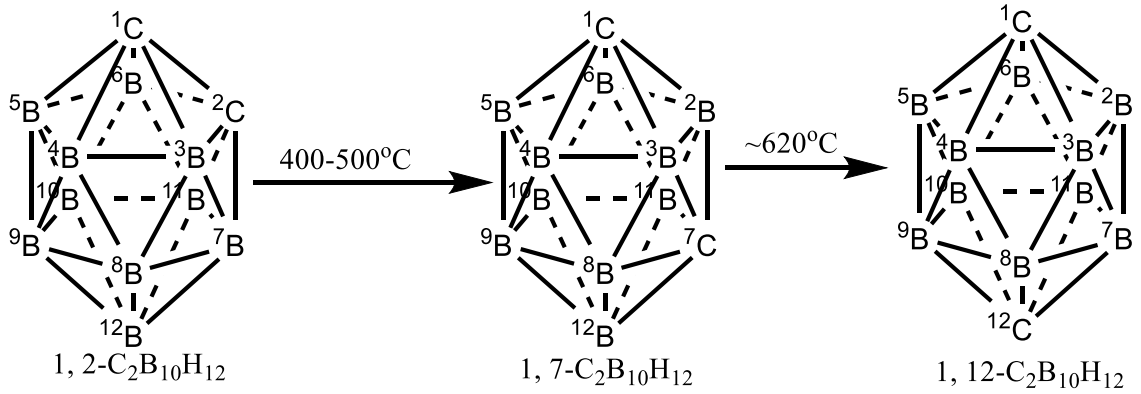

Scheme 1.2. Synthesis and structures of *m*- and *p*-carboranes from *o*-carborane

highest polarity of the three isomers and as a result reacts readily with lithium or Grignard reagents in organic solvents to form metallated derivatives (Scheme 1.3) which can readily react with suitable electrophiles such as organic halides or metal halides to give carbon-substituted carborane derivatives. Many examples of carboranes with groups 13-16 elements bonded to carbon have been well characterized.[14]

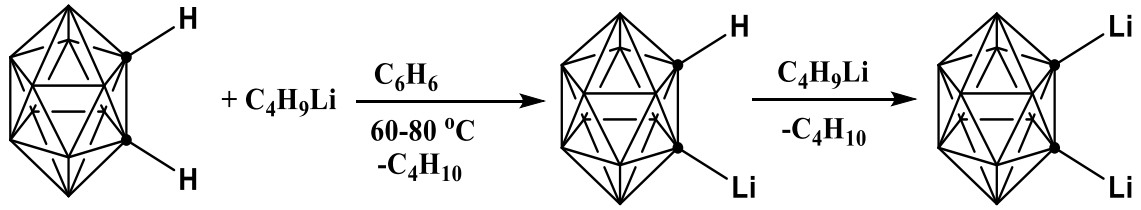

Scheme 1.3. Metallation of *o*-carborane cage carbons

Of the hundreds of carboranes with exopolyhedral transition metals known, only a few have direct cage C-M bonds.[15] Most of the transition metal carboranes known have atoms or groups such as silyl[16], thiolates[17] or selenites[18] bridging the carborane carbon and the metal. Although thio-carboranes were one of the earliest known derivatives since the 1960s[19], their coordination chemistry did not receive much attention until 10-15 years ago. Chalcogenocarboranes provide new opportunities to synthesize and characterize new coordinatively unsaturated molecules with rich chemistry.[20] They are also readily

obtained from C-lithiated *o*-carboranes by the corresponding group 16 elements (S, Se, Te).[18-19, 21] Chalcogenalate carborane ligands are of particular interest as chemically robust and chelating legands.[22] Direct cage carbon-metal bonding in *o*-carborane is accomplished through the reaction of C-lithiated carboranes with organometallic reagents resulting in coordination of a metal to one carbon (Scheme 1.4)[23] or to both cage carbons as was shown by the synthesis of $(Ph_3P)_2Ni(C_2B_{10}H_{10})$ from the reaction of $(Ph_3P)_2NiCl_2$ and $Li_2C_2B_{10}H_{10}$.[24]

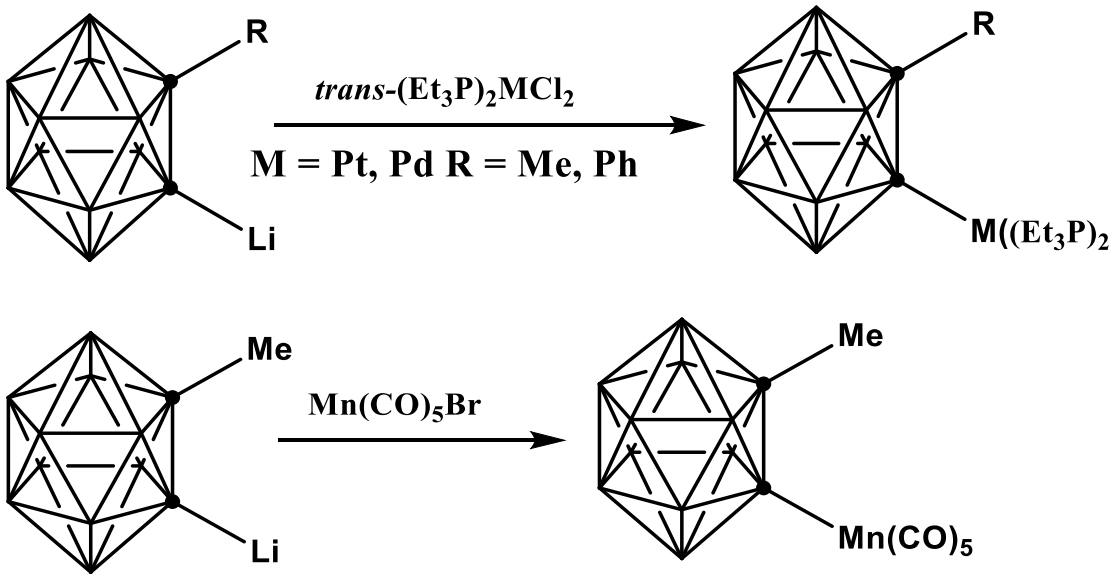

Scheme 1.4. The preparation of *o*- carborane cages with direct carbon-metal bonds

Carborane chemistry is mainly dominated by C-substituted derivatives due to the difficulty of selectively introducing substituents at cage B atoms.[25] Substitution at boron atoms in 1,2-$C_2B_{10}H_{10}$ is more challenging synthetically than substitution at the carbon atoms for two reasons: The presence of ten "B" vertices in four different electronic environments often leads to complex substitution patterns and secondly because of the lower electronegativity of boron, the B-H bonds are much less polar compared to C-H bonds, and hence are less reactive to nucleophiles. The *o*-carborane, however, behaves

much like aromatic hydrocarbons because of electron delocalization and is therefore susceptible to attack by electrophiles.[25] Introduction of substituents at boron can usually be accomplished by reactions on an existing *closo*-$C_2B_{10}H_{12}$ cage, however they can also be obtained indirectly from other polyborane substrates. Syntheses by indirect substitution have been accomplished starting with $B_{10}H_{14}$ derivatives or C_2B_9 and C_2B_{10} dianions. Halodecaboranes for instance react with alkynes to generate *o*-carboranyl B-halo derivatives[26] while a BX unit can be inserted into a *nido* C_2B_9 to generate a *closo*-C_2B_{10} with an X substituent on B(3) or B(6).[13b, 27] Direct substitution methods are diverse and are most commonly employed for substitutions in *ortho meta* and *para* carboranes. They include electrophilic alkylation,[28] nucleophilic displacement,[29] thermal iodination[30] and electrophilic halogenation[14f] (Scheme 1.5).

1.2 Addition of Transition Metals at Boron

Many metallaboranes have been obtained by substituting boron vertices in *ortho* and *meta*-carboranes with transition metals, but very few icosahedral-carboranes having *exo*-polyhedral transition metals σ-bonded to boron are known.[14f, 31] There are several approaches to boron-metallated carboranes: Firstly, treatment of a B(3)-carboxylyl chloride 1,2/1,7 carborane with an anionic metals species such as $Na[CpFe(CO)_2]$ leads to the formation of a B-carboxymetal product which undergoes decarbonylation when heated to form a B-M bond (Scheme 1.6-A). [28, 31] A second approach involves an intramolecular oxidative addition of a transition metal to B-H bond which is assisted by donor ligands such as phosphines (Scheme 1.6-B) [32] or phosphinite pincer ligands[33] present on the carborane cage. Boron-mercurated carborane derivatives offer another approach to transition metal substituted species as seen in the reaction of 1,2/1,7-

Electrophylic alkylation

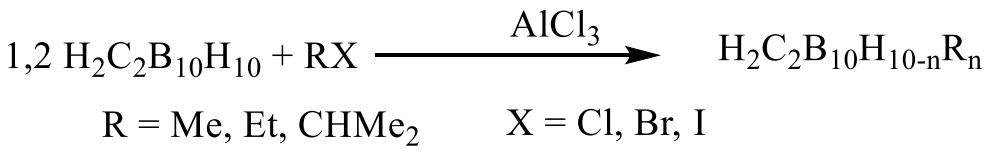

Nucleophilic displacement

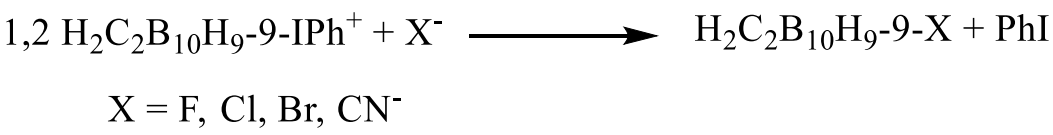

Thermal iodination

Electrophilic halogenation

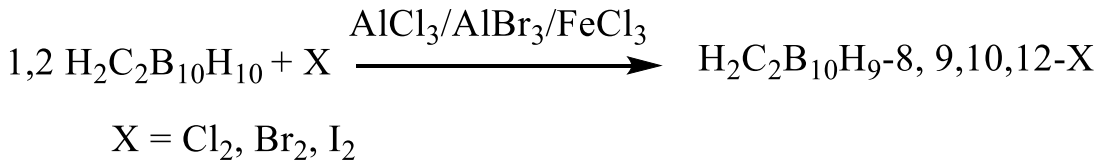

Scheme 1.5. The preparation of boron-substituted carboranes by direct methods

$C_2B_{10}H_{11}$-9-HgCl with $(Ph3)_3Pt$ to yield 1,2/1,7-$C_2B_{10}H_{11}$-9-$PtCl(PPh)_2$.[31, 34] Finally, direct addition of a single metal to *ortho/meta/para*-carborane has also been achieved by the reaction of $IrCl(EPh_3)_2$ (E = P or As)[32a](Scheme 1.6-C)

1.3 Cage-opening of C_2B_{10} Icosahedra

A unique feature of icosahedral carboranes is their ability to undergo substitution reactions at either the cage boron, carbon atoms or substituent groups attached to the carborane with the cage remaining intact. It has been shown however that the most electron deficient boron atoms on the cage can undergo attack by bases leading to cage rupture and in most cases complete removal of a BH group.[35] Cage opening

transformations of carborane cages almost always occur with the loss of a boron group (deboronation). Bases such as alkoxides[36], alkyl amines[37], ammonia[38] and piperidine[39] remove a BH unit to create a *nido*-C_2B_9 mono anion or base adduct (Scheme 1.7). The

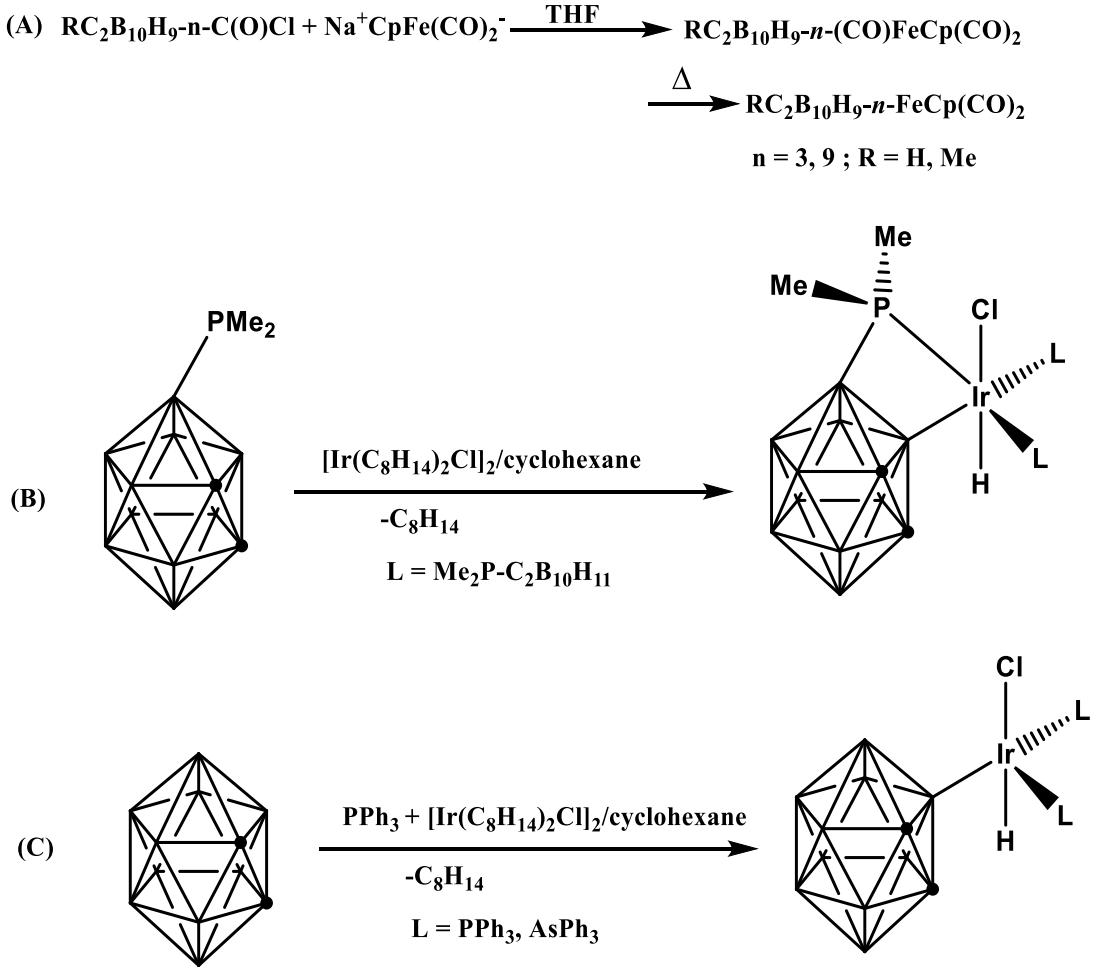

Scheme 1.6. Synthesis of boron-substituted carboranes

anion can undergo protonation to form a neutral *nido*-carborane or deprotonation to the dianion. *o*-Carboranyl C-P bonded derivatives however undergo degradation to *nido*-C_2B_9 with the cleavage of the C-P bond in the presence of bases. The C-P bond can be preserved by using piperidine as the base with a 1:10 carborane to base ratio in ethanol or 1:50 in toluene.[40] 1,2/1,7 arylphosphino carboranes can also undergo conversion to *nido*-

carboranyl phosphonium salts by methylation with methyl iodide followed by degradation with cesium fluoride. The 1, 12 carborane phosphino complex does not undergo degradation under similar conditions highlighting its more robust nature compared to the 1,2/1,7 carborane.[41]

Icosahedral cage opening without deboronation to form *nido*-C_2B_{10} is less common and prior to our work with triosmium carbonyl and *closo*-*o*-$C_2B_{10}H_{12}$ and *closo*-*o*-(1-SCH_3)[42], it had only been accomplished with *o*-carboranes bearing bulky phosphino ligands (Scheme 1.7)[43] and observed in solution in the base-promoted 2 electron reduction of diphenyl derivatives of *o*- and *m*-carborane. Reduction of 1, 2/1, 7-C_2B_{10} results in the formation of *nido*-7,9-$Ph_2C_2B_{10}H_{10}^{2-}$ and *nido*-7,10-$Ph_2C_2B_{10}H_{10}^{2-}$ dianions respectively.[44]

1.4 Summary

Icosahedral carboranes possess exceptional thermal and chemical stabilities which can limit their derivatization. B-H bond activation induced by transition metals offers a new approach to the synthesis of boron functionalized carboranes because it avoids the need for pre-functionalization. Reported functionalization of icosahedral carboranes B-H bonds mainly relies on the use of strong electrophiles or cross coupling reactions utilizing iodinated carborane cages. The highly symmetrical icosahedral cage presents challenges in electrophilic substitution because of a lack of control over the degree of substitution or regioselectivity. Transition metal B-H bond activation offers a new route for the selective functionalization of carboranes that may not be achievable by other means. In this thesis, the synthesis and characterization of new transition metal carboranes cluster complexes via multi-center B-H activations and the cage opening of the resulting complexes will be

discussed along with the B-H activation coordination chemistry of thioether carboranes by rhenium carbonyl complexes. We have synthesized several new rare transition metal clusters with direct B-M bonds on *o*-$C_2B_{10}H_{12}$ and also several clusters with a sulfur containing carboranyl ligand.

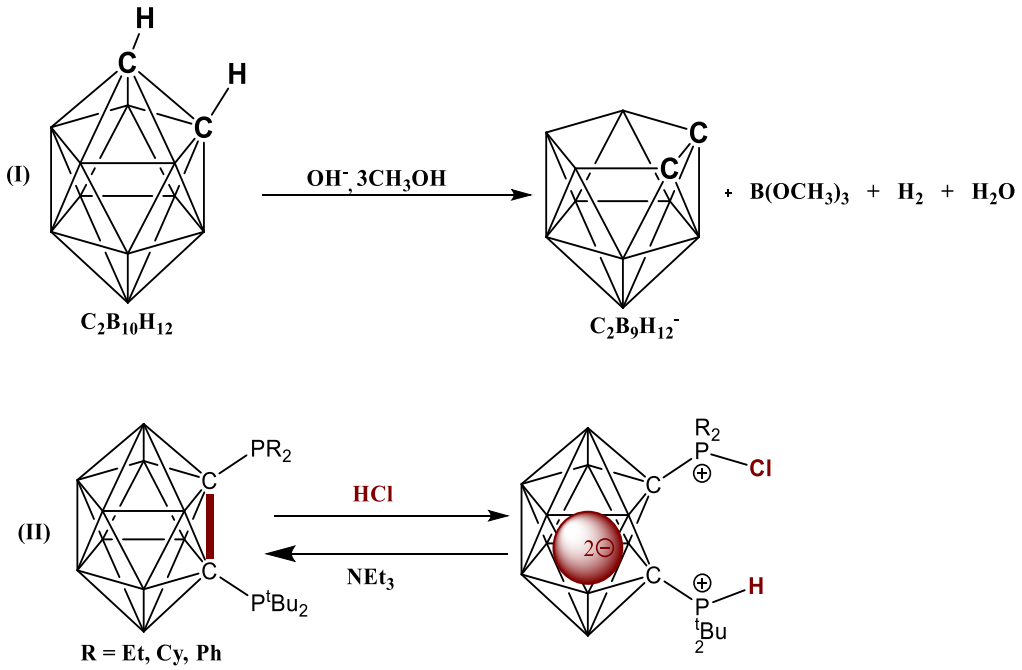

Scheme 1.7. Cage opening of a carborane ligand with deboronation (I) and without deboronation (II)

1.5 References

1. (a)Heying, T. L.; Ager, J. W.; Clark, S. L.; Mangold, D. J.; Goldstein, H. L.; Hillman, M.; Polak, R. J.; Szymanski, J. W. *Inorg. Chem.* **1963,** 2, (6), 1089-1092; (b)Fein, M. M.; Cohen, M. S.; Mayes, N.; Schwartz, N.; Bobinski, J. *Inorg. Chem.* **1963,** 2, (6), 1111-1115.

2. Grimes, R. N. *Carboranes, 2nd Edition* **2011**.

3. (a)Tutusaus, O.; Vinas, C.; Nunez, R.; Teixidor, F.; Demonceau, A.; Delfosse, S.; Noels, A. F.; Mata, I.; Molins, E. *J. Am. Chem. Soc.* **2003,** 125, (39), 11830-11831; (b)Qiu, Z. Z.; Ren, S. K.; Xie, Z. W. *Acc. Chem. Res.* **2011,** 44, (4), 299-309.

4. (a)Tanaka, K.; Chujo, Y. *Macromol. Rapid Commun.* **2012,** 33, (15), 1235-1255; (b)Weber, L.; Kahlert, J.; Brockhinke, R.; Bohling, L.; Halama, J.; Brockhinke, A.; Stammler, H. G.; Neumann, B.; Nervi, C.; Harder, R. A.; Fox, M. A. *Dalton Trans.* **2013,** 42, (30), 10982-10996; (c)Ferrer-Ugalde, A.; Gonzalez-Campo, A.; Vinas, C.; Rodriguez-Romero, J.; Santillan, R.; Farfan, N.; Sillanpaa, R.; Sousa-Pedrares, A.; Nunez, R.; Teixidor, F. *Chem. Eur. J.* **2014,** 20, (32), 9940-9951.

5. (a)Winberg, K. J.; Barbera, G.; Eriksson, L. B.; Teixidor, F.; Tolmachev, V.; Vinas, C.; Sjoberg, S. *J. Organomet. Chem.* **2003,** 680, (1-2), 188-192; (b)Tiwari, R.; Toppino, A.; Agarwal, H. K.; Huo, T. Y.; Byun, Y.; Gallucci, J.; Hasabenaby, S.; Khalil, A.; Goudah, A.; Baiocchi, R. A.; Darby, M. V.; Barth, R. F.; Tjarks, W. *Inorg. Chem.* **2012,** 51, (1), 629-639.

6. (a)Barth, R. F.; Coderre, J. A.; Vicente, M. G. H.; Blue, T. E. *Clin. Cancer Res.* **2005,** 11, (11), 3987-4002; (b)Takagaki, M.; Tomaru, N.; Maguire, J. A.; Hosmane, N. S., Future Applications of Boron and Gadolinium Neutron Capture Therapy. In *Boron*

Science: New Technologies and Applications, Hosmane, N. S., Ed. CRC Press-Taylor & Francis Group: Boca Raton, 2012; pp 243-275.

7. (a)Fujii, S.; Masuno, H.; Taoda, Y.; Kano, A.; Wongmayura, A.; Nakabayashi, M.; Ito, N.; Shimizu, M.; Kawachi, E.; Hirano, T.; Endo, Y.; Tanatani, A.; Kagechika, H. *J. Am. Chem. Soc.* **2011,** 133, (51), 20933-20941; (b)Fujii, S.; Sekine, R.; Kano, A.; Masuno, H.; Songkram, C.; Kawachi, E.; Hirano, T.; Tanatani, A.; Kagechika, H. *Biorg. Med. Chem.* **2014,** 22, (21), 5891-5901; (c)Soriano-Ursua, M. A.; Das, B. C.; Trujillo-Ferrara, J. G. *Expert Opinion on Therapeutic Patents* **2014,** 24, (5), 485-500.

8. (a)Ohta, K.; Goto, T.; Fujii, S.; Kawahata, M.; Oda, A.; Ohta, S.; Yamaguchi, K.; Hirono, S.; Endo, Y. *Biorg. Med. Chem.* **2011,** 19, (11), 3540-3548; (b)Wilkinson, S. M.; Gunosewoyo, H.; Barron, M. L.; Boucher, A.; McDonnell, M.; Turner, P.; Morrison, D. E.; Bennett, M. R.; McGregor, I. S.; Rendina, L. M.; Kassiou, M. *ACS Chem. Neurosci.* **2014,** 5, (5), 335-339.

9. (a)Jude, H.; Disteldorf, H.; Fischer, S.; Wedge, T.; Hawkridge, A. M.; Arif, A. M.; Hawthorne, M. F.; Muddiman, D. C.; Stang, P. J. *J. Am. Chem. Soc.* **2005,** 127, (34), 12131-12139; (b)Ludlow, J. M.; Tominaga, M.; Chujo, Y.; Schultz, A.; Lu, X. C.; Xie, T. Z.; Guo, K.; Moorefield, C. N.; Wesdemiotis, C.; Newkome, G. R. *Dalton Trans.* **2014,** 43, (25), 9604-9611.

10. Beall, H. *Inorg. Chem.* **1972,** 11, (3), 637-638.

11. Qiu, Z. Z. *Tetrahedron Lett.* **2015,** 56, (8), 963-971.

12. (a)Zakharkin, L. I.; Kovderov, A. I.; Olshevskaya, V. A. *Bull. Acad. Sci. USSR, Div. Chem. Sci.* **1986,** 35, (6), 1260-1266; (b)Kovredov, A. I.; Shaugumbekova, Z. S.; Kazantsev, V. A.; Zakharkin, L. I. *Zh. Obshch. Khim.* **1986,** 56, (10), 2316-2320.

13. (a)Kovredov, A. I.; Shaugumbekova, Z. S.; Petrovskii, P. V.; Zakharkin, L. I. *Zh. Obshch. Khim.* **1989,** 59, (3), 607-611; (b)Li, J.; Logan, C. F.; Jones, M. *Inorg. Chem.* **1991,** 30, (25), 4866-4868.

14. (a)Schroeder, H.; Papetti, S.; Alexander, R. P.; Sieckhaus, J. F.; Heying, T. L. *Inorg. Chem.* **1969,** 8, (11), 2444-2449; (b)Bregadze, V. I.; Usiatinsky, A. Y.; Godovikov, N. N. *J. Organomet. Chem.* **1985,** 292, (1-2), 75-80; (c)Bregadze, V. I.; Usyatinskii, A. Y.; Kampel, V. T.; Golubinskaya, L. M.; Godovikov, N. N. *Bull. Acad. Sci. USSR, Div. Chem. Sci.* **1985,** 34, (5), 1113-1113; (d)Lee, T.; Jeon, J.; Song, K. H.; Jung, I.; Baik, C.; Park, K. M.; Lee, S. S.; Kang, S. O.; Ko, J. J. *Dalton Trans.* **2004**, (6), 933-937; (e)Lee, Y. J.; Lee, J. D.; Kim, S. J.; Keum, S.; Ko, J. J.; Suh, I. H.; Cheong, M.; Kang, S. O. *Organometallics* **2004,** 23, (2), 203-214; (f)Grimes, R. N. *Carboranes, 2nd Edition* **2011**, 301-540.

15. Silvano, B., closo-Carborane-Metal Complexes Containing Metal-Carbon and Metal-Boron σ-Bonds In *Metal Interactions with Boron Clusters*, Grimes, R. N., Ed. Springer: Boston, MA, 1982; pp 173-237.

16. Lee, Y. J.; Lee, J. D.; Kim, S. J.; Yoo, B. W.; Ko, J. J.; Suh, I. H.; Cheong, M.; Kang, S. O. *Organometallics* **2004,** 23, (3), 490-497.

17. Jin, G. X. *Coord. Chem. Rev.* **2004,** 248, (7-8), 587-602.

18. Crespo, O.; Gimeno, M. C.; Ilie, A.; Laguna, A.; Ospino, I.; Silvestru, C. *Dalton Trans.* **2013,** 42, (29), 10454-10459.

19. Smith, H. D.; Obenland, C. O.; Papetti, S. *Inorg. Chem.* **1966,** 5, (6), 1013-1015.

20. Jain, L.; Jain, V. K.; Kushwah, N.; Pal, M. K.; Wadawale, A. P.; Bregadze, V. I.; Glazun, S. A. *Coord. Chem. Rev.* **2014,** 258, 72-118.

21. Laromaine, A.; Teixidor, F.; Kivekas, R.; Sillanpaa, R.; Arca, M.; Lippolis, V.; Crespo, E.; Vinas, C. *Dalton Trans.* **2006**, (44), 5240-5247.

22. Yao, Z. J.; Jin, G. X. *Coord. Chem. Rev.* **2013,** 257, (17-18), 2522-2535.

23. (a)Bresadola, S.; Longato, B. *Inorg. Chem.* **1974,** 13, (3), 539-542; (b)Lee, Y. J.; Kim, S. J.; Kang, C. H.; Ko, J.; Kang, S. O.; Carroll, P. J. *Organometallics* **1998,** 17, (6), 1109-1115.

24. Sayler, A. A.; Sieckhaus, J. F.; Beall, H. *J. Am. Chem. Soc.* **1973,** 95, (17), 5790-5792.

25. Bregadze, V. I. *Chem. Rev.* **1992,** 92, (2), 209-223.

26. (a)Zakharkin, L. I.; Kalinin, V. N. *Zh. Obshch. Khim.* **1966,** 36, (2), 376-; (b)Plesek, J.; Hermanek, S.; Stibr, B. *Collect. Czech. Chem. Commun.* **1970,** 35, (1), 344-346.

27. Roscoe, J. S.; Kongpric.S; Papetti, S. *Inorg. Chem.* **1970,** 9, (6), 1561-1563.

28. Zakharkin, L. I.; Pisareva, I. V.; Bikkineev, R. K. *Bull. Acad. Sci. USSR, Div. Chem. Sci.* **1977,** 26, (3), 577-580.

29. Grushin, V. V.; Shcherbina, T. M.; Tolstaya, T. P. *J. Organomet. Chem.* **1985,** 292, (1-2), 105-117.

30. Barbera, G.; Vaca, A.; Teixidor, F.; Sillanpaa, R.; Kivekas, R.; Vinas, C. *Inorg. Chem.* **2008,** 47, (16), 7309-7316.

31. Grimes, R. N. *Carboranes, 2nd Edition* **2011**, 541-674.

32. (a)Hoel, E. L.; Hawthorne, M. F. *J. Am. Chem. Soc.* **1975,** 97, (22), 6388-6395; (b)Kalinin, V. N.; Usatov, A. V.; Zakharkin, L. I. *Zh. Obshch. Khim.* **1981,** 51, (9), 2151-2152.

33. (a)Eleazer, B. J.; Smith, M. D.; Peryshkov, D. V. *Organometallics* **2016,** 35, (2), 106-112; (b)Eleazer, B. J.; Smith, M. D.; Peryshkov, D. V. *J. Organomet. Chem.* **2017,** 829, 42-47; (c)Eleazer, B. J.; Smith, M. D.; Popov, A. A.; Peryshkov, D. V. *Chem. Sci* **2017,** 8, (8), 5399-5407.

34. (a)Zakharkin, L. I.; Pisareva, I. V. *Bull. Acad. Sci. USSR, Div. Chem. Sci.* **1978,** 27, (1), 222-222; (b)Saleh, L. M. A.; Dziedzic, R. M.; Khan, S. I.; Spokoyny, A. M. *Chem. Eur. J.* **2016,** 22, (25), 8466-8470.

35. (a)Hawthorne, M. F.; Young, D. C.; Wegner, P. A. *J. Am. Chem. Soc.* **1965,** 87, (8), 1818-1819; (b)Yoo, Y.; Hwang, J. W.; Do, Y. *Inorg. Chem.* **2001,** 40, (3), 568-570; (c)Willans, C. E.; Kilner, C. A.; Fox, M. A. *Chem. Eur. J.* **2010,** 16, (35), 10644-10648.

36. Hawthorne, M. F.; Young, D. C.; Garrett, P. M.; Owen, D. A.; Schwerin, S. G.; Tebbe, F. N.; Wegner, P. A. *J. Am. Chem. Soc.* **1968,** 90, (4), 862-868.

37. Yoshizaki, T.; Shiro, M.; Nakagawa, Y.; Watanabe, H. *Inorg. Chem.* **1969,** 8, (3), 698-699.

38. Zhigach, A. F.; Svitsyn, R. A.; Sobolev, E. S. *Zh. Obshch. Khim.* **1977,** 47, (1), 228-229.

39. Hawthorne, M. F.; Wegner, P. A.; Stafford, R. C. *Inorg. Chem.* **1965,** 4, (11), 1675-1675.

40. Teixidor, F.; Vinas, C.; Abad, M. M.; Nunez, R.; Kivekas, R.; Sillanpaa, R. *J. Organomet. Chem.* **1995,** 503, (2), 193-203.

41. Ioppolo, J. A.; Clegg, J. K.; Rendina, L. M. *Dalton Trans.* **2007**, (20), 1982-1985.

42. (a)Adams, R. D.; Kiprotich, J.; Peryshkov, D. V.; Wong, Y. O. *Chem. Eur. J.* **2016,** 22, (19), 6501-6504; (b)Adams, R. D.; Kiprotich, J.; Peryshkov, D. V.; Wong, Y. O. *Inorg. Chem.* **2016,** 55, (16), 8207-8213.

43. Charmant, J. P. H.; Haddow, M. F.; Mistry, R.; Norman, N. C.; Orpen, A. G.; Pringle, P. G. *Dalton Trans.* **2008**, (11), 1409-1411.

44. Zakharkin, L. I.; Kalinin, V. N.; Antonovich, V. A.; Rys, E. G. *Bull. Acad. Sci. USSR, Div. Chem. Sci.* **1976,** 25, (5), 1009-1014.

CHAPTER 2

Cage Opening of a Carborane Ligand by Metal Cluster Complexes[1]

[1] Adams, R. D.; Kiprotich, J.; Peryshkov, D. V.; Wong, Y. O. *Chem. Eur. J.* **2016**, *22*, 6501 – 6504.
Reprinted here with permission of publisher

2.1 Introduction

Cage stability is one of the hallmarks of the closo polyhedral boranes and carboranes.[1] The stability is created by electron delocalization manifested in their highly delocalized bonding molecular orbitals. Carboranes are structures in which some of the BH groups of the boranes are replaced by CH groups.[1b] These substitutions lead to inequivalences and differences in reactivity of the remaining BH groups.[2] Studies have shown the strong bases can attack the most electron deficient BH groups leading to cage rupture including, in many cases, complete removal (deboronation) of a BH group from the cage.[3]

We have now prepared some of the first polynuclear metal carbonyl cluster complexes where a closo-carborane cage serves as a ligand on the face of one and two trimetallic clusters, and most interestingly, in the presence of two metal clusters, the cage can be opened. Although there are many examples of transition metal groupings incorporated into the cages of boranes and carboranes,[4] we have found only one previously reported example of an unsubstituted closo-carborane serving as a ligand in a polynuclear metal complex.[5]

2.2 Experimental Details

General Data

All reactions were performed under a nitrogen atmosphere using standard Schlenk Techniques. Reagent grade solvents were dried by the standard procedures and were freshly distilled prior to use. Infrared spectra were recorded on a Thermo Nicolet Avatar 360 FT-IR spectrophotometer. ^{1}H NMR spectra were recorded on a Varian Mercury 300 spectrometer operating at 300.1 MHz, Mass spectrometric (MS) measurements

performed by a direct-exposure probe using electron impact ionization (EI) were made on a VG 70S instrument. $C_2B_{10}H_{12}$ was obtained from STREM and Boron Specialties LLC and was used without further purification. $Os_3(CO)_{10}(NCMe)_2$ was prepared according to a previously reported procedure.[6] Product separations were performed by TLC in air on Analtech 0.25 and 0.5 mm silica gel or alumina 60 Å F_{254} glass plates.

Reaction of $Os_3(CO)_{10}(NCMe)_2$ with $C_2B_{10}H_{12}$

7.4 mg (0.0513mmol) of $C_2B_{10}H_{12}$ was added to a 100 mL three neck flask with a solution of 48.0 mg (0.0515mmol) $Os_3(CO)_{10}(NCMe)_2$ in 30 mL of toluene. After refluxing for 1.5 h, the solvent was removed *in vacuo* and the products isolated by TLC on alumina. Elution in pure hexane yielded: 12.7 mg of $Os_3(CO)_9(\mu_3\text{-}4,5,9\text{-}C_2B_{10}H_{10})(\mu\text{-}H)_2$, **2.1**, (26 % yield), 4.3 mg of $Os_3(CO)_9(\mu_3\text{-}3,4,8\text{-}C_2B_{10}H_{10})(\mu\text{-}H)_2$, **2.2,** (9 % yield), 2.0 mg of the known compound $Os_2(CO)_9(\mu_3\text{-}C_6H_3Me)(\mu\text{-}H_2)$[2] and 4.0 mg of $Os_3(CO)_{12}$. At reaction times greater than 2 h, a hexaosmium complex $Os_3(CO)_9(\mu\text{-}H)_2(\mu_3\text{-}4,5,9\text{-}\mu_3\text{-}7,11,12\text{-}C_2B_{10}H_7)Os_3(CO)_9(\mu\text{-}H)_3$, **2.3** (*vide infra*) was formed in addition to **2.1** and **2.2**. Spectral data for **2.1**: IR (υ_{CO}, cm^{-1}, in hexane): 2103 (s), 2083 (vs), 2051 (s), 2030 (s), 2015 (m), 2008 (s), 1973 (s). ^1H NMR (in toluene-d_8): δ = 2.41 ppm (s, 1H, CH), 2.52 (s, 1H, CH), -9.97 (q, br, agostic B-H→Os), $^1J_{B\text{-}H}$ = 76 Hz, -17.90 (s, hydride, 1H), -20.25 (s, hydride, 1H). ^{11}B NMR (in toluene-d_8): δ = -1.34(d, 1B), $^1J_{B\text{-}H}$ = 159 Hz, -5.38(d, 2B), $^1J_{B\text{-}H}$ = 162 Hz, -11.49(d, 2B), $^1J_{B\text{-}H}$ = 223 Hz, -13.20(d, 2B), $^1J_{B\text{-}H}$ = 190 Hz, -20.39(s, 2B), -29.69(1B, agostic BH), $^1J_{B\text{-}H}$ = 76 Hz. Figure **A 1** (appendix A) is a copy of the H-coupled ^{11}B NMR spectrum of **2.1**. Figure **A 2** (appendix A) is a copy of the H-decoupled ^{11}B NMR spectrum of **2.1**. EI/MS, m/z, M^+ = 967. Spectral data for **2.2**: IR (υ_{CO}, cm^{-1}, in hexane): 2104 (s), 2084 (vs), 2052 (s), 2032 (s), 2019 (m), 2013 (s), 2006 (w), 1972

(s). ^{1}H NMR (in toluene-d_8): δ = 2.42 ppm (s, 1H, CH), 2.64 (s, 1H, CH), -9.91 (q br, agostic B-H→Os), $^1J_{B-H}$ = 78 Hz, -17.93 (s, hydride, 1H), -20.22 (s, hydride, 1H). EI/MS m/z, M^+ = 967.

Conversion of 2.1 to 2.2 and vice versa

A pure sample of **2.1** (isomer 1) was dissolved in toluene-d_8 and heated in an oil bath at 108° C. The sample was monitored by NMR for a period of 43 h. Formation of isomer **2.2** was observed after 7 h. After 42 h at this temperature, the ratio of the two isomers had achieved their equilibrium ratio of **2.1**/**2.2** of 0.63. In reverse, a pure sample of **2.2** was dissolved in toluene-*d*$_8$ and heated at 90° C for 26.5 h after which the temperature was raised to 105° C and heated for a further 40 h. Formation of isomer **2.1** was only observed after the temperature was raised to 105° C. The two isomers reached equilibrium after 67 h.

Reaction of 2.1 with $Os_3(CO)_{10}(NCMe)_2$.

Compound **2.3** was obtained from the reaction of a mixture of the compounds **2.1** with $Os_3(CO)_{10}(NCMe)_2$. 27.0 mg (0.0279 mmol) of **2.1** was added to a 100 mL three neck flask with a solution of 22.5 mg (0.0241mmol) $Os_3(CO)_{10}(NCMe)_2$ in 30 mL of heptane. After refluxing for 1.25 h, the solvent was removed *in vacuo* and the products were isolated by TLC by using hexane solvent. The following products were obtained in order of elution: 2.7 mg of $Os_3(CO)_{12}$, 16.6 mg of $Os_3(CO)_9(\mu\text{-}H)_2(\mu_3\text{-}4,5,9\text{-}\mu_3\text{-}7,11,12\text{-}C_2B_{10}H_6)Os_3(CO)_9(\mu\text{-}H)_3$, **2.3** (38% yield), 2.1 mg of $Os_3(CO)_9(\mu\text{-}H)(\mu_3\text{-}3,4,8\text{-}\mu_3\text{-}7,11,12\text{-}C_2B_{10}H_6)Os_3(CO)_9(\mu\text{-}H)$, **2.4** (5% yield), and 3.3 mg of the known compound $Os_3(CO)_{10}(\mu\text{-}H)_2$.[7] Spectral data for **2.3**: IR (υ_{CO}, cm^{-1}, in hexane): 2104 (vw), 2097 (s), 2088 (vs), 2085 (vs), 2050 (m), 2033 (vs), 2019 (s) 2016 (s), 2005 (w), 1971 (m), 1988

(w). ^{1}H NMR (in CD_2Cl_2): δ = 3.63 ppm (s, 1H, CH), 3.74 (s, 1H, CH), -9.70 (q, br, agostic B-H→Os) $^1J_{B\text{-}H}$ ~ 82 Hz, -17.67 (s, hydride, 1H), -17.93 (s, hydride, 1H), -20.03 (s, hydride, 1H), -20.20 (s, hydride, 1H), -20.65 (s, hydride, 1H). EI/MS m/z = 1787(M^+-2H). Note: Compound **2.3** loses H_2 when heated to form compound **2.4** (see below). Spectral data for **2.4**: IR (υ_{CO}, cm^{-1}, in hexane): 2106 (m), 2095 (s), 2076 (vs), 2070 (s), 2061 (vs), 2037 (m), 2031 (s) 2013 (s), 2008 (sh), 1991 (w), 1988 (w). ^{1}H NMR (^{11}B decoupled in CD_2Cl_2): δ = 1.67 ppm (s, 1H, CH), 2.04 (s, 1H, CH), -11.84 (br, B-H→Os), -13.56 (br, agostic B-H→Os), -21.93 (s, hydride, 1H), -22.48 (s, hydride, 1H). EI/MS m/z = 1788.

Conversion of 2.3 to 2.4

A solution of **2.3** (25.9 mg, 0.0145 mmol) in nonane solvent was heated to reflux for 1.25 h. The products were separated by TLC by using pure hexane solvent to yield: 6.1 mg of **2.4** (15% yield), 4.7 mg of $Os_3(CO)_{10}(\mu\text{-}H)_2$, 2.5 mg of a mixture of **2.1** and **2.2** plus some uncharacterizable trace products.

Crystallographic Analyses

Yellow single crystals of **2.1, 2.2, 2.3** and **2.4** suitable for x-ray diffraction analyses were obtained by slow evaporation of solvent from a hexane/methylene chloride solvent mixture at room temperature. Each data crystal was glued onto the end of a thin glass fiber. X-ray intensity data were measured by using a Bruker SMART APEX CCD-based diffractometer using Mo Kα radiation (λ = 0.71073 Å). The raw data frames were integrated with the SAINT$^+$ program by using a narrow-frame integration algorithm.[8] Correction for Lorentz and polarization effects were also applied with SAINT$^+$. An empirical absorption correction based on the multiple measurement of equivalent

reflections was applied using the program SADABS. All structures were solved by a combination of direct methods and difference Fourier syntheses, and refined by full-matrix least-squares on F^2, using the SHELXTL software package.[9] All non-hydrogen atoms were refined with anisotropic displacement parameters. Hydrogen atoms were placed in geometrically idealized positions and included as standard riding atoms during the least-squares refinements. Crystal data, data collection parameters, and results of the analyses are listed in Tables 2.1 and 2.2.

Compounds **2.1, 2.2, 2.3** and **2.4** all crystallized in the monoclinic crystal system. The space group $P2_1/n$ was assumed for **2.1, 2.2** and **2.3** and confirmed by the successful solution and refinement of the structures. For compound **2.4**, the space group $C2/c$ was indicated by the systematic absences in the data and confirmed by the successful solution and refinement of the structure. Compound **2.4** co-crystallized with half methylene chloride solvent molecule. The bridging Os–H distances in all 3 compounds were refined with distance constraints of 1.80 Å.

2.3 Results and Discussion

Two products, $Os_3(CO)_9(\mu_3\text{-}4,5,9\text{-}C_2B_{10}H_8)(\mu\text{-}H)_2$, **2.1** and $Os_3(CO)_9(\mu_3\text{-}3,4,8\text{-}C_2B_{10}H_8)(\mu\text{-}H)_2$, **2.2** were obtained from the reaction of $Os_3(CO)_{10}(NCMe)_2$ with closo-o-$C_2B_{10}H_{10}$ in toluene solvent at 110 ^oC for 1.5 h. ORTEP diagrams of the molecular structures **2.1** and **2.2** are shown in Figures 2.1 and 2.2 respectively. Compounds **2.1** and **2.2** are isomers formed the loss of the two NCMe ligands and one CO ligand from the $Os_3(CO)_{10}(NCMe)_2$, and the addition of one equivalent of closo-$C_2B_{10}H_{10}$ to the triosmium cluster. The carborane is a triply bridging ligand containing two direct Os – B bonds, and one agostically-coordinated BH group to the third metal atom in each isomer.

The distances of the direct Os – B bonds, Os(1) – B(5) = 2.168(10) Å, Os(3) – B(4) = 2.181(10) Å, for **2.1**, and Os(1) – B(3) = 2.189(11) Å, Os(3) – B(4) = 2.176(12) Å for **2.2**, are considerably shorter than the distance to the agostically-coordinated BH groups, B(9) – H(9a) bond, B(9) – H(9a) **=** 1.41(16**)** Å and Os(2) – B(9) = 2.624(10) Å and Os(2) – H(9a) = 1.64(16) Å, in **2.1**, and B(8) – H(8a) = 1.03(18) Å, Os(2) – B(8) = 2.629(13) Å and Os(2) – H(8a) = 1.70(18) Å for **2.2**. Agostically, coordinated B-H bonds exhibit characteristically longer M – B distances.[10] Two B-H bonds were cleaved from the cage in the ligation process and the hydrogen atoms were shifted to the metal atoms to become bridging hydrido ligands as shown in the figures, ^{1}H NMR, δ = -17.90 (s, 1H), -20.25 (s, 1H) for **2.1** and δ = -17.93 (s, 1H), -20.22 (s, 1H) for **2.2**. The boron atoms from the cleaved B-H bonds are the ones coordinated directly to the metal atoms. The hydrogen atoms of the agostically coordinated BH groups are also characteristically shifted upfield and appear as a quartet due to ^{1}J-coupling to the neighboring boron atom: for **2.1**, δ = -9.97 (q, br, B-H→Os), $^{1}J_{B\text{-}H}$ = 76 Hz; for **2.2** and δ = -9.91 (q, br, B-H→Os), $^{1}J_{B\text{-}H}$ = 78 Hz.[11] Isomers **2.1** and **2.2** differ principally by the B_3 triangle to which the carborane is coordinated to the Os_3 triangle. For **2.1** it is coordinated to the 4,5,9 triangle, but for **2.2** it is coordinated to the 3,4,8 triangle. The locations of the carbon atoms in each carborane ligand were identified by their characteristically short C – C bond distance.

Compounds **2.1** and **2.2** can be interconverted thermally. The equilibrium ratio **2.1**/**2.2** = 0.63 in toluene solvent was achieved by heating **2.1** at 108^{o} C for 48 h. In the transformation of **2.1** to **2.2**, the carborane cage must shift by two B_3 triangles and must involve, the addition of a hydrogen atom to B5 and a cleavage of the hydrogen atom from

B3. It is likely that the hydrido ligands on the metal cluster participate in these hydrogen exchanges, but details of the mechanism are not available at this time.

Interestingly, **2.1** and **2.2** react with a second equivalent of $Os_3(CO)_{10}(NCMe)_2$ at 97° C to yield two new hexaosmium compounds: $Os_3(CO)_9(\mu\text{-}H)_2(\mu_3\text{-}4,5,9\text{-}\mu_3\text{-}7,11,12\text{-}C_2B_{10}H_7)Os_3(CO)_9(\mu\text{-}H)_3$, **2.3** (38% yield) and $Os_3(CO)_9(\mu\text{-}H)(\mu_3\text{-}3,4,8\text{-}\mu_3\text{-}7,11,12\text{-}C_2B_{10}H_8)Os_3(CO)_9(\mu\text{-}H)$, **2.4** (5% yield). Compound **2.3** can be converted to **2.4** in 15% yield by heating a solution of **2.3** in nonane solvent to reflux for 1.25 h. Compounds **2.3** and **2.4** have both been characterized by a combination of IR, NMR and single-crystal X-ray diffraction analyses. An ORTEP diagram of the molecular structure of **2.3** is shown in Figure 2.3.

Compound **2.3** contains a $C_2B_{10}H_7$ cage sandwiched between two triangular triosmium carbonyl clusters. The metal clusters bridge the 4,5,9 and 7,11,12 B_3 triangles of the closo-$C_2B_{10}H_7$ cage. Two boron atoms, Os(1) – B(4) = 2.169(11) Å, Os(3) – B(5) = 2.188(11) Å, and one agostically-coordinated BH group, Os(2) – B(9) = 2.593(11) Å, Os(2) – H(9A) = 1.86(10) Å, ^{1}H NMR δ = -9.70 (q, 1H), $^1J_{B\text{-}H} \sim 82$ Hz, are bonded to the Os(1)-Os(2)-Os(3) triangle. The Os(1)-Os(2)-Os(3) triangle also contains two bridging hydrido ligands that were presumably transferred to the cluster from the two boron atoms that are directly-bonded bonded to the osmium atoms. Three boron atoms, Os(4) – B(11) = 2.189(11) Å, Os(5) – B(7) = 2.185(11) Å and Os(6) – B(11) = 2.211(11) Å are directly coordinated to the Os(4)-Os(5)-Os(6) triangle. Accordingly, this Os_3 triangle contains three hydrido ligands with one bridging each of the three Os – Os bonds. Except for the presence of one of the bridging hydrido ligand, H(2), on the Os(1)-Os(2)-Os(3) triangle,

compound **2.3** contains overall an approximate reflection symmetry with the symmetry plane passing through the cage atoms C(1), C(2), B(9) and B(12).

An ORTEP diagram of the molecular structure of **2.4** is shown in Figure 4. Compound **2.4** also contains two triangular triosmium clusters that coordinated to a significantly ruptured $C_2B_{10}H_8$ cage. Each triosmium cluster contains two directly-coordinated boron atoms, one triply-bridging agostic BH group and one hydrido ligand. The Os – B distances to the triply-bridging agostic BH groups, B(3) and B(7), are significantly shorter, Os(1) – B(3) = 2.132(10), Os(2) – B(3) = 2.200(10), Os(3) – B(3) = 2.199(10), Os(1) – H(3A) = 1.85(15), Os(5) – B(7) = 2.150(11), Os(4) – B(7) = 2.235(10), Os(6) – B(7) = 2.191(11) Å than that to the agostically-coordinated BH groups that are coordinated to only one metal atom as found in compounds **2.1**, **2.2** and **2.3**. The resonances of the triply bridging agostic BH groups are shifted to slightly higher field values, δ = -11.83 (br, 1H), and -13.56 (br, 1H), than those of **2.1**, **2.2** and **2.3**. The osmium triangle Os(4)-Os(5)-Os(6) is bonded to the same group of boron atoms, **7**,11,12, as found in **2.3**, but the Os(1)-Os(2)-Os(3) group is bonded instead to the B_3 group 3,4,8 and thus was shifted in the course of the conversion of **2.3** to **2.4**.

We have analyzed the transformation of **2.3** into **2.4** in terms a two-step mechanism as shown in scheme 2.1. The process begins with a shift of the Os(1)-Os(2)-Os(3) cluster from the 4,5,9 B_3-triangle to the 3,4,8 B_3-triangle. In the process a hydrogen atom is shifted to B(5) and one is cleaved from B(3). This step would lead to the formation of an intermediate represented as **2.3a** in the Scheme. This step of the rearrangement is formally equivalent to the isomerization of **2.1** to **2.2** described above. The opening of the C_2B_{10} cage requires the cleavage of five cage bonds, B(3) – B(7),

B(3) – C(1), B(3) – C(2), B(7) – C(2) and B(7) – B(8). The sequence of these cleavages is not known at present, but we are willing to speculate that the process begins with cleavage of the bonds between B(3) and the two carbon atoms, C(1) and C(2), because previous studies have shown that these B(3) – C cage bonds are the first to cleave upon the addition of bases to 1,2-$C_2B_{10}H_{12}$.[4] Hydrogen atoms, presumably from the metal atoms, are added to the boron atoms B(3) and B(7). These additions would facilitate cleavage of the bonds to B(7), particularly B(3) – B(7), and also B(7) – C(2) and B(7) – B(8), to complete the cage opening process. Two hydrogen atoms were eliminated, presumably as H_2, in the transformation of **2.3** to **2.4**.

2.4 Summary

The metalated boroncages reported herein are rare examples of the unsupported metal–boryl complexes of unsubstituted icosahedral carboranes. The formation of transition metal B-carboranyl bonds by nondirected B-H activation has been reported only for the reaction of *o*-$C_2B_{10}H_{12}$ and [$Ir(PPh_3)_3Cl$] or [$Ir(AsPh_3)_3Cl$][12]. Furthermore, compound **2.3** is the first example of the complex containing a total of five metal– boryl bonds on a single icosahedral carborane cage.

It is anticipated that similar cluster-induced cage opening reactions can be obtained with other carboranes and by using clusters of different transition metals. Indeed, Du et al. have shown that reaction of the carborane, *closo*-4-CB_8H_9, reacts with $Ru_3(CO)_{12}$ by formation of an Ru_6 raft from which three of the ruthenium atoms have been inserted into the carborane cage to form a 12-vertex triruthenacarborane.[13] It will be interesting to see if carboranes will also open when they are deposited on clean metal

surfaces and, if so, could carboranes serve as precursors to “carborene” hybrids of graphenes[14] and borophenes[15] on metal surfaces?

Table 2.1. Crystallographic Data for Compounds **2.1** and **2.2**

Compound	**2.1**	**2.2**
Empirical formula	$Os_3O_9C_{11}B_{10}H_{12}$	$Os_3O_9C_{11}B_{10}H_{12}$
Formula weight	966.91	966.91
Crystal system	Monoclinic	Monoclinic
Lattice parameters		
a (Å)	8.1347(12)	8.2829(8)
b (Å)	20.133(3)	19.6941(19)
c (Å)	13.984(2)	14.0536(14)
α (deg)	90.00	90.00
β (deg)	94.286(3)	96.960(2)
γ (deg)	90.00	90.00
V (Å^3)	2283.9(6)	2275.6(4)
Space group	$P2_1/n$	$P2_1/n$
Z value	4	4
ρcalc (g/cm3)	2.812	2.822
μ (Mo Kα) (mm−1)	16.690	16.750
Temperature (K)	293(2)	294(2)
2Θmax (°)	56.70	52.18
No. Obs. (I > 2σ(I))	3738	4015
No. Parameters	315	318
Goodness of fit (GOF)	1.077	1.024
Max. shift/error on final cycle	0.001	0.028
Residuals*: R_1; wR_2	0.0509; 0.1307	0.0363; 0.0850
Absorption Correction,	Multi-scan	Multi-scan
Transmission (Max/min)	1.00/0.264	1.00/0.560
Largest peak in Final Diff. Map (e$^-$/Å^3)	4.105	1.697

*$R_1 = \Sigma_{hkl}(\,|\,|F_{obs}|-|F_{calc}|\,|)/\Sigma_{hkl}|F_{obs}|$; $wR_2 = [\Sigma_{hkl}w(|F_{obs}|-|F_{calc}|)^2/\Sigma_{hkl}wF^2_{obs}]^{1/2}$; $w = 1/\sigma^2(F_{obs})$; GOF = $[\Sigma_{hkl}w(|F_{obs}|-|F_{calc}|)^2/(n_{data}-n_{vari})]^{1/2}$.

Table 2.2. Crystallographic Data for Compounds **2.3** and **2.4**.

Compound	**2.3**	**2.4**
Empirical formula	$Os_6O_{18}C_{20}B_{10}H_{12}$	$Os_6O_{18}C_{20.5}B_{10}ClH_{10}$
Formula weight	1789.79	1808.31
Crystal system	Monoclinic	Monoclinic
Lattice parameters		
a (Å)	9.6636(2)	19.2832(13)
b (Å)	15.4422(4)	18.0798(12)
c (Å)	25.6755(6)	23.6626(16)
α (deg)	90.00	90.00
β (deg)	90.5760(10)	108.5790(10)
γ (deg)	90.00	90.00
V (Å3)	3831.29(16)	7819.7(9)
Space group	$P2_1/n$	$C2/c$
Z value	4	8
ρcalc (g/cm3)	3.103	3.072
μ (Mo Kα) (mm−1)	19.888	19.523
Temperature (K)	294(2)	294(2)
2Θmax (°)	56.67	56.78
No. Obs. (I > 2σ(I))	5836	6178
No. Parameters	514	517
Goodness of fit (GOF)	1.409	1.108
Max. shift in cycle	0.012	0.016
Residuals*: R_1; wR_2	0.0378; 0.0961	0.0321; 0.0832
Absorption Correction,	Multi-scan	Multi-scan
Transmission (Max/min)	1.00/0.547	1.00/0.322
Largest peak in Final Diff. Map ($e^-/Å^3$)	2.068	1.477

*$R_1 = \Sigma_{hkl}(||F_{obs}|-|F_{calc}||)/\Sigma_{hkl}|F_{obs}|$; $wR_2 = [\Sigma_{hkl}w(|F_{obs}|-|F_{calc}|)^2/\Sigma_{hkl}wF^2_{obs}]^{1/2}$; $w = 1/\sigma^2(F_{obs})$; GOF = $[\Sigma_{hkl}w(|F_{obs}|-|F_{calc}|)^2/(n_{data} - n_{vari})]^{1/2}$.

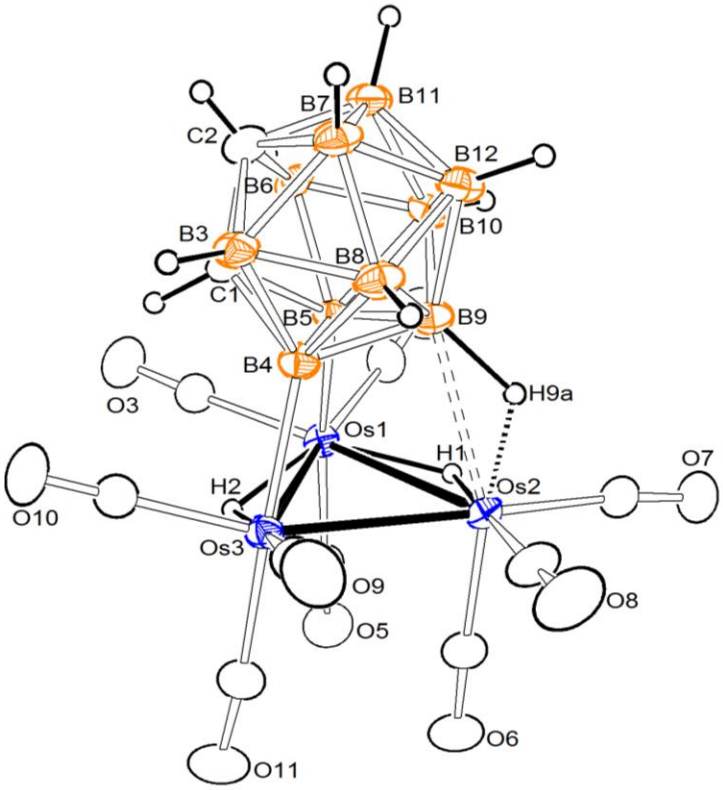

Figure 2.1. An ORTEP diagram of the molecular structure of $Os_3(CO)_9(\mu_3\text{-}4,5,9\text{-}C_2B_{10}H_{10})(\mu\text{-}H)_2$, **2.1** showing 30% thermal ellipsoid probability. Selected interatomic bond distances (Å) are as follow: Os(1) – Os(2) = 3.0395(6), Os(1) – Os(3) = 3.0865(6), Os(2) – Os(3) = 2.8698(6), Os(1) – B(5) = 2.168(10), Os(3) – B(4) = 2.181(10), Os(2) – B(9) = 2.624(10), Os(2) – H(9a) = 1.64(16), B(9) – H(9a) = 1.41(16), C(1) – C(2) = 1.594(13).

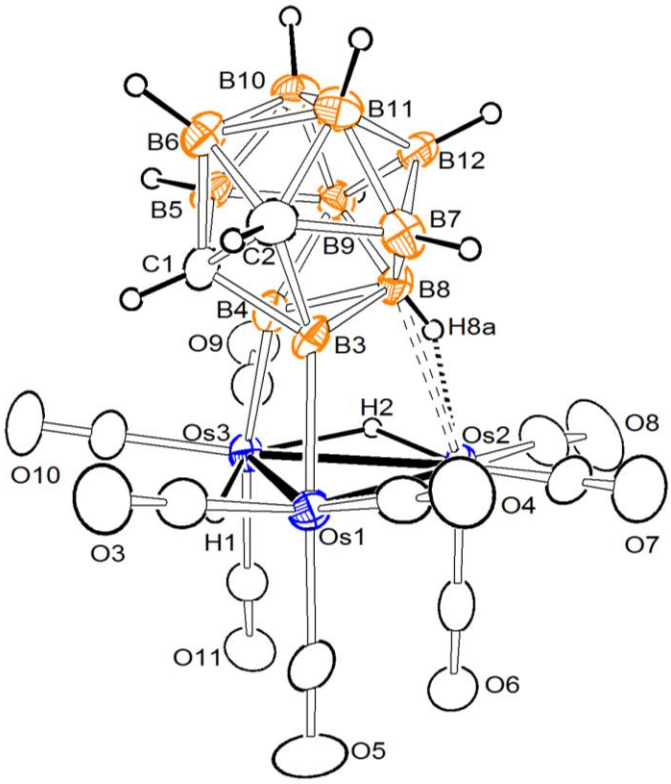

Figure 2.2. An ORTEP diagram of the molecular structure of $Os_3(CO)_9(\mu_3\text{-}3,4,8\text{-}C_2B_{10}H_{10})(\mu\text{-}H)_2$, **2.2** showing 30% thermal ellipsoid probability. Selected interatomic bond distances (Å) are as follow: Os(1) – Os(2) = 2.8917(6), Os(1) – Os(3) = 3.0923(6), Os(2) – Os(3) = 3.0148(6), Os(1) – B(3) = 2.189(11), Os(3) – B(4) = 2.176(12), Os(2) – B(8) = 2.629(13), Os(2) – H(8a) = 1.70(18), B(8) – H(8a) = 1.03(18), C(1) – C(2) = 1.645(15).

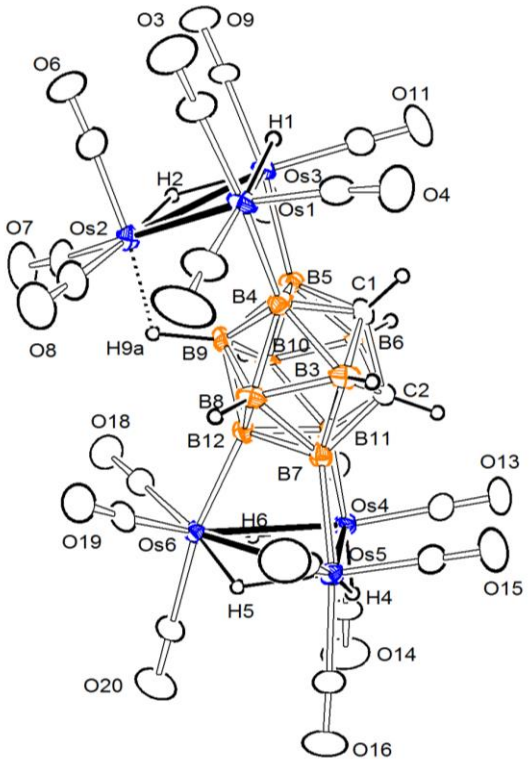

Figure 2.3. An ORTEP diagram of the molecular structure of $Os_3(CO)_9(\mu\text{-}H)_2(\mu_3\text{-}4,5,9\text{-}\mu_3\text{-}7,11,12\text{-}C_2B_{10}H_7)Os_3(CO)_9(\mu\text{-}H)_3$, **2.3** showing 25% thermal ellipsoid probability. Selected interatomic bond distances (Å) are as follow: Os(1) – Os(2) = 2.8827(6), Os(1) – Os(3) = 3.0825(5), Os(2) – Os(3) = 3.0381(5), Os(4) – Os(5) = 3.1060(5), Os(4) – Os(6) = 3.1356(5), Os(5) – Os(6) = 3.1291(5), Os(1) – B(4) = 2.169(11), Os(2) – B(9) = 2.593(11), Os(3) – B(5) = 2.188(11), Os(4) – B(11) = 2.189(11), Os(5) – B(7) = 2.185(11), Os(6) – B(11) = 2.211(11), Os(2) – H(9A) = 1.86(10), B(9) – H(9A) = 1.30(9), C(1) – C(2) = 1.603(14).

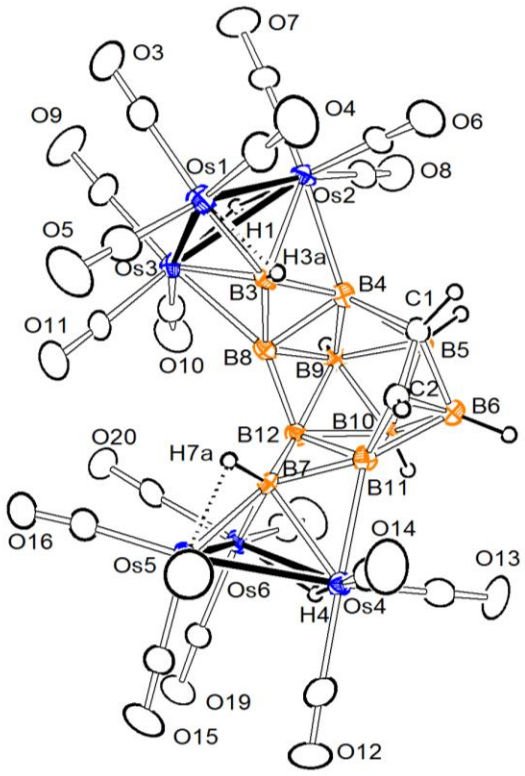

Figure 2.4. An ORTEP diagram of the molecular structure of $Os_3(CO)_9(\mu\text{-}H)(\mu_3\text{-}3,4,8\text{-}\mu_3\text{-}7,11,12\text{-}C_2B_{10}H_8)Os_3(CO)_9(\mu\text{-}H)$, **2.4** showing 20% thermal ellipsoid probability. Selected interatomic bond distances (Å) are as follows: Os(1) – Os(2) = 2.8526(6), Os(1) – Os(3) = 2.8538(6), Os(2) – Os(3) = 2.9647(5), Os(4) – Os(5) = 2.8370(5), Os(4) – Os(6) = 2.9714(5), Os(5) – Os(6) = 2.8647(5), Os(1) – B(3) = 2.132(10), Os(2) – B(3) = 2.200(10), Os(3) – B(3) = 2.199(10), Os(1) – H(3A) = 1.85(15), Os(2) – B(4) = 2.291(11), Os(3) – B(8) = 2.304(10), Os(5) – B(7) = 2.150(11), Os(4) – B(7) = 2.235(10), Os(6) – B(7) = 2.191(11), Os(4) – B(11) = 2.307(10), Os(6) – B(12) = 2.335(10).

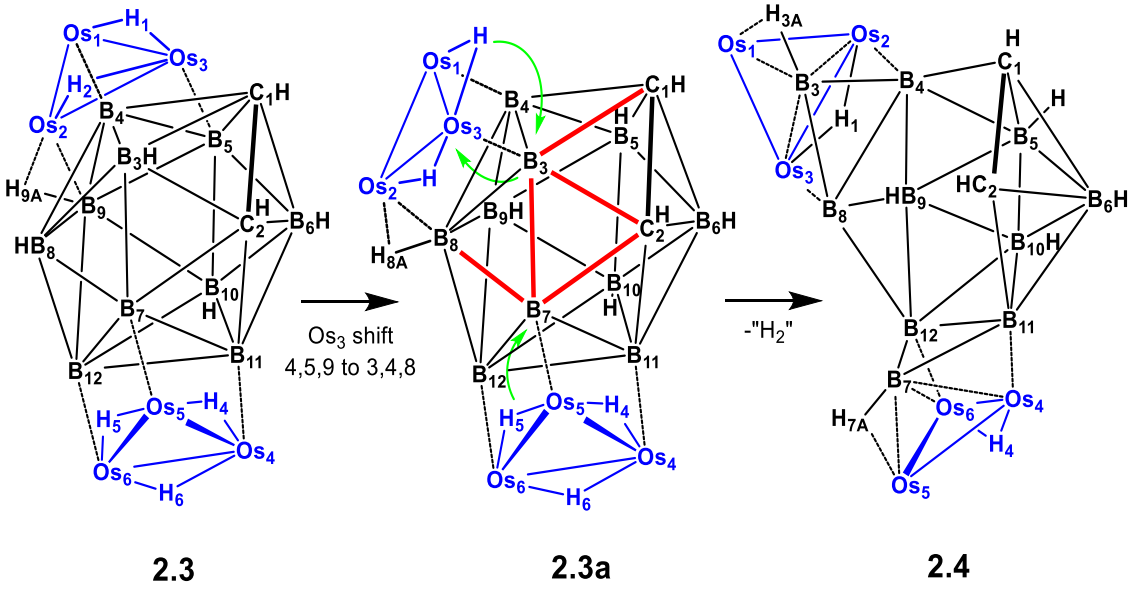

Scheme 2.1. A proposed mechanism for the transformation of **2.3** to **2.4**. The red lines in the Intermediate **2.3a** indicate the cage bonds that must be cleaved in the cage-opening process.

2.5 References

1. (a)D. M. P. Mingos, D. J. W., *Introduction to Cluster Chemistry*. Prentice Hall: Cliffs, N.J., 1990; (b)Grimes, R. N. *Carboranes, 2nd Edition* **2011**.

2. (a)Hermansson, K.; Wojcik, M.; Sjoberg, S. *Inorg. Chem.* **1999,** 38, (26), 6039-6048; (b)Teixidor, F.; Barbera, G.; Vaca, A.; Kivekas, R.; Sillanpaa, R.; Oliva, J.; Vinas, C. *J. Am. Chem. Soc.* **2005,** 127, (29), 10158-10159.

3. (a)Batsanov, A. S.; Copley, R. C. B.; Davidson, M. G.; Fox, M. A.; Hibbert, T. G.; Howard, J. A. K.; Wade, K. *J. Cluster Sci.* **2006,** 17, (1), 119-137; (b)Willans, C. E.; Kilner, C. A.; Fox, M. A. *Chem. Eur. J.* **2010,** 16, (35), 10644-10648.

4. Grimes, R. N. *Coord. Chem. Rev.* **2000,** 200, 773-811.

5. Molinos, E.; Brayshaw, S. K.; Kociok-Kohn, G.; Weller, A. S. *Dalton Trans.* **2007**, (42), 4829-4844.

6. Braga, D.; Grepioni, F.; Parisini, E.; Johnson, B. F. G.; Martin, C. M.; Nairn, J. G. M.; Lewis, J.; Martinelli, M. *J. Chem. Soc.-Dalton Trans.* **1993**, (12), 1891-1895.

7. Mason, R.; Mingos, D. M. P. *J. Organomet. Chem.* **1973,** 50, (1), 53-61.

8. *SAINT+*, Version 6.2a; Bruker Analytical X-ray Systems, Inc.: Madison, WI 2001.

9. Sheldrick, G. M. *SHELXTL*, Version 6.1; Bruker Analytical X-ray Systems, Inc.: Madison, WI, 1997.

10. (a)Jan, D. Y.; Shore, S. G. *Organometallics* **1987,** 6, (2), 428-430; (b)Chung, J. H.; Knoeppel, D.; McCarthy, D.; Columbie, A.; Shore, S. G. *Inorg. Chem.* **1993,** 32, (16), 3391-3392; (c)Chung, J. H.; Boyd, E. P.; Liu, J. P.; Shore, S. G. *Inorg. Chem.* **1997,** 36, (21), 4778-4781.

11. (a)Brew, S. A.; Stone, F. G. A. *Adv. Organomet. Chem.* **1993,** 35, 135-186; (b)Lebedev, V. N.; Mullica, D. F.; Sappenfield, E. L.; Stone, F. G. A. *J. Organomet. Chem.* **1997,** 536, (1-2), 537-539; (c)Ellis, D. D.; Franken, A.; Stone, F. G. A. *Organometallics* **1999,** 18, (12), 2362-2369.

12. Hoel, E. L.; Hawthorne, M. F. *J. Am. Chem. Soc.* **1975,** 97, (22), 6388-6395.

13. Du, S.; Hodson, B. E.; Lei, P.; McGrath, T. D.; Stone, F. G. A. *Inorg. Chem.* **2007,** 46, (16), 6613-6620.

14. Geim, A. K.; Novoselov, K. S. *Nat. Mater.* **2007,** 6, (3), 183-191.

15. (a)Zhai, H. J.; Zhao, Y. F.; Li, W. L.; Chen, Q.; Bai, H.; Hu, H. S.; Piazza, Z. A.; Tian, W. J.; Lu, H. G.; Wu, Y. B.; Mu, Y. W.; Wei, G. F.; Liu, Z. P.; Li, J.; Li, S. D.; Wang, L. S. *Nat. Chem.* **2014,** 6, (8), 727-731; (b)Mannix, A. J.; Zhou, X. F.; Kiraly, B.; Wood, J. D.; Alducin, D.; Myers, B. D.; Liu, X. L.; Fisher, B. L.; Santiago, U.; Guest, J. R.; Yacaman, M. J.; Ponce, A.; Oganov, A. R.; Hersam, M. C.; Guisinger, N. P. *Science* **2015,** 350, (6267), 1513-1516.

CHAPTER 3

Opening of Carborane Cages by Metal Cluster Complexes: The Reaction of a Thiolate-Substituted Carborane with Triosmium Carbonyl Cluster Complexes[2]

[2]Adams, R. D.; Kiprotich, J.; Peryshkov, D. V.; Wong, Y. O. *Inorg. Chem.* **2016,** 55, (16), 8207-8213.
Reprinted here with permission of publisher

3.1 Introduction

Polyhedral borane and carborane cage compounds are distinguished by their high stability which is a consequence of the delocalized bonding within their molecular frameworks.[1,2] Recent studies have shown that strong nucleophiles can attack the boron atoms of certain carboranes and open the cages by cleaving some of the B - C bonds.[3] The stability, rigidity, considerable steric bulk and electronic properties of carboranes make them a highly attractive class of ligands for transition metal complexes. The unique three-dimensional icosahedral geometry of the boron cage provides multiple coordination sites for multiple metal centers through B-H activation.[2]

In 2008, Du et al. reported that the reaction of the carborane anion [*closo*-4-CB_8H_9] with $Ru_3(CO)_{12}$ yielded the hexaruthenium compound [PPh_4][2,3,7-{$Ru(CO)_3$}-2,6,11-{$Ru(CO)_3$}-7,11,12-{Ru-$(CO)_3$}-3,6,12-(μ-H)$_3$-2,2,7,7,11,11-$(CO)_6$-*closo*-2,7,11,1-$Ru_3CB_8H_6$], **A** by a cage opening reaction in combination with a cluster fusing process that led to the formation of an Ru_6 raft to which the opened carborane cage, formally a "{*hypho*-CB_8H_9}$^{7-}$" ligand, was coordinated to the Ru_6 raft.[4] Carborane complexes of the late transition metals have shown promising applications as reaction catalysts.[2c]

In recent studies, we have found that the reaction of the carborane, closo-*o*-$C_2B_{10}H_{12}$, with $Os_3(CO)_{10}(NCMe)_2$ can also result in opening of the *o*-$C_2B_{10}H_{12}$ cage upon addition of two triosmium clusters to the surface of the cage. The reaction of closo-*o*-$C_2B_{10}H_{12}$ with $Os_3(CO)_9(NCMe)_2$ first yielded the compound $Os_3(CO)_9(\mu\text{-H})_2(\mu_3$-4,5,9-$\mu_3$-7,11,12-$C_2B_{10}H_7)Os_3(CO)_9(\mu\text{-H})_3$, **2.3** which contains two triosmium carbonyl clusters on the surface of a *closo*-$C_2B_{10}H_7$ bridging ligand. When heated, **2.3** was

transformed to the compound $Os_3(CO)_9(\mu\text{-}H)(\mu_3\text{-}3,4,8\text{-}\mu_3\text{-}7,11,12\text{-}C_2B_{10}H_8)Os_3(CO)_9(\mu\text{-}H)$, **C** by loss of H_2 and an opening of the carborane cage by cleavage of a combination of three B – C and two B – B bonds, see Scheme 3.1.[5]

We have now investigated the reaction of the thiolate substituted derivative of *o*-$C_2B_{10}H_{12}$, closo-*o*-(1-SCH_3)$C_2B_{10}H_{11}$, with $Os_3(CO)_9(NCMe)_2$. As with *o*-$C_2B_{10}H_{12}$, it is possible to add one and two $Os_3(CO)_9$ cluster units to the surface of the carborane and in the latter case, the carborane cage is also opened, but more importantly, in this case the opening occurs in a stepwise process that provides new insight into the mechanism of the cage opening process.

3.2 Experimental

General Data.

All reactions were performed under a nitrogen atmosphere by using standard Schlenk techniques. Reagent grade solvents were dried by the standard procedures and were freshly distilled prior to use. Infrared spectra were recorded on a Thermo Scientific Nicolet IS10. ^{1}H NMR spectra were recorded on a Varian Mercury 300 spectrometer operating at 300.1 MHz. ^{11}B NMR spectra were recorded on a Bruker Avance III at 128.42 MHz with reference to $BF_3{\cdot}OEt_2$. Mass spectrometric (MS) measurements performed by a direct-exposure probe using electron impact ionization (EI) were made on a VG 70S instrument. closo-*o*-(1-SCH_3)$C_2B_{10}H_{11}$[6] and $Os_3(CO)_{10}(NCMe)_2$[7] were prepared according to previously reported procedures. Product separations were performed by TLC in air on Analtech 0.25 and 0.5 mm silica gel or alumina 60 Å F_{254} glass plates.

Synthesis of $Os_3(CO)_9[\mu_3\text{-}\eta^3\text{-}C_2B_{10}H_9(SCH_3)](\mu\text{-}H)_2$, 3.1.

12 µL (0.063 mmol) of closo-*o*-(1-SCH_3)$C_2B_{10}H_{11}$ was added to a 100 mL 3-neck, round bottomed flask containing a 30 mL solution of 67.0 mg (0.072 mmol) of $Os_3(CO)_{10}(NCMe)_2$ in toluene. After refluxing for 3 h, the solvent was removed *in vacuo*, and the product was isolated by TLC on silica by using a 5:1 hexane/methylene chloride solvent mixture to yield 51.7 mg of $Os_3CO)_9(\mu_3\text{-}\eta^3\text{-}C_2B_{10}H_9SCH_3)(\mu\text{-}H)_2$, **3.1**, (71 %) followed by a trace of $Os_3(CO)_{12}$. Spectral Data for **3.1**: IR νCO (cm^{-1} in hexane): 2102(s), 2080(vs), 2054(vs), 2030(s), 2019(vs) 2011(s) 2004(m), 1990(s), 1977(m). ^1H NMR (CD_2Cl_2, 25ºC, TMS) δ = 3.05 (s, CH), δ = 3.98 (s, br, CH), 3.05 (s, 3H, CH_3), -16.89 (s, OsH, 1H), -19.12 (s, OsH, 1H). ^{11}B {^1H} NMR (in $CDCl_3$): δ = -13.03 ppm (1 B), -11.11 (4 B), -9.99 (1B), -7.83 (1 B), -1.35 (1 B), -0.60 (1 B), 6.71 (1 B). EI/MS m/z, 1014 (M^+).

Synthesis of $Os_3(CO)_9(\mu\text{-}H)[(\mu_3\text{-}\eta^3\text{-}1,4,5\text{-}\mu_3\text{-}\eta^3\text{-}6,10,11\text{-}C_2B_{10}H_8S(CH_3)]Os_3(CO)_9(\mu\text{-}H)_2$, 3.2.

20.0 mg (0.019 mmol) of compound **3.1** was added to a solution of 44.0 mg (0.047 mmol) $Os_3(CO)_{10}(NCMe)_2$ in a 30 mL toluene and the solution was heated to reflux for 8 h. The solvent was then removed *in vacuo* and the products were isolated by TLC on silica by using hexane as the eluent. In order of elution they were, 7.7 mg of $Os_3(CO)_{12}$, 14.1 mg of **3.2** (39 %)**,** 1.7 mg of $Os_3(CO)_{10}(\mu\text{-}OH)(\mu\text{-}H)$,[8] 7.3 mg of $Os_3(CO)_9((\mu_3\text{-}C_6H_3Me)(\mu\text{-}H)$[9] and 1.7 mg of $Os_3(CO)_{10}(\mu\text{-}H)_2$.[10] Compound **3.2** could also be obtained albeit at a low yield (2%) by refluxing **3.1** in nonane for 3.5 h. Spectral data for **3.2**: IR (υ_{CO}, cm^{-1}, in hexane): 2112 (m), 2092 (vs), 2075 (vs), 2065 (s), 2052(vs), 2029 (sh, m), 2025 (vs), 2016 (w), 2004 (m), 1996 (w), 1985 (w), 1974 (w). ^1H

NMR (^{11}B decoupled, in $CDCl_3$): δ = 3.05 ppm (s, 1H, CH), 2.29 (s, 3H, CH_3), -8.43 (s, B-H→Os), -11.64 (s, B-H→Os), -17.28 (s, hydride, 1H), -17.84 (s, hydride, 1H), -22.57 (s, hydride, 1H). EI/MS m/z, 1834 (M^+ - 2H).

Synthesis of $Os_3(CO)_9(\mu\text{-}H)[(\mu_3\text{-}\eta^3\text{-}\mu_3\text{-}\eta^3\text{-}C_2B_{10}H_7S(CH_3)]Os_3(CO)_9(\mu\text{-}H)$, 3.3.

31.0 mg of compound **3.2** was heated to reflux in a nonane solution (150 ^oC) for 6.5 h. The solvent was then removed *in vacuo* and the products were isolated by TLC on silica by using hexane as the eluent. In order of elution 2.5 mg of **3.2** (unreacted), 2.0 mg of **3.3** (7%) and some uncharacterized products were obtained. Spectral data for **3.3**: IR (υ_{CO}, cm^{-1}, in hexane): 2104 (m), 2094 (s), 2075 (vs), 2060 (vs), 2035(w), 2030 (s), 2023 (vw), 2013 (m), 2008 (m), 1998 (vw), 1989 (w), 1978 (vw). ^{1}H NMR (^{11}B decoupled, in $CDCl_3$): δ = 2.44 ppm (s, 1H, CH), 2.29 (s, 3H, CH_3), -11.70 (s, B-H→Os), -12.98 (s, B-H→Os), -21.70 (s, hydride, 1H), -22.53 (s, hydride, 1H). EI/MS m/z, 1834 (M^+).

Synthesis of $Os_3(CO)_6)(\mu_3\text{-}\eta^3\text{-}C_2B_{10}H_9\text{-}R\text{-}SCH_3)(\mu_3\text{-}\eta^3\text{-}C_2B_{10}H_{10}\text{-}S\text{-}SCH_3)(\mu\text{-}H)_3$, 3.4.

14 µL (0.073 mmol) of closo-*o*-(1-SCH_3)$C_2B_{10}H_{11}$ was added to 32.0 mg (0.0315 mmol) of a solution of **3.1** in octane and the solution was heated to reflux for 3 h. The solvent was removed *in vacuo* and the product was isolated by TLC on silica by using a 5:1 hexane/methylene chloride solvent mixture. In order of elution, 27.8 mg (79 % yield) of $Os_3(CO)_6(\mu_3\text{-}\eta^3\text{-}C_2B_{10}H_9\text{-}R\text{-}SCH_3)(\mu_3\text{-}\eta^3\text{-}C_2B_{10}H_{10}\text{-}S\text{-}SCH_3)(\mu\text{-}H)_3$, **3.4**, 1.8 mg of unreacted **3.1**. Compound **3.4** could also be obtained albeit at a lower yield (28 %) by refluxing **3.1** with closo-*o*-(1-SCH_3)$C_2B_{10}H_{11}$ in nonane for 3.5 h. Spectral data for **3.4**: IR (υ_{CO}, cm^{-1}, in hexane): 2060 (w), 2050 (m), 2044 (vs), 1996 (m), 1986 (vs). ^{1}H NMR (in $CDCl_3$): δ = 3.00 ppm (s, 3H, CH_3), 3.03 (s, 3H, CH_3), 3.48 (s, 1H, CH), 3.61 (s, 1H,

CH), -6.40 (br, B-H→Os), -12.83 (s, hydride, 1H), -13.61 (s, hydride, 1H), -15.65 (s, hydride, 1H). EI/MS m/z, 1117 (M^+ - 2H).

Isomerization of 3.4 to 3.5.

33 mg (0.029 mmol) of a sample of pure **3.4** was heated to reflux in decane for 2.5 h. The solvent was then removed *in vacuo* and the product was isolated by TLC on alumina. This yielded 14.3 mg of yellow $Os_3(CO)_6(\mu_3\text{-}\eta^3\text{-}C_2B_{10}H_9\text{-}R\text{-}SCH_3)(\mu_3\text{-}\eta^3\text{-}C_2B_{10}H_{10}\text{-}R\text{-}SCH_3)(\mu\text{-}H)_3$, **3.5** (43%) and 2.2 mg of unconverted **3.4**. Spectral data for **3.5**: IR (υCO, cm^{-1}, in hexane): 2058 (w), 2047 (vw), 2045 (vs), 1995 (m), 1986 (vs). ^1H NMR (in $CDCl_3$): δ = 3.55 (s, 1H, CH), 3.48 (s, 1H, CH), 3.09 ppm (s, 3H, CH_3), 3.03 (s, 3H, CH_3), -6.42 (br, B-H→Os), -12.96 (s, hydride, 1H), -13.35 (s, hydride, 1H), -15.60 (s, hydride, 1H). EI/MS m/z, 1117 (M^+ - 2H).

Crystallographic Analyses

Yellow single crystals of **3.1**, **3.2** and **3.3** suitable for x-ray diffraction analyses were obtained by slow evaporation of solvent from a hexane/methylene chloride solvent mixture at room temperature. Crystals of **3.4** and **3.5** were also obtained by slow evaporation of solvent at room temperature from hexane/benzene mixtures. X-ray intensity data for of **3.1**, **3.2**, **3.4** and **3.5** were measured by using a Bruker SMART APEX CCD-based diffractometer using Mo K_α radiation (λ = 0.71073 Å).[11] X-ray intensity data from a yellow needle crystal of **3.3** were collected at 100(2) K by using a Bruker D8 QUEST diffractometer equipped with a PHOTON 100 CMOS area detector and an Incoatec microfocus source (Mo K_α radiation, λ = 0.71073 Å).[12] All structures were solved by a combination of direct methods and difference Fourier syntheses, and refined by full-matrix least-squares on F^2 by using the SHELXTL program library.[13]. All

non-hydrogen atoms were refined with anisotropic thermal parameters. Hydrogen atoms on the cages and methyl groups were placed in geometrically idealized positions and included as standard riding atoms during the least-squares refinements. Crystal data, data collection parameters and results of the analyses are summarized in Tables 3.1.and 3.2

Compounds **3.1**, **3.2, 3.4** and **3.5** crystallized in the monoclinic crystal system while compound **3.3** crystallized in the triclinic crystal system. The space group $P2_1/n$ was indicated by the systematic absences in the data for each of the compounds **3.1**, **3.2, 3.4** and **3.5** and subsequently confirmed by the successful solution and refinement of the structures. Compound **3.2** co-crystallized with a methylene chloride molecule (50% occupancy) which was satisfactorily refined without restraints. The bridging hydrido ligands were refined with Os – H distance constraints of 1.80 Å. The hydrogen atom H(5a) in **3.3** was located in a diff. Fourier map, but it could not be adequately refined and was included as a fixed contribution in the final cycles of refinement. Compound **3.5** co-crystallized with a molecule of hexane that was disordered in the solid state and was modeled with constrained C-C bond lengths and angles by using the DFIX and DANG commands.

3.3 Results and Discussion

Only one product $Os_3(CO)_9[(\mu_3\text{-}\eta^3\text{-}C_2B_{10}H_9(SCH_3)](\mu\text{-}H)_2$, **3.1**, (71 % yield) was obtained from the reaction of closo-*o*-$(1\text{-}SCH_3)C_2B_{10}H_{11}$ with $Os_3(CO)_{10}(NCMe)_2$ in a solution in toluene solvent when heated to reflux for 3h. Compound **3.1** was characterized by IR, ^{1}H NMR and ^{11}B NMR spectroscopy, mass spec and single-crystal X-ray diffraction analyses. An ORTEP diagram of the molecular structure **3.1** is shown in Figure 3.1. Compound **3.1** consists of a triangular cluster of three osmium atoms with a

triply bridging $C_2B_{10}H_9(SCH_3)$ ligand. The $C_2B_{10}H_9(SCH_3)$ ligand was formed by the oxidative addition of two B – H bond at the B(3) and B(4) atoms to the cluster. These boron atoms became coordinated to the metal atoms Os(3) and Os(1), respectively, Os(3) – B(3) = 2.175(11) Å and Os(1) – B(4) = 2.210(11) Å. The Os – B distances are very similar to those found for the triply-bridging ligand found in the complex $Os_3(CO)_9(\mu_3\text{-}\eta^3\text{-}C_2B_{10}H_{10})(\mu\text{-}H)_2$, 2.168(10) Å and 2.181(10) Å.[5] The hydrogen atoms were transferred to the metal atoms to become bridging hydrido ligands on the Os(1) - Os(2) and Os(1) – Os(3) bonds. They resonate at δ = -16.89 and -19.12 in the ^{1}H NMR spectrum. The ^{11}B and ^{11}B{^{1}H} NMR spectra of **3.1** (see Figure **B 1** and **B 2** in appendix B) reflect its C_1 symmetry of the complex and exhibit a set of partially overlapping signals from ten boron atoms in the range from -6.8 ppm to -14.8 ppm. The signals from two metalated boron atoms overlap with signals from B(H) atoms of the cage and cannot be distinguished. As expected, the hydride ligands cause a lengthening of the metal – metal bonds that they bridge, Os(1) – Os(2) = 3.0440(6) Å, Os(1) – Os(3) = 3.1037(6) Å in comparison to the nonhydride bridged bond, Os(2) – Os(3) = 2.8795(6) Å.[14] The $C_2B_{10}H_9(SCH_3)$ ligand is also coordinated to the cluster at Os(2) by the thioether sulfur atom S(1), Os(2) – S(1) = 2.401(3) Å.

When compound **3.1** was allowed to react with a second equivalent of $Os_3(CO)_{10}(NCMe)_2$ in a solution in toluene solvent at reflux for 8 h, the compound $Os_3(CO)_9(\mu\text{-}H)[(\mu_3\text{-}\eta^3\text{-}1,4,5\text{-}\mu_3\text{-}\eta^3\text{-}6,10,11\text{-}C_2B_{10}H_8S(CH_3)]Os_3(CO)_9(\mu\text{-}H)_2$, **3.2**, was obtained in 39 % yield. Compound **3.2** was characterized by IR, ^{1}H NMR spectroscopy, mass spec and single-crystal X-ray diffraction analyses. An ORTEP diagram of the molecular structure **3.2** is shown in Figure 3.2. Compound **3.2** contains two individual

Os_3 clusters attached to a $C_2B_{10}H_8S(CH_3)$ ligand. The sulfur atom of the thiolate group is bonded to Os(2), Os(2) – S(1) = 2.450(3) Å. Assuming that the thioether-coordinated osmium atom is the same one as found in **3.1**, then the cluster labeled Os(1), Os(2), Os(3) in Figure 3.2 is the same one that was coordinated to the carborane in **3.1**. This cluster was repositioned slightly because in **3.1** it was coordinated to the atoms B(3) and B(4) and in **3.2** it is coordinated to B(4) and B(5) and the latter contains a hydrogen atom, see below. The cluster Os(4), Os(5), Os(6) must then be the one that was added to **3.1** in the formation of **3.2**. Most importantly, the C_2B_{10} cage in **3.2** was opened by cleavage of the B(6) – C(1), B(6) – C(2) and the B(5) – B(6) bonds of the closed $C_2B_{10}H_9$ cage in **3.1**. The ^{1}H NMR spectrum shows three high-field resonances at δ = -17.28 (1H), -17.84 (1H), -22.57 (1H) that are attributed to hydrido ligands bridging Os - Os bonds. They were located and partially refined in the structural analysis and they bridge the Os(1) – Os(3), Os(2) – Os(3) and Os(5) – Os(6) bonds, 3.0520(6) Å, 3.0297(6) Å, 3.0002(6) Å, respectively, which are elongated.[14] Three boron atoms, B(4), B(10) and B(11), have no hydrogen atoms and are bonded directly to osmium atoms, Os(3), Os(5), Os(6): Os(3) – B(4) = 2.196(11) Å, Os(5) – B(11) = 2.319(10) Å and Os(6) – B(10) = 2.358(11) Å. Atom B(5) contains a hydrogen atom B(5) – H(5a) = 1.28(7) Å and forms an agostic B – H interaction with Os(1), Os(1) – H(5a) = 1.82(7) Å, Os(1) – B(5) = 2.615(10) Å. Agostic B – H groups such as these have been observed previously, and they exhibit characteristically longer M–B distances.[5,15] Atom B(6) is bonded to three osmium atoms, Os(4), Os(5), Os(6): Os(4) – B(6) = 2.144(10) Å, Os(5) – B(6) = 2.191(11) Å, Os(6) – B(6) = 2.173(10) Å but it still contains its hydrogen atom B(6) – H(6a) = 1.17(2) Å that forms an agostic-like bridge to the metal atom Os(4), Os(4) – H(6a) = 1.70(2) Å. The

exo-cage B – B bonds to B(6), B(6) – B(10) = 1.659(15) Å and B(6) – B(11) = 1.675(14) Å are significantly shorter than the B – B bonds in the cage, e.g. B(10) – B(11) = 1.791(16) Å, but they are significantly longer that the C – C bond in the cage, C(1) – C(2) = 1.545(13) Å. As expected, both of the agostic B – H groups have characteristically high-field resonance shifts, δ = -8.43 (s, B-H→Os), -11.64 (s, B-H→Os), that are also broad due to partial coupling to their attached boron atom.[16]

When compound **3.2** was heated to reflux in nonane solvent (150 ^{o}C), the new compound $Os_3(CO)_9(\mu\text{-}H)[(\mu_3\text{-}\eta^3\text{-}\mu_3\text{-}\eta^3\text{-}C_2B_{10}H_7S(CH_3)]Os_3(CO)_9(\mu\text{-}H)$, **3.3** was obtained in 7% yield. Compound **3.3** was characterized by IR, ^{1}H NMR spectroscopy, mass spec and single-crystal X-ray diffraction analyses. An ORTEP diagram of the molecular structure **3.3** is shown in Figure 3.3. Compound **3.3** contains two individual Os_3 clusters attached to a $C_2B_{10}H_7S(CH_3)$ ligand. The sulfur atom of the thiolate group is not coordinated to a metal atom in **3.3**. The Os(1), Os(2), Os(3) cluster is bonded to three boron atoms B(4), B(5) and B(9). Atom B(5) has been pulled out of the carborane cage by cleaving the C(1) – B(5) and the the B(5) – B(10) bonds of the cage in **3.2**, and the B(5) - H(5a) group bridges all three metal atoms, Os(1) – B(5) = 2.153(10) Å, Os(2) – B(5) = 2.211(11) Å and Os(3) – B(5) = 2.181(11) Å, but B(5) remains attached to the cage through bonds to B(4) and B(9), B(4) – B(5) = 1.813(14) Å and B(5) – B(9) = 1.677(15) Å. The hydrogen atom on B(5) forms an agostic bridge to Os(1), Os(1) – H(5a) = 2.20 Å. B(4) and B(9) are also bonded to Os(2) and Os(3), respectively, Os(2) – B(4) = 2.300(13) Å and Os(3) – B(9) = 2.312(11) Å. As it was in **3.2**, the Os(4), Os(5), Os(6) cluster is bonded to the boron atoms B(6), B(10) and B(11) and the B(6) – H(6a) group, B(6) – H(6a) = 1.31(7) Å, is a triply-bridging, agostic group: Os(4) – B(6) = 2.154(12) Å, Os(5)

– B(6) = 2.221(12) Å, Os(6) – B(6) = 2.207(12) Å, Os(4) – H(6A) = 1.87(7) Å, Os(5) – B(11) = 2.302(13) Å, Os(6) – B(6) = 2.207(12) Å, Os(6) – B(10) = 2.308(12) Å. Compound **3.3** contains two hydrido ligands, one on each of the osmium clusters. H(1) bridges the Os(2) – Os(3) bond (2.9512(6) Å) and H(5) bridges the Os(5) – Os(6) bond (2.9856(6) Å) and they resonate in the ^{1}H NMR spectrum at δ = -21.70 and -22.53. The H atoms of agostically, coordinated triply bridging BH groups resonate at δ = -11.70 and -12.98. Overall, compound **3.2** loses one equivalent of H_2 in its conversion of **3.3**. The opened carborane cage in **3.3** is similar to that of the compound $Os_3(CO)_9(\mu\text{-}H)(\mu_3\text{-}3,4,8\text{-}\mu_3\text{-}7,11,12\text{-}C_2B_{10}H_8)Os_3(CO)_9(\mu\text{-}H)$ represented as structure **2.3** shown in Scheme 3.1.

When compound **3.1** was allowed to react with an additional quantity of closo-*o*-(1-SCH_3)$C_2B_{10}H_{11}$ in octane solvent at reflux, the compound $Os_3(CO)_6)(\mu_3\text{-}\eta^3\text{-}C_2B_{10}H_9$-*R*-$SCH_3$) ($\mu_3\text{-}\eta^3\text{-}C_2B_{10}H_{10}$-*S*-$SCH_3)(\mu\text{-}H)_3$, **3.4** was obtained in 79% yield. Compound **3.4** was characterized by IR, ^{1}H NMR spectroscopy, mass spec and single-crystal X-ray diffraction analyses. An ORTEP diagram of the molecular structure **3.4** is shown in Figure 3.4. Compound **3.4** contains two closo-carborane ligands, one on each side of a triangular Os_3 cluster. The carborane labeled S(1) – C(1a) ··· B(12a) is coordinated to the metal atoms in the same manner as that in **3.1** and is therefore believed to be the one that was carried over from **3.1** to **3.4**, Os(2) – S(1) = 2.4361(12) Å Os(2) – B(3b) =2.105(6) Å, Os(3) – B(3a) = 2.122(6) Å. Thus, the carborane labeled S(2) – C(1b) ··· B(12b) is believed to be the one that was added to **3.1**, Os(1) – S(2) = 2.4523(13) Å. One B – H bond was cleaved in this ligand at B(3b), and the boron atom is bonded to Os(2), Os(2) – B(3b) = 2.105(6) Å. The hydrogen atom was transferred to the Os_3 cluster, see below. One B – H bond is agostically-coordinated to an osmium, Os**(**3) – B(4b) = 2.800(6) Å,

Os(3) – H(4b) = 1.94(4) Å, B(4b) – H(4b) = 1.21(4) Å and the BH resonance of this group is shifted upfield as expected, δ = -6.40 (br, B-H→Os). There are three bridging metal hydride ligands, one on each Os – Os bond, Os(1) – Os(2) = 3.1271(3) Å, Os(1) – Os(3) = 3.0525(3) Å, Os(2) – Os(3) = 3.0167(3) Å,[14] and δ = -12.83 (s, 1H), -13.61 (s, 1H), -15.65 (s, 1H). The stereochemistry of the sulfur atoms shown in Figure 3.4 is *R*- for S(1) and *S*- for S(2), but the crystal is a racemic mixture so the enantiomer with the sulfur stereochemistries, *S*- for S(1) and *R*- for S(2) is present in an equimolar amount.

When a solution of **3.4** was heated to reflux in decane solvent (174 ^{o}C), it was converted to an isomer $Os_3(CO)_6(\mu_3\text{-}\eta^3\text{-}C_2B_{10}H_9\text{-}R\text{-}SCH_3)(\mu_3\text{-}\eta^3\text{-}C_2B_{10}H_{10}\text{-}R\text{-}SCH_3)(\mu\text{-}H)_3$, **3.5** in 43% yield. Compound **3.5** was characterized by single-crystal X-ray diffraction analyses. An ORTEP diagram of the molecular structure **3.5** is shown in Figure 3.5. Like **3.4**, compound **3.5** contains two closo-carborane ligands, one on each side of a triangular Os_3 cluster. There is one agostic B- H group, Os(3) – B(4b) = 2.783(8) Å, Os(3) – H(4b) = 1.87(4) Å, δ = -6.42 (br, 1H) and three bridging hydrido ligands, one each Os – Os bond, δ = -12.96 (1H), -13.35 (1H), -15.60 (1H). The only significant difference between **3.4** and **3.5** is the relative chirality of the sulfur atoms. In **3.5**, S(1) and S(2) both have an *R*-chirality, while in **3.4**, they have opposite chiralities, i.e. one of the sulfur atoms S(2) has inverted its configuration in the transformation of **3.4** to **3.5**. Note: the crystal of **3.5** is also a racemic mixture, so the enantiomer with *S*-, *S*-chirality is also present in the crystal of **3.5**. The inversion of configuration of thioether sulfur atoms has been observed in thioether ligands previously and generally occurs under milder conditions than those observed for the **3.4** – **3.5** conversion reported here.[17]

3.4 Summary

In recent studies, we have shown that the reaction of $Os_3(CO)_{10}(NCMe)_2$ with *o*-$C_2B_{10}H_{12}$ leads to the addition of one and two triosmium carbonyl cluster complexes to the surface of the carborane cage by activation of selected B-H bonds. In the presence of two Os_3 clusters, the carborane cage can be opened by thermal treatment with the formation of two triply-bridging BH groups, one on each Os_3 cluster, at the cage opening site, see Scheme 1.[5] In that reaction two of the BH groups were pulled from the *closo*-structure to give the opened cage **C** by cleavage of five bonds in the cage.

The reaction of $Os_3(CO)_{10}(NCMe)_2$ with closo-*o*-(1-SCH_3)$C_2B_{10}H_{11}$ also proceeds first by the addition of one triosmium cluster to the carborane to yield the compound **3.1**, but a second cluster can subsequently be added to **3.1** to give the compound **3.2** in a good yield. The cluster additions are facilitated by the formation of Os – S bonds to the SMe group on the carborane,[18] but the cleavage of B – H bonds is also important by forming additional attachments of the carborane to the other metal atoms in the cluster. The second cluster adds to the triangular group of three boron atoms, B(6), B(10) and B(11), see Scheme 3.2.

Upon addition of the second cluster to **3.1**, the carborane is opened at the B(6) cage atom by the cleavage of three bonds, two B - C bonds, B(6) – C(1) and B(6) – C(2) to its neighboring carbon atoms, and one B – B bond, B(6) – B(6). Atom B(6) with its hydrogen atom H(6a) became a triply bridging group on the added Os_3 cluster Os(4), Os(5), Os(6), but B(6) remains attached to cage by bonds to two boron atoms, B(10) and B(11). In the process, the original Os(1), Os(2), Os(3) cluster is shifted from the B3 B4 edge of the carborane to the B4 B5 edge and a hydrogen atom is, probably from the Os_3

cluster, shifted to B3. Atom B(6) is symmetry equivalent to B(3) in the free carborane molecule. Computational studies of *o*-$C_2B_{10}H_{12}$ have shown that the atoms B(3) and B(6) are electron deficient in comparison to the other boron atoms in the cage.[19] If B(3) and B(6) are also electron deficient in closo-*o*-(1-SCH_3)$C_2B_{10}H_{11}$, and if this results in weaker bonds to the atoms B(3)/B(6), this could explain why the cage is opened at B(6) and B(3) in the reactions described here and elsewhere.[5]

When **3.2** was heated to reflux in nonane solvent (150 ^oC), two hydrogen atoms were eliminated, presumably as H_2, and it was converted into the new compound **3.3** by a rearrangement that resulted in further opening of the carborane cage by the cleavage of two of the cage bonds to boron B(5), B(5) – C(1) and B(5) – B(10), see Scheme 3.3. The sulfur atom is released from Os(2) and the Os(1), Os(2), Os(3) cluster shifts off the B(4), B(5), B(9) triangle, Os(2) to B(4) and Os(3) to B(9).

We expect that the opening of the cage in the transformation of **2.3** to **2.4** shown in Scheme 3.1[5] probably also occurs by a similar two-step process, but this was not observed in that study.

A second carborane cage was added to **3.1** to yield the compound **3.4**. Compound **3.4** was isomerized to **3.5** by heating to high temperature, but this isomerization involved only an inversion of configuration at the sulfur atom.

Clearly, the coordination of metal clusters to the surface of carborane cage compounds leads to weakening of the bonds among the atoms in the cage to the extent that cages begin to rupture. These cage rupture reactions should open the door to new chemistry at the bond rupture sites. Opening of the carborane cages should make it easier to functionalize the cage atoms at the rupture sites. It may be possible to fuse the metal

clusters on the surface of the ruptured carboranes by inducing decarbonylations at higher temperatures. It may be possible to add even more than two trimetallic clusters to a single carborane cage. Carborane cages of different sizes may undergo cage opening more readily than the highly stable icosahedral carboranes that we have studied.[4]

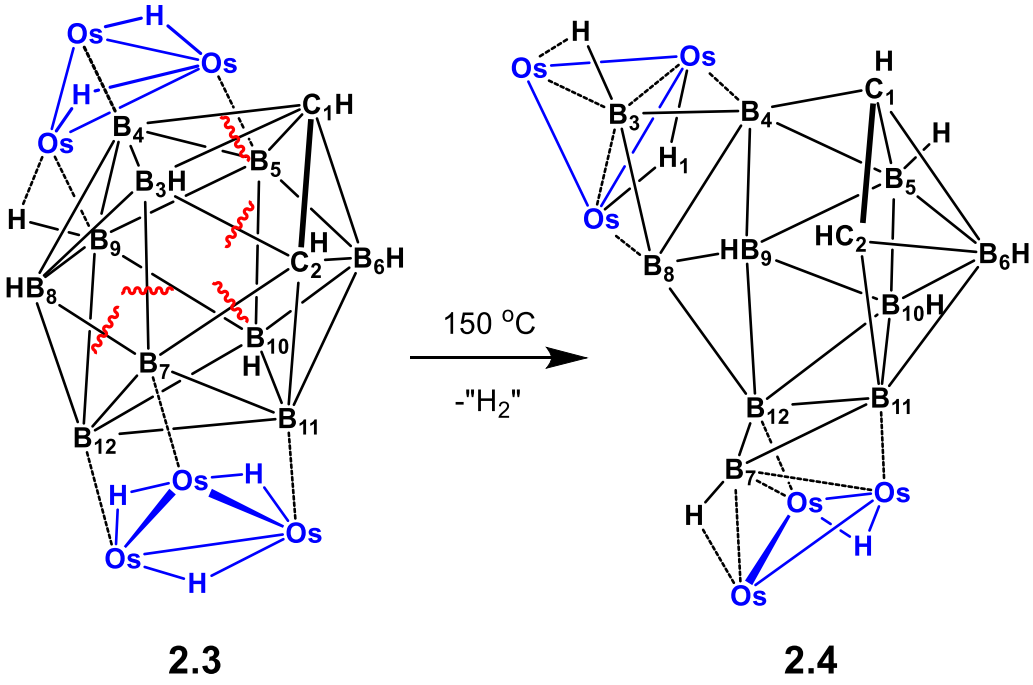

Scheme 3.1. A schematic of the transformation of $Os_3(CO)_9(\mu\text{-}H)_2(\mu_3\text{-}4,5,9\text{-}\mu_3\text{-}7,11,12\text{-}C_2B_{10}H_7)Os_3(CO)_9(\mu\text{-}H)_3$, **2.3** into $Os_3(CO)_9(\mu\text{-}H)(\mu_3\text{-}3,4,8\text{-}\mu_3\text{-}7,11,12\text{-}C_2B_{10}H_8)Os_3(CO)_9(\mu\text{-}H)$, **2.4**. Red lines indicate bonds in the carborane cage of **2.3** that are cleaved.

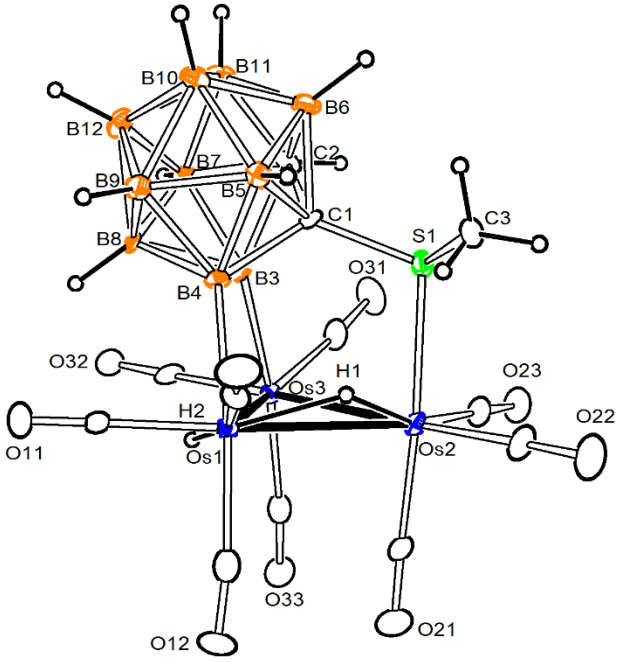

Figure 3.1. An ORTEP diagram of the molecular structure of $Os_3(CO)_9[\mu_3\text{-}\eta^3\text{-}C_2B_{10}H_9(SCH_3)](\mu\text{-}H)_2$, **3.1**, showing 40% thermal ellipsoid probability. Selected interatomic bond distances (Å) are as follow: Os(1) – Os(2) = 3.0440(6), Os(1) – Os(3) = 3.1037(6), Os(2) – Os(3) = 2.8795(6), Os(1) – B(4) = 2.210(11), Os(3) – B(3) = 2.175(11), Os(2) – S(1) = 2.401(3), S(1) – C(1) = 1.801(10), C(1) – C(2) = 1.653(13).

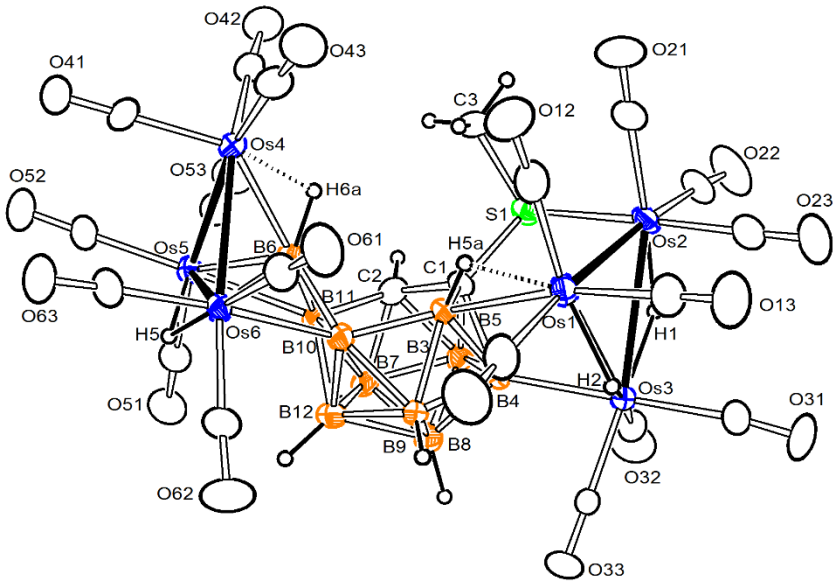

Figure 3.2. An ORTEP diagram of the molecular structure of $Os_3(CO)_9(\mu\text{-}H)[(\mu_3\text{-}\eta^3\text{-}1,4,5\text{-}\mu_3\text{-}\eta^3\text{-}6,10,11\text{-}C_2B_{10}H_8S(CH_3)]Os_3(CO)_9(\mu\text{-}H)_2$, **3.2** showing 25% thermal ellipsoid probability. Selected interatomic bond distances (Å) are as follow: Os(1) – Os(2) = 2.8794(5), Os(1) – Os(3) = 3.0520(6), Os(2) – Os(3) = 3.0297(6), Os(4) – Os(5) = 2.8629(5), Os(4) – Os(6) = 2.8717(5), Os(5) – Os(6) = 3.0002(6), Os(2) – S(1) = 2.450(3), Os(1) – B(5) = 2.615(10), Os(3) – B(4) = 2.196(11), Os(4) – B(6) = 2.144(10), Os(5) – B(6) = 2.191(11), Os(6) – B(6) = 2.173(10), Os(5) – B(11) = 2.319(10), Os(6) – B(10) = 2.358(11), B(6) – H(6a) = 1.17(2), B(5) – H(5a) =1.28(7), B(6) – B(10) = 1.659(15), B(6) – B(11) = 1.675(14), B(10) – B(11) = 1.791(16) S(1) – C(1) = 1.80(2), C(1) – C(2) = 1.545(13).

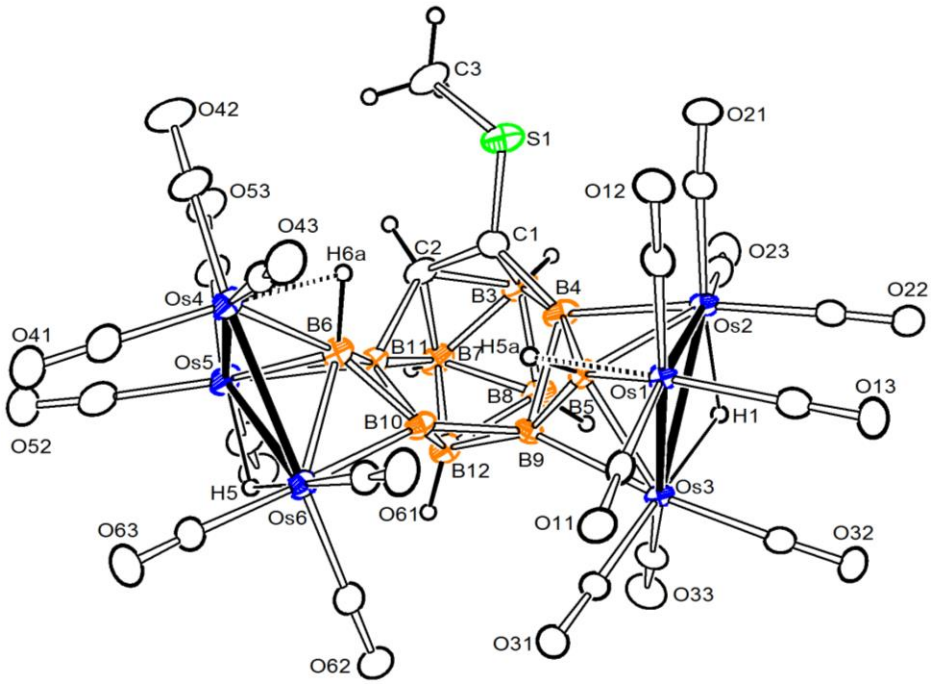

Figure 3.3. An ORTEP diagram of the molecular structure of $Os_3(CO)_9(\mu{-}H)[(\mu_3{-}\eta^3{-}\mu_3{-}\eta^3{-}C_2B_{10}H_7S(CH_3)]Os_3(CO)_9(\mu\text{-}H)$, **3.3** showing 25% thermal ellipsoid probability. Selected interatomic bond distances (Å) are as follow: Os(1) – Os(2) = 2.8516(5), Os(1) – Os(3) = 2.8517(5), Os(2) – Os(3) = 2.9512(6), Os(4) – Os(5) = 2.8429(6), Os(4) – Os(6) = 2.8519(6), Os(5) – Os(6) = 2.9856(6), Os(3) – B(9) = 212(11), Os(1) – B(5) = 2.153(10), Os(2) – B(4) = 2.300(13), Os(2) – B(5) =2.211(11), Os(3) – B(5) = 2.181(11), Os(3) – B(9) = 2.312(11), Os(4) – B(6) = 2.154(12), Os(5) – B(6) = 2.221(12), Os(6) – B(6) = 2.207(12), Os(5) – B(11) = 2.302(13), Os(6) – B(6) = 2.207(12), Os(6) – B(10) = 2.308(12), Os(1) – H(5a) = 2.20, Os(4) – H(6A) = 1.87(7), B(6) – H(6a) = 1.31(7), B(4) – B(5) = 1.813(14); B(4) – B(9) = 1.898(16), B(5) – B(9) = 1.677(15), B(6) – B(11) = 1.677(16), B(6) – B(10) = 1.690(17), B(10) – B(11) = 1.738(15), S(1) – C(1) = 1.745(11), C(1) – C(2) = 1.460(15).

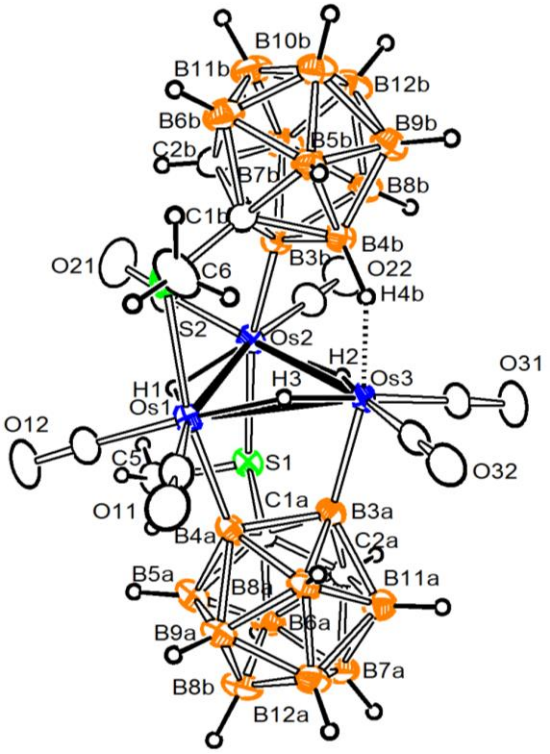

Figure 3.4. An ORTEP diagram of the molecular structure of $Os_3(CO)_6(\mu_3\text{-}\eta^3\text{-}C_2B_{10}H_9\text{-}R\text{-}SCH_3)$ $(\mu_3\text{-}\eta^3\text{-}C_2B_{10}H_{10}\text{-}S\text{-}SCH_3)(\mu\text{-}H)_3$, **3.4** showing 25% thermal ellipsoid probability. Selected interatomic bond distances (Å) are as follow: Os(1) – Os(2) = 3.1271(3), Os(1) – Os(3) = 3.0525(3), Os(2) – Os(3) = 3.0167(3), Os(1) – S(2) = 2.4523(13), Os(2) – S(1) = 2.4361(12), Os(2) – B(3b) =2.105(6), Os(3) – B(3a) = 2.122(6), Os(1) – B(4a) =2.168(6), Os(3) – B(4b) = 2.800(6), Os(3) – H(4b) = 1.94(4), B(4b) – H(4b) = 1.21(4).

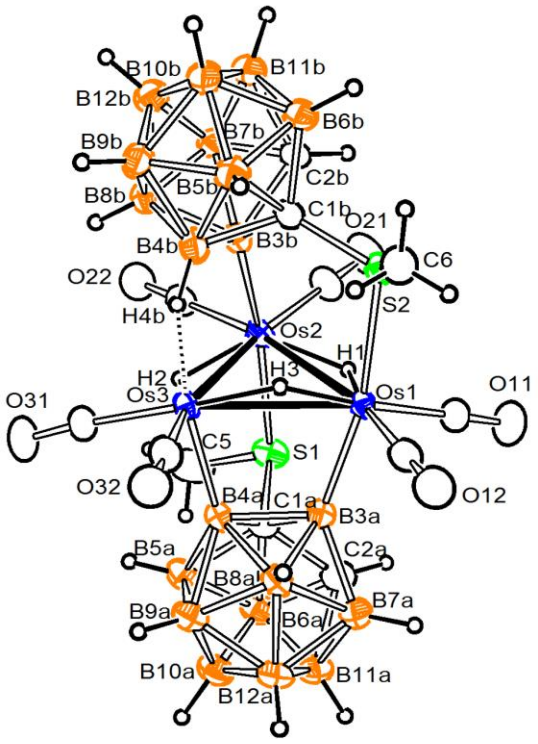

Figure 3.5. An ORTEP diagram of the molecular structure of $Os_3(CO)_6(\mu_3\text{-}\eta^3\text{-}C_2B_{10}H_9\text{-}R\text{-}SCH_3)(\mu_3\text{-}\eta^3\text{-}C_2B_{10}H_{10}\text{-}R\text{-}SCH_3)(\mu\text{-}H)_3$, **3.5** showing 25% thermal ellipsoid probability. Selected interatomic bond distances (Å) are as follow: Os(1) – Os(2) = 3.0918(5), Os(1) – Os(3) = 3.0524(4), Os(2) – Os(3) = 3.0659(5), Os(1) – S(2) = 2.4599(15), Os(2) – S(1) = 2.4370(17), Os(2) – B(3b) = 2.126(7), Os(3) – B(4a) = 2.142(7), Os(1) – B(3a) = 2.138(7), Os(3) – B(4b) = 2.783(8), Os(3) – H(4b) = 1.87(4).

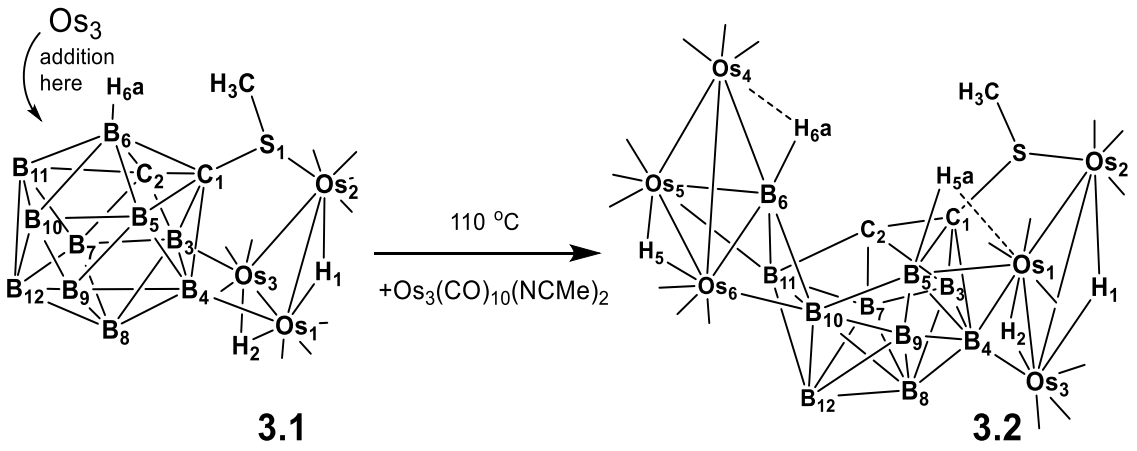

Scheme 3.2. A schematic of the addition of a second Os_3 cluster to **3.1** and the opening of the carborane cage.

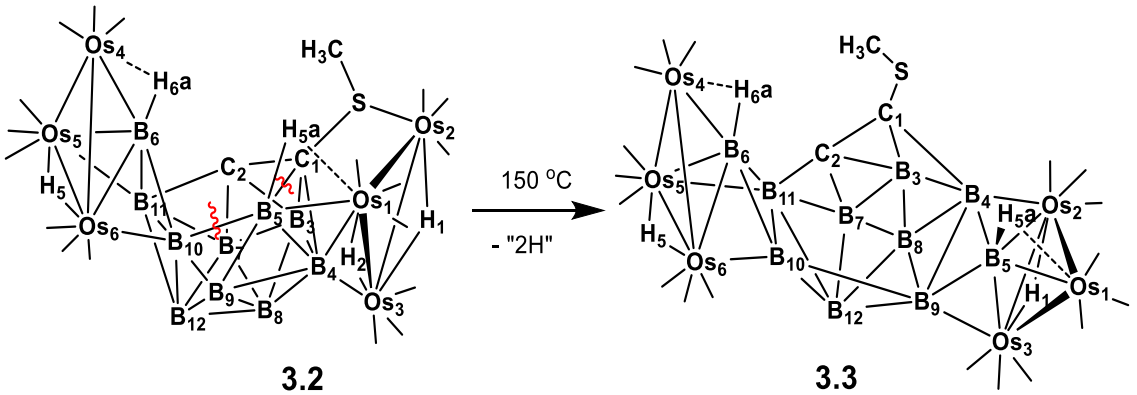

Scheme 3.3. A schematic of the opening of the carborane cage in going from **3.2** to **3.3**. Red lines indicate the bonds that are cleaved in **3.2**.

Table 3.1. Crystallographic Data for Compounds **3.1**, **3.2** and **3.3**

Compound	**3.1**	**3.2**	**3.3**
Empirical formula	$Os_3SO_9C_{12}B_{10}H_{14}$	$Os_6SO_{18}C_{21}B_{10}H_{13}0.5CH_2Cl_2$	$Os_6SO_{18}C_{21}B_{10}H_{12}$
Formula weight	1012.99	1877.14	1833.67
Crystal system	Monoclinic	Monoclinic	Triclinic
Lattice parameters			
a (Å)	9.1412(11)	17.2821(13)	9.5168(7)
b (Å)	18.055(2)	9.6253(7)	11.8739(10)
c (Å)	14.5660(17)	26.284(2)	17.8436(14)
α (deg)	90.00	90.00	77.450(2)
β (deg)	91.265(2)	102.942(2)	77.567(2)
γ (deg)	90.00	90.00	87.628(2)
V (Å3)	2403.4(5)	4261.1(6)	1922.0(3)
Space group	$P2_1/n$	$P2_1/n$	P-1
Z value	4	4	2
ρcalc (g/cm3)	2.800	2.928	3.168
μ (Mo Kα) (mm−1)	15.950	17.997	19.879
Temperature (K)	100(2)	294(2)	100(2)
2Θmax (°)	56.52	56.62	54.26
No. Obs. (I > 2σ(I))	4361	10587	8445
No. Parameters	329	558	522
Goodness of fit (GOF)	1.037	1.027	1.053
Max. shift in cycle	0.001	0.022	0.001
Residuals*: R1; wR2	0.0327; 0.0812	0.0473; 0.1224	0.0332; 0.0681
Absorption Correction, Max/min	Multi-scan 1.00/0.373	Multi-scan 1.00/0.316	Semi-empirical from equivalents 0.1506/0.0844
Largest peak in Final Diff. Map ($e^-/Å^3$)	2.660	2.737	2.682

*$R1 = \Sigma_{hkl}(\,|\,|F_{obs}|-|F_{calc}|\,|)/\Sigma_{hkl}|F_{obs}|$; $wR2 = [\Sigma_{hkl}w(|F_{obs}|-|F_{calc}|)^2/\Sigma_{hkl}wF^2_{obs}]^{1/2}$; $w = 1/\sigma^2(F_{obs})$; $GOF = [\Sigma_{hkl}w(|F_{obs}|-|F_{calc}|)^2/(n_{data}-n_{vari})]^{1/2}$.

Table 3.2. Crystallographic Data for Compounds **3.4** and **3.5**

Compound	**3.4**	**3.5**
Empirical formula	$Os_3S_2O_6C_{12}B_{20}H_{28}$	$Os_3S_2O_6C_{18}B_{20}H_{42}$
Formula weight	1119.26	1205.44
Crystal system	Monoclinic	Monoclinic
Lattice parameters		
a (Å)	14.4603(12)	12.2286(19)
b (Å)	15.4906(13)	12.0151(19)
c (Å)	16.0060(14)	28.330(4)
α (deg)	90.00	90.00
β (deg)	115.583(2)	97.590(3)
γ (deg)	90.00	90.00
V (Å3)	3233.8(5)	4126.0(11)
Space group	$P2_1/n$	$P2_1/n$
Z value	4	4
ρcalc (g/cm3)	2.299	1.941
μ (Mo Kα) (mm−1)	11.917	9.348
Temperature (K)	294(2)	294(2)
2Θmax (°)	56.68	56.22
No. Obs. (I > 2σ(I))	8057	10207
No. Parameters	414	423
Goodness of fit (GOF)	1.046	1.026
Max. shift in cycle	0.001	0.016
Residuals*: R1; wR2	0.0262; 0.0617	0.0353; 0.0918
Absorption Correction,	Multi-scan	Multi-scan
Max/min	1.00/0.563	1.00/0.481
Largest peak in Final Diff. Map ($e^-/Å^3$)	1.609	2.182

*$R1 = \Sigma_{hkl}(\,|\,|F_{obs}|-|F_{calc}|\,|)/\Sigma_{hkl}|F_{obs}|$; $wR2 = [\Sigma_{hkl}w(|F_{obs}|-|F_{calc}|)^2/\Sigma_{hkl}wF^2_{obs}]^{1/2}$; $w = 1/\sigma^2(F_{obs})$; $GOF = [\Sigma_{hkl}w(|F_{obs}|-|F_{calc}|)^2/(n_{data} - n_{vari})]^{1/2}$.

3.5 References

1. Mingos, D. M. P.; Wales, D. J., *Introduction to Cluster Chemistry*, Prentice Hall, Engelwood Cliffs, N. J., 1990.
2. (a) Grimes R. N., *Carboranes*, 2nd Edition, Elsevier, Amsterdam, 2011. (b) Grimes, R. N. *Dalton Trans.* **2015**, *44*, 5939 – 5956. (c) Grimes R. N., *Carboranes*, 2nd Edition, Elsevier, Amsterdam, 2011, section 15.4, pp 1039 – 1044.
3. (a) Wong, Y. O.; Smith, M. D.; Peryshkov, D. V. *Chem.-Eur. J.* **2016**, *22*, 6764-6767. (b) Willans, C. E.; Kilner, C. A.; Fox, M. A. *Chem. Eur. J.* **2010**, *16*, 10644 – 10648. (c) Davidson, M. G.; Fox, M. A.; Hibbert, T. G.; Howard, J. A. K.; Mackinnon, A.; Neretin, I. S.; Wade, K. *Chem. Commun.* **1999**, 1649 – 1650. (d) Wiesboeck, R. A.; Hawthorne, M. F. *J. Am. Chem. Soc.* **1964**, *86*, 1642–1643. (e) Dunks, G. B.; Wiersema, R. J. Hawthorne, M. F. *J. Am. Chem. Soc.* **1973**, *95*, 3174–3179. (f) Tomita, H.; Luu, H.; Onak, T. *Inorg Chem.* **1991**, *30*, 812–815. (g) Zheng, F.; Xie, Z. *Dalton Trans.* **2012**, *41*, 12907 – 12914.
4. Du, S.; Hodson, B. E.; Lei, P. McGrath, T. D.; Stone, F. G. A. *Inorg. Chem.* **2007**, *46*, 6613 – 6620.
5. Adams, R. D.; Kiprotich, J.; Peryshkov, D. V.; Wong, Y. O. *Chem. Eur. J.* **2016**, *22*, 6501 – 6504.
6. Timofeev, S. V.; Zakharova, M. V.; Mosolova, E. M.; Godovikov, I. A.; Ananyev, I. V.; Sivaev, I. B.; Bregadze, V. I. *J. Organomet. Chem.* **2012**, *721–722*, 92.
7. Braga, D.; Grepioni, F.; Parisini, E.; Johnson, B. F. G.; Martin, C. M.; Nairn, J. G. M.; Lewis, J.; Martinelli, M. *J. Chem. Soc. Dalton Trans.* **1993**, 1891- 1895.
8. Ho, W. G.-Y.; Wong W.-T., *Polyhedron* **1005**, *14*, 2848 – 2855.

9. Goudsmit, R. J.; Johnson, B. F. G.; Lewis, J.; Raithby, P. R.; Rosales, M. J. *J. Chem. Soc. Dalton Trans.* **1983**, 2257 - 2261.
10. Lewis, J., Johnson, B. F. G., *Pure Appl. Chem*. **1975**, *44*, 43 - 79.
11. SAINT^{+}, Version 6.2a, Bruker Analytical X-ray Systems, Inc., Madison, WI (2001)
12. APEX2 Version 2014.9-0, SAINT Version 8.34A and SADABS Version 2014/4. Bruker Analytical X-ray Systems, Inc., Madison, Wisconsin, USA, 2014.
13. G.M. Sheldrick, SHELXTL, Version 6.1, Bruker Analytical X-ray Systems, Inc., Madison, WI (1997).
14. (a) Bau, R.; Drabnis, M. H., *Inorg. Chim. Acta* **1997**, *259*, 27 - 50. (b) Teller, R. G.; Bau, R., *Struct. Bonding*, Berlin, Ger.**1981**, *41*, 1 - 82.
15. Chung, J.-H.; Boyd, E. P.; Liu, J.; Shore, S. G., *Inorg. Chem.* **1997**, *36*, 4778 - 4781. b) Chung, J.-H.; Knoeppel, D.; McCarthy, D.; Columbie, A.; Shore, S. G., *Inorg. Chem.*, **1993**, *32*, 3391–3392. (c) Jan, D.-Y.; Shore, S. G., *Organometallics* **1987**, *6*, 428 - 430.
16. a) Brew, S. A.; Stone, F. G. A., *Adv. Organomet. Chem*. **1993**, *35*, 135–186. b) Lebedev, V. N.; Mullica, D. F.; Sappenfield, E. L.; Stone, F. G. A., *J. Organomet. Chem*. **1997**, *536-537*, 536–539. c) Ellis, D. D.; Franken, A.; Stone, F. G. A., *Organometallics* **1999**, *18*, 2362–2369.
17. (a) Wu, H.; Lucas, C. R., *Inorg. Chem.* **1992**, *31*, 2354 - 2358. (b) Abel, E. W.; Booth, M.; Orrell, K. G. *J. Chem Soc., Dalton Trans.* **1979**, 1994 - 2002**.**
18. (a) Fey, N.; Haddow, M. F.; Mistry, R.; Norman, N. C.; Orpen, A. G.; Reynolds, T. J.; Pringle, P. G. *Organometallics* **2012**, *31*, 2907 – 2913. (b) Yao, Z.-J.; Yu, W.-B.; Lin, Y.-J.; Huang, S.-L.; Li, Z.-H.; Jin, G.-X. *J. Am. Chem. Soc.* **2014**, *136*, 2825 –

2832. (c) Estrada, J.; Lee, S. E.; McArthur, S. G.; El-Hellani, A.; Tham, F. S.; Lavallo, V. *J. Organomet. Chem.* **2015**, *798*, 214 – 217. (d) Spokoyny, A.; Saleh, L.; Dziedzic, R.; Khan, S. *Chem.–Eur. J.* **2016**, DOI: 10.1002/chem.201601292.

19. (a) Teixidor, F.; Barbera, G.; Vaca, A.; Kivakäs, R.; Sillanpää, R.; Oliva, J.; Viñas, C., *J. Am. Chem. Soc.* **2005**, *127*, 10158 – 10159. (b) Hermansson, K.; Wojik, M.; Sjöberg, S. *Inorg. Chem.*, **1999**, *38*, 6039 – 6048

CHAPTER 4

Coordination Chemistry of Thioether-Carboranes in Polynuclear Metal Carbonyl Cluster Complexes. B-H Activation of Thioether-Carboranes by Dirhenium Carbonyl Complexes[3]

[3]Adams R. D., Kiprotich J, *J. Organomet. Chem.*, **2017**, XX, 1-6. Accepted
Reprinted here with permission of publisher

4.1 Introduction

Polyhedral carborane cage compounds have now been studied extensively for over 50 years.[1] In recent years, transition metal carborane complexes and metallacarboranes have attracted considerable interest.[2] The addition of heteroatomic groupings to the carbon atoms in the carborane cage has provided new opportunities for studies of their coordination chemistry and associated reactivity.[3] We have recently found that triosmium carbonyl cluster complexes can be added to the surface of closo-*o*-$C_2B_{10}H_{12}$[4] and closo-*o*-(1-SCH_3)$C_2B_{10}H_{11}$,[5] and when two triosmium clusters are added to the surface of the same cage, some of the B – C and B – B bonds in the cage can be cleaved leading to opening of the cages. For example, the addition of an Os_3 cluster to the complex $Os_3(CO)_9[\mu_3\text{-}\eta^3\text{-}C_2B_{10}H_9(SCH_3)](\mu\text{-}H)_2$, **3.1** which leads to an opening of cage resulting in the product $Os_3(CO)_9(\mu\text{-}H)[(\mu_3\text{-}\eta^3\text{-}1,4,5\text{-}\mu_3\text{-}\eta^3\text{-}6,10,11\text{-}C_2B_{10}H_8S(CH_3)]Os_3(CO)_9(\mu\text{-}H)_2$, **3.2**, see Scheme 4.1.

To follow up on our studies of these interesting new cage opening reactions of the closo-carboranes, we have now investigated reactions of closo-*o*-(1-SCH_3)$C_2B_{10}H_{11}$ and closo-[o-1,2-$(SCH_3)_2$]$C_2B_{10}H_{10}$ with the dirhenium complex $Re_2(CO)_8[\mu\text{-}\eta^2\text{-}C(H)C(H)Bu^n](\mu\text{-}H)$.[6] We have obtained two isomers of the dirhenium complex $Re_2(CO)_8[\mu\text{-}\eta^2\text{-}1,3\text{-}C_2B_{10}H_{10}(1\text{-}SCH_3)](\mu\text{-}H)$, **4.1** and $Re_2(CO)_8[\mu\text{-}\eta^2\text{-}1,4\text{-}C_2B_{10}H_{10}(1\text{-}SCH_3)](\mu\text{–}H)$, **4.2** from the reaction of closo-*o*-(1-SCH_3)$C_2B_{10}H_{11}$ with $Re_2(CO)_8[\mu\text{-}\eta^2\text{-}C(H)C(H)Bu^n](\mu\text{-}H)$ and one product $Re_2(CO)_7[\mu\text{-}\eta^3\text{-}C_2B_{10}H_9(1,2\text{-}SCH_3)_2](\mu\text{–}H)$, **4.3** from the reaction of [o-1,2-$(SCH_3)_2$]$C_2B_{10}H_{10}$ with $Re_2(CO)_8[\mu\text{-}\eta^2\text{-}C(H)C(H)Bu^n](\mu\text{-}H)$. The results of our studies of the synthesis, characterization and reactivity of these new carborane complexes are reported herein.

4.2 Experimental Section

General Data.

All reactions were performed under a nitrogen atmosphere by using standard Schlenk techniques. Reagent grade solvents were dried by the standard procedures and were freshly distilled prior to use. Infrared spectra were recorded on a Thermo Fisher Scientific Nicolet IS10 FT-IR spectrophotometer. ^{1}H NMR spectra were recorded on a Varian Mercury 300 spectrometer operating at 300.1 MHz. ^{11}B NMR spectra were recorded on a Varian Mercury 300 at 96.28 MHz with reference to $BF_3{\cdot}OEt_2$. Mass spectrometric (MS) measurements performed by a direct-exposure probe using electron impact ionization (EI) were made on a VG 70S instrument. closo-*o*-(1-SCH_3)$C_2B_{10}H_{11}$,[7] [o-1,2-(SCH_3)$_2$]$C_2B_{10}H_{10}$[8] and $Re_2(CO)_8[\mu\text{-}\eta^2\text{-}C(H)C(H)Bu^n](\mu\text{-}H)$[6] were prepared according to previously reported procedures. Product separations were performed by TLC in the open air on Analtech 0.25 or 0.5 mm silica gel 60 Å F_{254} glass plates.

Synthesis of $Re_2(CO)_8[\mu\text{-}\eta^2\text{-}1,3\text{-}C_2B_{10}H_{10}(SCH_3)](\mu\text{-}H)$, 4.1 and $Re_2(CO)_8[\mu\text{-}\eta^2\text{-}1,4\text{-}C_2B_{10}H_{10}(SCH_3)](\mu\text{–}H)$, 4.2.

63.0 µL (0.331 mmol) of closo-*o*-(1-SCH_3)$C_2B_{10}H_{11}$ was added to a 100 mL round bottomed flask containing a 30 mL solution of 225.0 mg (0.331 mmol) of $Re_2(CO)_8[\mu\text{-}\eta^2\text{-}C(H)C(H)Bu^n](\mu\text{-}H)$ in octane solvent. The solution was then heated to reflux (125 ^{o}C) for 2h with intermittent monitoring by IR spectroscopy. The solvent was then removed *in vacuo* and the products were isolated by TLC on silica by using pure hexane to yield 5.7 mg of $Re_2(CO)_8[\mu\text{-}\eta^2\text{-}1,3\text{-}C_2B_{10}H_{10}(1\text{-}SCH_3)](\mu\text{-}H)$, **4.1** (3.2 % yield), 54.2 mg of $Re_2(CO)_8[\mu\text{-}\eta^2\text{-}1,4\text{-}C_2B_{10}H_{10}(1\text{-}SCH_3)](\mu\text{–}H)$, **4.2** (31 % yield), and 71.5 mg of $Re_2(CO)_{10}$. Spectral data for **4.1**: IR νCO (cm^{-1} in hexane): 2113(m), 2080(m),

2020(vs), 2002(m), 1984(s) 1967(m), 1957(m). ^{1}H NMR (CD_2Cl_2, 25^{o}C) δ = 3.77 (s, CH), 3.06 (s, 3H, CH_3), -14.30 (s, ReH, 1H). EI/MS m/z, 787, M^+; the ions displayed isotopic distribution patterns consistent with the presence of two rhenium atoms and ten boron atoms. Spectral Data for **4.2**: IR νCO (cm^{-1} in hexane): 2118(m), 2097(m), 2027(sh), 2022(vs), 2014(sh) 1994(s), 1971(m), 1957(vw). ^{1}H NMR (CD_2Cl_2, 25^{o}C) δ = 3.77 (s, CH), 3.08 (s, 3H, CH_3), -13.08 (s, ReH, 1H). ^{11}B {^{1}H} NMR (in $CDCl_3$): δ = -8.77 ppm (2 B), -7.48 (2 B), -5.27 (4 B), -2.41 (1 B), -1.68 (1 B). EI/MS m/z, 787, M^+; the ions displayed isotopic distribution patterns consistent with the presence of two rhenium atoms and ten boron atoms.

Conversion of 4.1 to 4.2.

A pure sample of **4.1** was dissolved in toluene-d_8 in an NMR tube and was then heated in an oil bath at 107 ^{o}C. After 5 h and 20 min at this temperature, the conversion to **2** was complete (100%). As expected, it was not possible to convert isomer **4.2** back to **4.1** under similar conditions.

Synthesis of $Re_2(CO)_7[\mu\text{-}\eta^3\text{-}C_2B_{10}H_9(SCH_3)_2](\mu\text{-}H)$, 4.3

20.2 mg (0.085 mmol) of $[o\text{-}1,2\text{-}(SCH_3)_2]C_2B_{10}H_{10}$ was added to a 100 mL round bottomed flask with 30 mL solution of 58.0 mg (0.085 mmol) of $Re_2(CO)_8[\mu\text{-}\eta^2\text{-}C(H)C(H)Bu^n](\mu\text{-}H)$ in octane. The solution was then heated to reflux (125^o C) for 2h with intermittent monitoring by IR spectroscopy. The solvent was then removed *in vacuo* and the products were separated by TLC on silica by using pure hexane solvent to yield 16.4 mg of $Re_2(CO)_7[\mu\text{-}\eta^3\text{-}C_2B_{10}H_9(1,2\text{-}SCH_3)_2](\mu\text{–}H)$, **4.3**, (38 %) and 21.3 mg of $Re_2(CO)_{10}$. Spectral Data for **4.3**: IR νCO (cm^{-1} in hexane): 2088(m), 2049(s), 1999(m), 1987(vs), 1972(m), 1945(m), 1931(vw). ^{1}H NMR (CD_2Cl_2, 25^{o}C, TMS) δ = 3.06 (s, 6H,

$2CH_3$), -15.68 (s, ReH, 1H). EI/MS m/z, 805, M^+; 790, M^+- CH_3; 762, M^+-CO. These ions displayed isotopic distributions consistent with the presence of two rhenium atoms and ten boron atoms.

Crystallographic Analyses

Colorless single crystals of **4.1** and **4.2**, suitable for X-ray analyses, were obtained by slow evaporation of solvent from a hexane-dichloromethane solution at room temperature while crystals of **4.3** were obtained by slow evaporation of a hexane solution at room temperature. Crystals of **4.2** and **4.3** were each glued onto the end of a thin glass fiber. X-ray intensity data were measured by using a Bruker SMART APEX CCD-based diffractometer using Mo Kα radiation (λ = 0.71073 Å).[9] The raw data frames were integrated with the SAINT$^+$ program by using a narrow-frame integration algorithm.[10] Corrections for Lorentz and polarization effects were also applied with SAINT$^+$. Empirical absorption corrections based on the multiple measurements of equivalent reflections were applied by using the program SADABS.[11] X-ray intensity data from a colorless crystal of **4.1** were collected at 300(2) K by using a Bruker D8 QUEST diffractometer equipped with a PHOTON-100 CMOS area detector and an Incoatec Microfocus source (Mo Kα radiation, λ = 0.71073 Å).[12] The data collection strategy consisted of five 180° ω-scans at different φ settings and two 360° φ-scans, with a scan width per image of 0.5°. The crystal-to-detector distance was 5.0 cm and each image was measured for 15 s. The average reflection redundancy was 18.9. The raw area detector data frames were reduced, scaled and corrected for absorption effects using the SAINT and SADABS programs.[12-13] All structures were solved by a combination of direct methods and difference Fourier syntheses, and refined by full-matrix least-squares on F^2

by using the SHELXTL software package.[14] All non-hydrogen atoms were refined with anisotropic thermal parameters. Hydrogen atoms were placed in geometrically idealized positions and included as standard riding atoms during the least-squares refinements. Compounds **4.1**, **4.2,** and **4.3** all crystallized in the monoclinic crystal system. The space group $P2_1/n$ was indicated by the systematic absences in the data for compounds **4.1** and **4.2**. The space group $P2_1/c$ was indicated by the systematic absences in the data for compound **4.3**. The space group assignments were confirmed by the successful solution and refinement of each of the structures. The bridging hydrido ligands were refined with Re – H distance constraints of 1.80 Å for each of the analyses. Crystal data, data collection parameters and refinement results for each of the analyses are summarized in Table 4.1.

4.3 Results and Discussion

The reaction of closo-*o*-(1-SCH_3)$C_2B_{10}H_{11}$ with $Re_2(CO)_8[\mu\text{-}\eta^2\text{-}C(H)C(H)Bu^n](\mu\text{-}H)$ in an octane solution at reflux (125^o C) for 2h yielded two new compounds $Re_2(CO)_8[\mu\text{-}\eta^2\text{-}1,3\text{-}C_2B_{10}H_{10}(1\text{-}SCH_3)](\mu\text{-}H)$, **4.1** (3.2 % yield) and $Re_2(CO)_8[\mu\text{-}\eta^2\text{-}1,4\text{-}C_2B_{10}H_{10}(1\text{-}SCH_3)](\mu\text{–}H)$, **4.2** (31 % yield). Both compounds were formed by the elimination of 1-hexene from the dirhenium cluster followed by the coordination the sulfur atom and an accompanying oxidative-addition of one of the B – H bonds of the closo-*o*-(1-SCH_3)$C_2B_{10}H_{11}$ to the remaining dirhenium octacarbonyl fragment. Compounds **4.1** and **4.2** are isomers. Both products were characterized by IR and ^{1}H NMR spectroscopy, mass spec and single-crystal X-ray diffraction analyses.

An ORTEP diagram of the molecular structure **4.1** is shown in Figure 4.1. Compound **4.1** contains two mutually-bonded rhenium atoms that are bridged by a

$C_2B_{10}H_{10}(SCH_3)$ ligand and one hydrido ligand. The $C_2B_{10}H_{10}(SCH_3)$ ligand is coordinated to rhenium atom Re(2) by the thioether sulfur atom S(1), Re(2) – S(1) = 2.4791(15) Å and to Re(1) by the boron atom B(3), Re(1) – B(3) = 2.255(7) Å. The Re – Re bond is significantly longer, Re(1) – Re(2) = 3.2790(4) Å than the Re – Re bond in $Re_2(CO)_{10}$ which is 3.041(1) Å.[15] The bond lengthening effect can be attributed in part to the presence of the hydrido ligand H(1) which also bridges the Re – Re bond.[16] As expected, the resonance of the hydrido ligand is highly shielded at δ = -14.30. The location of the carbon atom C(1) in the carborane cage was determined in part by recognition of the short length of the C – C bond, C(1) – C(2) = 1.631(8) Å.[1b] Compound **4.1** contains eight linear terminal carbonyl ligands distributed as shown in Figure 4.1.

An ORTEP diagram of the molecular structure **4.2** is shown in Figure 4.2. Compound **4.2** is structurally very similar to **4.1** with a bridging by a $C_2B_{10}H_{10}(SCH_3)$ ligand and one bridging hydrido ligand, Re(2) – S(1) = 2.4801(14) Å. The main difference is that the carborane cage is coordinated to the rhenium atom at the boron B(4) of the cage, Re(1) – B(4) = 2.243(5) Å. The Re – Re bond length in **4.2** is similar to that in **4.1**, Re(1) – Re(2) = 3.2861(3) Å. The bond lengthening effect can be attributed in part to the presence of the hydrido ligand H(1) which also bridges the Re – Re bond.[15] The resonance of the hydrido ligand in **4.2** is also highly shielded at δ = -13.08.

As indicated by the structures, it appears that both compounds were formed by the addition the thioether sulfur atom S(1) to one rhenium atom and an oxidative-addition of one of the B – H bonds of the closo-*o*-(1-SCH_3)$C_2B_{10}H_{11}$ to the other rhenium atom of the dirhenium complex. The structures would suggest that it was the B(3) – H that was oxidatively added to form **4.1** and the B(4) – H that was oxidatively added to form **4.2**,

but the mechanisms of the processes have not been established. Oxidative addition of the BH bonds at the B(3) and B(4) sites in closo-*o*-(1-SCH_3)$C_2B_{10}H_{11}$ has been observed previously.[5]

In further studies, we found that compound **4.1** was converted to compound **4.2** quantitatively by heating to 107° C for 5h 20 min. This helps to explain the low yield of **4.1** in the original reaction. Compound **4.2** does not convert to **4.1** under these conditions. This raises a question as to whether all of the observed **4.2** was formed via **4.1** as an intermediate or whether **4.2** was formed simultaneously and in a reaction that competes with the formation of **4.1**. We cannot answer that question with certainty with the studies at hand. However, these studies do confirm that **4.1** does convert to **4.2**. This conversion may occur intramolecularly via a transient reductive-elimination involving the formation of a B – H bond between B(3) and H(1) in **4.1**, see Intermediate **C** in Scheme 4.2. In **C**, the B(3) – H(1) group would most probably remain coordinated to the rhenium atom Re(1) via an agostic-like interaction. There are many examples of such interactions among the many structurally-characterized carborane metal complexes.[4, 17] A small rotation of the carborane cage about the C(1) – S(1) bond in **C** would allow the formation of a second closely-related intermediate, **D**, in which the B(4) – H(4) bond replaces the B(3) – H(1) bond to form a new agostic interaction at Re(1). The isomerization to **4.2** would then be completed by an oxidative addition of the B(4) – H(4) bond to Re(1).

The reaction of [o-1,2-(SCH_3)$_2$]$C_2B_{10}H_{10}$ with $Re_2(CO)_8$[μ-η^2-C(H)C(H)Bu^n](μ-H) in an octane solution at reflux (125° C) for 2h yielded only one new product $Re_2(CO)_7$[μ-η^3-$C_2B_{10}H_9$(1,2-(SCH_3)$_2$](μ–H), **4.3** in 38 % yield. An ORTEP diagram of the molecular structure **4.3** is shown in Figure 4.3. Compound **4.3** contains two mutually-

bonded rhenium atoms that are bridged by a $C_2B_{10}H_9(SCH_3)_2$ ligand and one hydrido ligand. The $C_2B_{10}H_9(SCH_3)_2$ ligand is coordinated to rhenium atom Re(2) by both of the thioether sulfur atoms, Re(2) – S(1) = 2.461(2) Å and Re(2) – S(2) = 2.474(3) Å, and to Re(1) by the boron atom B(3), Re(1) – B(3) = 2.264(11) Å. As in **4.1** and **4.2**, the Re – Re bond is long, Re(1) – Re(2) = 3.3273(6) Å which can also be attributed in part to the presence of the hydrido ligand H(1) which also bridges the Re – Re bond.[16] The resonance of the hydrido ligand is also highly shielded at δ = -15.68. The C – C bond distance, C(1) – C(2) = 1.655(12) Å is significantly shorter than that bonds in the free molecule of [o-1,2-$(SCH_3)_2$]$C_2B_{10}H_{10}$, 1.8033(18) Å.[18] This might be due to the removal of electron density from the sulfur atoms because of their coordination to the metal atom Re(2). The formation of the Re(1) – B(3) bond involved the oxidation addition of the B(3) – H bond in of the [o-1,2-$(SCH_3)_2$]$C_2B_{10}H_{10}$ to Re(1). The hydrogen atom became the hydrido ligand following the elimination of the hexane form the original dirhenium reagent. Compound **4.3** contains only seven linear terminal carbonyl ligands which are distributed as shown in Figure 4.3, but both metal atom achieve 18 electron configurations as a result of the existence of a Re – Re single bond.

4.4 Summary

Two new dirhenium compounds **4.1** and **4.2** were obtained from the reaction of closo-*o*-(1-SCH_3)$C_2B_{10}H_{11}$ with $Re_2(CO)_8[\mu\text{-}\eta^2\text{-}C(H)C(H)Bu^n](\mu\text{-}H)$. Compounds **4.1** and **4.2** are isomers and compound **4.1** is cleanly converted to **4.2** by heating in solution to 107 ^{o} C. In both products the carborane is coordinated to one Re atom by the sulfur atom and to the second Re atom by a cage boron atom by an oxidative-addition of one of the BH bonds in the carborane. An intramolecular isomerization process involving

reductive-elimination and oxidative-addition of B-H bonds in the carborane cage at one of the rhenium atoms has been proposed for the conversion of **4.1** to **4.2**. The bis-thioether carborane [o-1,2-$(SCH_3)_2$]$C_2B_{10}H_{10}$ reacts with $Re_2(CO)_8$[μ-η^2-C(H)C(H)Bu^n](μ-H) to yield the new compound $Re_2(CO)_7$[μ-η^3-$C_2B_{10}H_9$(1,2-$(SCH_3)_2$](μ–H), **4.3**. The bridging $C_2B_{10}H_9$(1,2-$(SCH_3)_2$ ligand is coordinated to one of the rhenium atoms by the two sulfur atoms and to the carborane boron atom B(3) which has under an oxidative-addition at the B(3) – H bond in order to form the Re – B(3) bond at the other Re atom Re(1). Unfortunately, we were not able to add additional metal groupings to any of these compounds and no carborane cage-opening transformations were observed with any of these new carboranyldirhenium compounds.

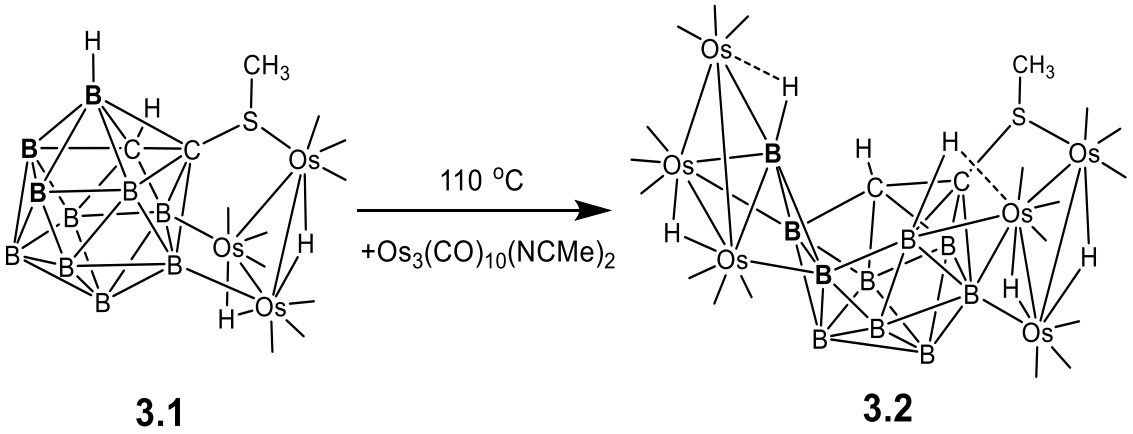

3.1 **3.2**

Scheme 4.1. A schematic of the cage opening of the carborane compound closo-[o-1,2-$(SCH_3)_2$]$C_2B_{10}H_{10}$ induced by the addition of two triosmium carbonyl clusters.[5]

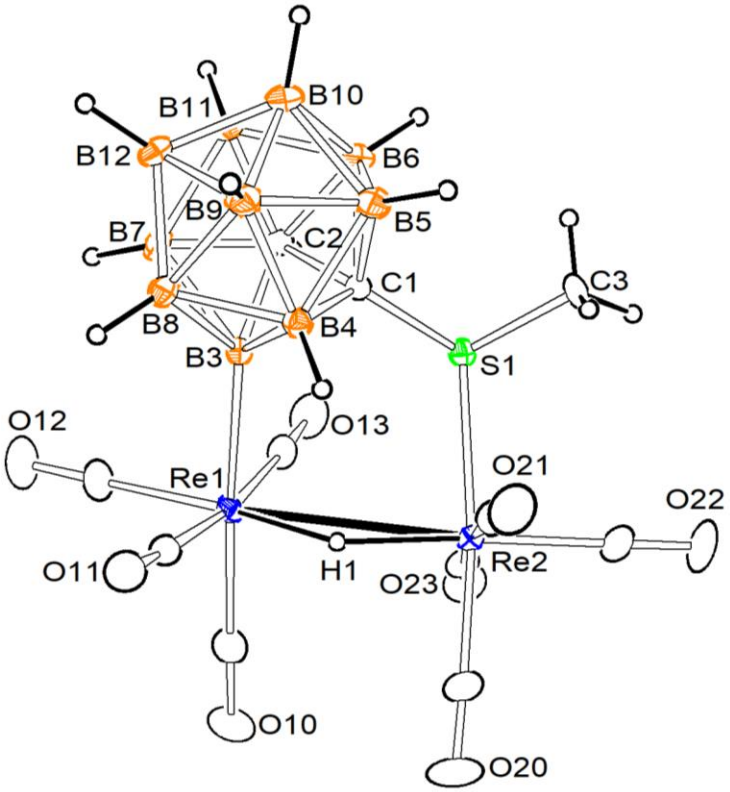

Figure 4.1. An ORTEP diagram of the molecular structure of $Re_2(CO)_8[\mu\text{-}\eta^2\text{-}1,3\text{-}C_2B_{10}H_{10}(SCH_3)](\mu\text{-}H)$, **4.1** showing 20% thermal ellipsoid probability. Selected interatomic bond distances (Å) are as follows: Re(1) – Re(2) = 3.2790(4), Re(1) – B(3) = 2.255(7), Re(2) – S(1) = 2.4791(15), C(1) – C(2) = 1.631(8).

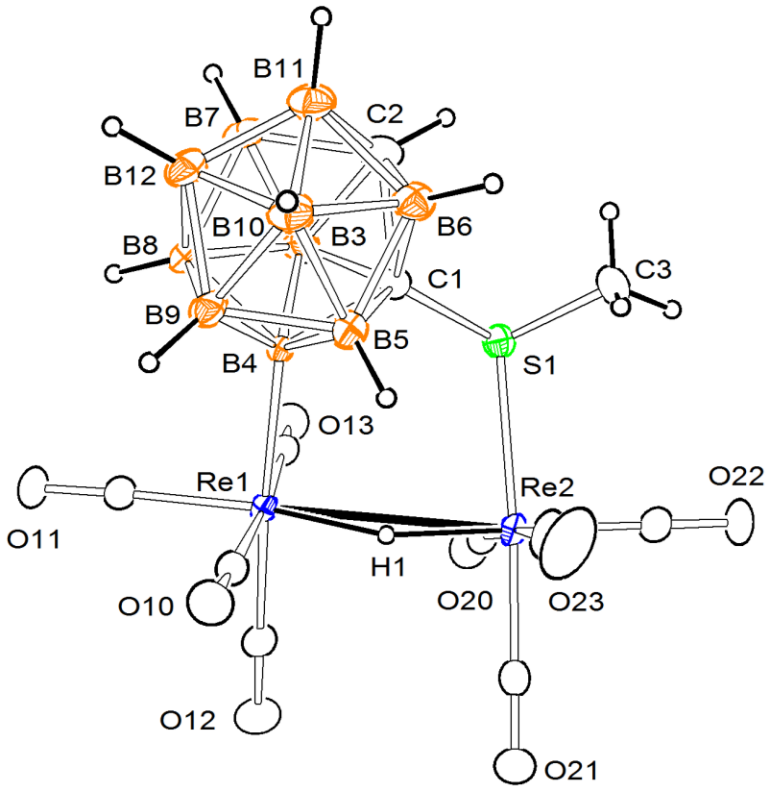

Figure 4.2. An ORTEP diagram of the molecular structure of $Re_2(CO)_8[\mu\text{-}\eta^2\text{-}1,4\text{-}C_2B_{10}H_{10}(1\text{-}SCH_3)](\mu\text{-}H)$, **4.2** showing 20% thermal ellipsoid probability. Selected interatomic bond distances (Å) are as follows: Re(1) – Re(2) = 3.2861(3), Re(1) – B(4) = 2.243(5), Re(2) – S(1) = 2.4801(14), C(1) – C(2) = 1.708(8).

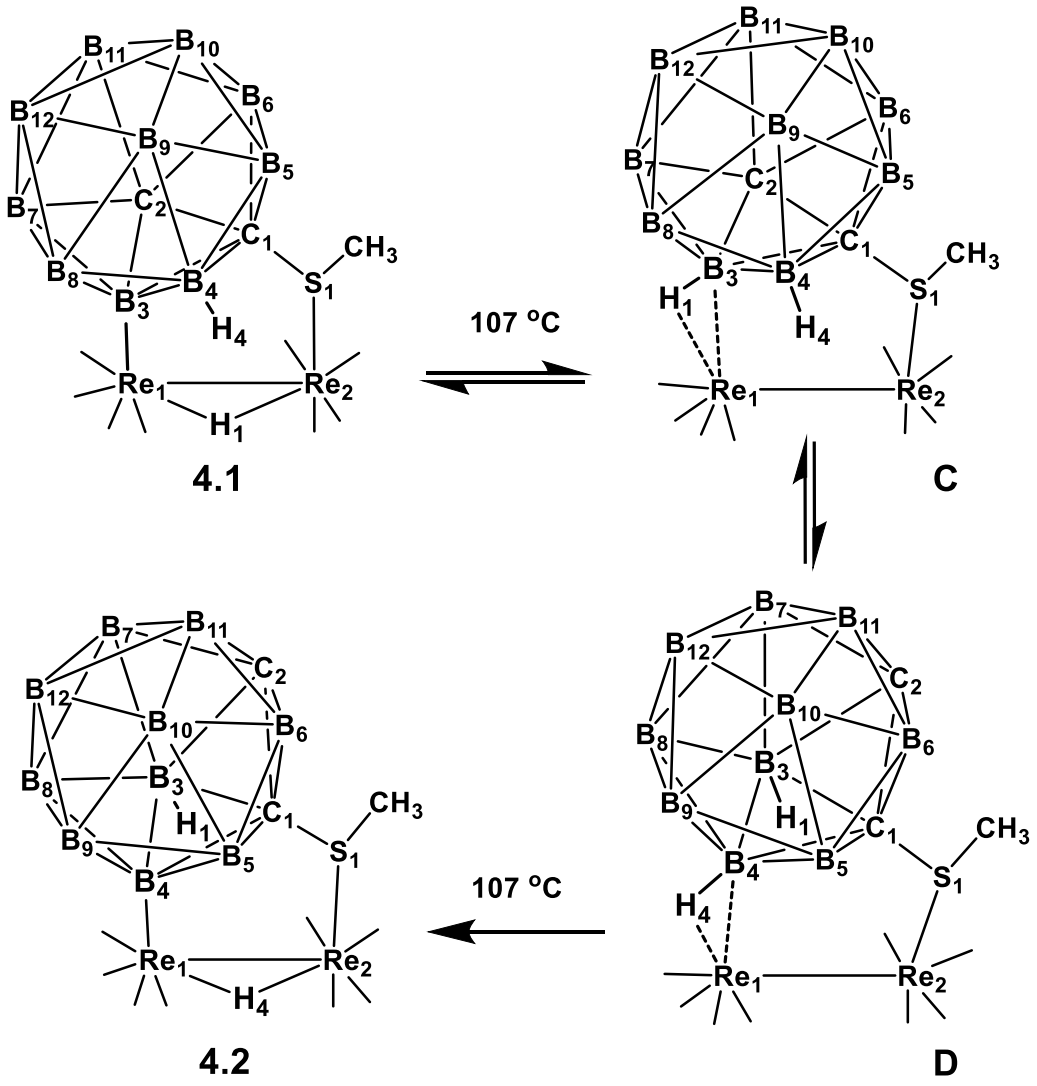

Scheme 4.2. A schematic of the proposed mechanism for the isomerization of compound **4.1** to **4.2**. The CO ligands are shown only as lines to the Re atoms. Most of the H atoms on the carborane cage are omitted for clarity.

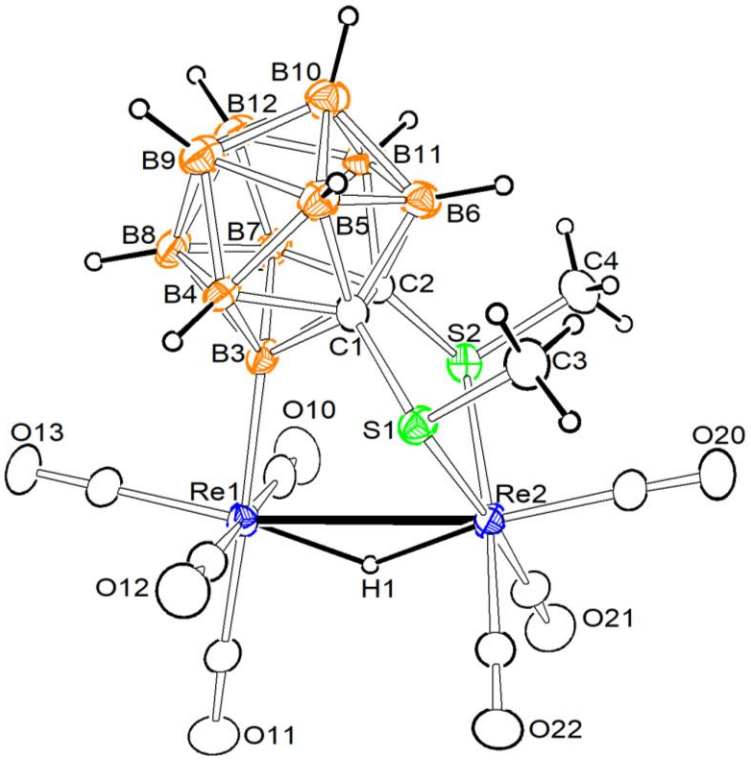

Figure 4.3. An ORTEP diagram of the molecular structure of $Re_2(CO)_7[\mu\text{-}\eta^3\text{-}C_2B_{10}H_9(1,2\text{-}SCH_3)_2](\mu\text{-}H)$, **4.3** showing 20% thermal ellipsoid probability. Selected interatomic bond distances (Å) are as follows: Re(1) – Re(2) = 3.3273(6), Re(1) – B(3) = 2.264(11), Re(2) – S(1) = 2.461(2), Re(2) – S(2) = 2.474(3), C(1) – C(2) = 1.655(12).

Table 4.1. Crystallographic Data for Compounds **4.1, 4.2** and **4.3.**

Compound	**4.1**	**4.2**	**4.3**
Empirical formula	$Re_2SO_8C_{11}B_{10}H_{14}$	$Re_2SO_8C_{11}B_{10}H_{14}$	$Re_2S_2O_7C_{11}B_{10}H_{16}$
Formula weight	786.78	786.78	804.86
Crystal system	Monoclinic	Monoclinic	Monoclinic
Lattice parameters			
a (Å)	7.2873(3)	9.4934(6)	14.9150(18)
b (Å)	14.1786(6)	27.0139(17)	10.2246(12)
c (Å)	21.9707(10)	9.5306(6)	15.9356(19)
α (deg)	90.00	90.00	90.00
β (deg)	95.565(1)	108.085(1)	102.332(2)
γ (deg)	90.00	90.00	90.00
V (Å3)	2259.39(17)	2323.4(3)	2374.1(5)
Space group	$P2_1/n$	$P2_1/n$	$P2_1/c$
Z value	4	4	4
ρ_{calc} (g/cm^3)	2.313	2.249	2.252
μ (Mo Kα) (mm^{-1})	10.834	10.535	10.395
Temperature (K)	294(2)	294(2)	294(2)
2Θmax (°)	50.06	50.06	50.06
No. Obs. (I > 2σ(I))	3798	3937	3457
No. Parameters	298	298	295
Goodness of fit (GOF)	1.271	1.197	1.056
Max. shift in cycle	0.000	0.001	0.001
Residuals*: R1; wR2	0.0232; 0.0542	0.0248; 0.0597	0.0404; 0.1025
Absorption Correction,	Multi-scan	Multi-scan	Multi-scan
Transmission (Max/min)	0.466/0.295	1.00/0.575	1.00/0.481
Largest peak in Final Diff. Map (e$^-$/Å^3)	1.773	0.925	2.163

*$R1 = \Sigma_{hkl}(\,|\,|F_{obs}|-|F_{calc}|\,|)/\Sigma_{hkl}|F_{obs}|$; $wR2 = [\Sigma_{hkl}w(|F_{obs}|-|F_{calc}|)^2/\Sigma_{hkl}wF^2_{obs}]^{1/2}$; $w = 1/\sigma^2(F_{obs})$; $GOF = [\Sigma_{hkl}w(|F_{obs}|-|F_{calc}|)^2/(n_{data} - n_{vari})]^{1/2}$

4.5 References

1. (a)Grimes, R. N. *Carboranes, 2nd Edition* **2011**; (b)Bregadze, V. I. *Chem. Rev.* **1992,** 92, (2), 209-223; (c)Grimes, R. N. *Dalton Trans.* **2015,** 44, (13), 5939-5956.

2. (a)Grimes, R. N. *Carboranes, 2nd Edition* **2011**, 773-1014; (b)Grimes, R. N. *Coord. Chem. Rev.* **2000,** 200, 773-811; (c)Saxena, A. K.; Hosmane, N. S. *Chem. Rev.* **1993,** 93, (3), 1081-1124.

3. (a)Grimes, R. N., Icosahedral carboranes: 1,2-C2B10H12. In *Carboranes, 2nd Edition*, Elsevier Science Bv: Amsterdam, 2011; pp 461-500; (b)Jain, L.; Jain, V. K.; Kushwah, N.; Pal, M. K.; Wadawale, A. P.; Bregadze, V. I.; Glazun, S. A. *Coord. Chem. Rev.* **2014,** 258, 72-118.

4. Adams, R. D.; Kiprotich, J.; Peryshkov, D. V.; Wong, Y. O. *Chem. Eur. J.* **2016,** 22, (19), 6501-6504.

5. Adams, R. D.; Kiprotich, J.; Peryshkov, D. V.; Wong, Y. O. *Inorg. Chem.* **2016,** 55, (16), 8207-8213.

6. Nubel, P. O.; Brown, T. L. *J. Am. Chem. Soc.* **1984,** 106, (3), 644-652.

7. Timofeev, S. V.; Zakharova, M. V.; Mosolova, E. M.; Godovikov, I. A.; Ananyev, I. V.; Sivaev, I. B.; Bregadze, V. I. *J. Organomet. Chem.* **2012,** 721, 92-96.

8. Llop, J.; Vinas, C.; Teixidor, F.; Victori, L.; Kivekas, R.; Sillanpaa, R. *Figshare* **2001**.

9. *APEX2*, 2014.9-0; Bruker AXS, Inc.: Madison, WI, USA, 2014.

10. *SAINT+*, Version 6.2a; Bruker Analytical X-ray Systems, Inc.: Madison, WI 2001.

11. *SADABS*, 2014/4; Bruker Analytical X-ray Systems, Inc.: Madison, Wisconsin, USA, 2014.

12. *APEX3*, 2016.5-0; Bruker AXS, Inc.: Madison, WI, USA, 2016.

13. *SADABS* 2016/2; Bruker Analytical X-ray Systems, Inc.: Madison, WI, USA, 2016.

14. Sheldrick, G. M. *SHELXTL*, Version 6.1; Bruker Analytical X-ray Systems, Inc.: Madison, WI, 1997.

15. Churchill, M. R.; Amoh, K. N.; Wasserman, H. J. *Inorg. Chem.* **1981,** 20, (5), 1609-1611.

16. (a)Bau, R.; Drabnis, M. H. *Inorg. Chim. Acta* **1997,** 259, (1-2), 27-50; (b)Teller R.G., B. R. *Struct. Bond.* **1981,** 44, 1-82.

17. (a)Chung, J. H.; Boyd, E. P.; Liu, J. P.; Shore, S. G. *Inorg. Chem.* **1997,** 36, (21), 4778-4781; (b)Chung, J. H.; Knoeppel, D.; McCarthy, D.; Columbie, A.; Shore, S. G. *Inorg. Chem.* **1993,** 32, (16), 3391-3392; (c)Jan, D. Y.; Shore, S. G. *Organometallics* **1987,** 6, (2), 428-430; (d)Brew, S. A.; Stone, F. G. A. *Adv. Organomet. Chem.* **1993,** 35, 135-186; (e)Lebedev, V. N.; Mullica, D. F.; Sappenfield, E. L.; Stone, F. G. A. *J. Organomet. Chem.* **1997,** 536, (1-2), 537-539.

18. Laromaine, A.; Vinas, C.; Sillanpaa, R.; Kivekas, R. *Acta Crystallogr. Sect. C* **2004,** 60, O524-O526.

CHAPTER 5

Multiple Activations of C-H bonds in a Furan Ligand by Transition Metal Clusters

5.1 Introduction

The growing demand, declining supplies of fossil fuels and in addition the threat of climate change have been driving forces for the chemical industry to find alternative sources for the production of important chemicals and fuels.[1] Biomass is an abundant sustainable source of organic carbon and can therefore serve as a renewable resource for the production of value added chemicals.[2] The conversion of biomass to fuels or chemicals can be accomplished in several ways including thermal pyrolysis,[3] high temperature gasification,[4] bioconversion[5] and chemical catalytic processes.[6] Chemical catalytic conversion of biomass has particularly received a lot of attention because of the wide array of chemical and fuels that can be produced by the different designed catalytic systems.[1c] Furans are a class of five-membered heterocyclic aromatic compounds with four carbon atoms and one oxygen atom. They are products from the processing of biomass and intermediates in the production of biofuels. The furan core is also present in many natural products and pharmaceuticals.[7] The most abundant biomass, lignocellulose is made up of mostly 3 components: cellulose, hemicellulose, and lignin. The catalytic dehydration of glucose and xylose which are the building blocks of cellulose and hemicellulose respectively can generate furfural and 5-hydroxymethylfuran (HMF) as intermediates respectively.[8] Both HMF and furfural are important intermediates that can be upgraded to generate high value chemicals such as furfuryl alcohol, tetrahydrofuran, tetrahydrofurfuryl alcohol, furan, dihydropyran, acetylfuran and methyltetrahydrofuran.[1c] HMF and its derivatives levulinic acid and 2, 5-Furan dicarboxylic acid (FDCA) are especially of high value and in 2004 the U.S. Department of Energy (DOE) listed them in the top 12 value added chemicals from biomass.[9] Levulinic acid is obtained in the acid

catalyzed dehydration of HMF and can be converted to levulinic esters or methyl-tetrahydrofuran for use as oxygenated diesel and gasoline fuel additives respectively.[2a] FDCA is a potential replacement of petrochemical-derived terephthalic acid and is used as polymer building block in polymer synthesis.[10] Copper and iron catalysts have been very promising in the conversion of furfural to 2-methyltetrahydrofuran (2-MTHF) with conversion up to 99% and selectivity of 98% for a Cu/Fe catalyst.[11] There has also been a recent increasing interest in the conversion of alkylfurans to BTX compounds (benezene, toluene, xylene) and the group of Dumesic has demonstrated that acidic oxides such as tungstated zirconia (WO_x–ZrO_2) demonstrate superior activity and selectivity for the production of aromatics compared to zeolites.[12] Despite a lot of progress in furfural and HMF upgrade to fuels typical time scales for many solid catalysts are still limited to just a few hours hence there is a need for further improvement in both homogeneous and solid catalytic methods.[13] In the catalytic conversion of biomass intermediates efficient C – O bond cleavage is needed since most metallated ethers are challenging to manipulate as they undergo rapid C-O bond cleavage.[14] Transition metal mediated functionalization via C – H bond activations can provide routes to facile and highly regioselective functionalization of biomass intermediates.[15]

The activation of C-H bonds is a critical determining first step in the transformation and functionalization of hydrocarbons to higher value products.[16] The first reports on the C–H activation in saturated hydrocarbons were by Bergman[17] and Graham[18] with (η^5-C_5R_5)Ir [R = Me (Cp^*); R = H (Cp)] complexes. Transition metal clusters with aromatic ligands have received a lot of attention because of the interesting bonding interactions between metals and arenes and they can also serve as models to

study the transformations of small molecules on metal surfaces. Activation of aromatic C-H bonds by polynuclear metal clusters are much less common compared to mononuclear clusters. [19] The activation of organic molecules at multinuclear metal sites offers unique advantages based on "cooperative reactivity" of the metal centers.[20] Multiple coordination of the substrate and multi-electron transfer are possible in multinuclear clusters. The C-H activation of the simplest arene, benzene, with transition metals has been well studied,[21] and different bonding modes of benzene and benzyne coordination have been identified. Examples of some bonding modes are presented in Scheme 5.1**.** The best known coordination mode of benzene is the η^6 bonding mode but it can also bond in other modes such as μ_3 -η^2:η^2:η^2 to three metals (**I)** of a triangular face,[22] as a bridge to two metal atoms as in $[Os_3(CO)_{10}(C_4H_6N)(\mu\text{-}C_6H_5)]$ (**II**),[23] via a σ interaction with 2 metals and a π interaction through a double bond with the 3rd metal[24] (**III)** and bonding mode **IV** in which benzene acts as a 5 electron donor.[24] Benzyne can bind to one metal center as a two-electron donor via 2 σ-bonds (**IA**)[21c, d], to two metals via a σ-bond to each of the metals (**IIA**)[21e, g] and to three metals atoms in two modes: In one mode the benzyne binds to one metal using one of the unpaired electrons to form a two-center 2 electron bond and the other pair to two metals to form a 3 center 2 electron σ-bond (**IIIA**)[21f, 25]. In the second mode, the benzyne can be a four-electron donor where both the unpaired electrons are σ-bonded to two metals, and the π bond between the two carbons donates two more electrons to the third metal (**IVA**).[21a, b] Several trimetallic type **IVA** clusters with only 2 metal-metal bonds and main group elements such as phosphorus[25] and antimony[26] bridging the cleaved bond have also been reported. Late transition metal-benzyne complexes can undergo addition reactions with acidic reagents

such as alcohols and ketones and insertion reactions with CO, CO_2, aldehydes, nitriles and unsaturated hydrocarbons.[27] Insertion reactions in benzyne complexes can lead to the formation of M – O/N bonds which are important in the study of transition metal heteroatom containing molecules[27b] and also C-C bond fomation[28] showing potential for use in synthetic reactions.

In the activation of furans the iron complexes Cp*Fe(CO)(NCMe)Ph[15] (Cp* = η^5-pentamethylcyclopentadienyl) and Cp*Fe[29] ($L^{'iPr}$ = $CH_2CH(CH_3)$(3-isopropyl-4,5-dimethylimidazol-2-ylidene-1-yl) have recently been shown to mediate facile and highly regioselective C−H activation of heteroaromatic substrates including furan, thiophene, thiazole, 2-methylfuran benzothiophene, and benzofuran. In both catalysts the C-H activation is regioselective for the 2 position except with 2-methylfuran where activation takes place at the 5 position over the methyl group. This selectivity has been rationalized for Cp*Fe(CO)(NCMe)Ph by the relative stability gained by formation of an Fe−C2(furyl) bond versus an Fe−C3(furyl) bond in the transition state.[15] Density functional calculations have indeed found that the most favorable C – H activation transition state (TS) corresponds to the most favorable metal aryl bond energy and therefore shown that M – C2(furyl) bond energy to be stronger than the M – C3(furyl) bond energy.[15, 30] The coordination of a free furan rings to metals mostly happens by *ortho*-metallation, however one example of coordination via the "O" heteroatom to a single metal[31] and coordination via an O, C- bridge[32] have been observed for copper and yttrium respectively.

Heteroaromatic species like furan can also oxidatively add like benzene to a triosmium cluster in different boding modes (Scheme 5.2): by ortho-metallation and η^2-

coordination of the furyl group (**IIB**), dehydrogenation in the α and β position to give compound **IIIB** and by one ortho C-H activation to give a μ-2-furyl cluster (**IVB**). The structural types **IB**[33], **IIB**[34] and **IIIB**[34] have been observed for the furan ligand, but prior to our work no crystal structure was reported for the Os_3 furyne (**IIB**). Structural types **IIIB**[35] and **IVB**[36] have also been observed for the 2-methylimidazolyl ligand. We report here the further studies of the reaction of $Os_3(CO)_{10}(\mu,\eta^2\text{-}C_4H_3O)(\mu\text{-}H)$, **5.1** and $Os_3(CO)_9(\mu_3,\eta^2\text{-}C_4H_2O)(\mu\text{-}H)_2$, **5.2** with dirhenium carbonyl cluster complexes.

5.2 Experimental

General Data.

All reactions were performed under a nitrogen atmosphere using standard Schlenk techniques. Reagent grade solvents were dried by the standard procedures and were freshly distilled prior to use. Infrared spectra were recorded on a Thermo Fisher Scientific Nicolet IS10 FT-IR spectrophotometer. ^{1}H NMR spectra were recorded on a Varian Mercury 300 spectrometer operating at 300.1 MHz. Mass spectrometric (MS) measurements performed by a direct-exposure probe using electron impact ionization (EI) were made on a VG 70S instrument. $Os_3(CO)_{10}(NCMe)_2$[37] and $Re_2(CO)_8(\mu\text{-}Ph)(\mu\text{-}H)$[23b] were prepared according to previously reported procedures. Product separations were performed by TLC in the air on Analtech 0.25 and 0.5 mm silica gel 60 Å F_{254} glass plates.

Synthesis of $Os_3(CO)_{10}(\mu\text{-}\eta^2\text{-}C_4H_3O)(\mu\text{-}H)$, 5.1 and $Os_3(CO)_9(\mu_3, \eta^2\text{-}C_4H_2O)(\mu\text{-}H)_2$, 5.2

$Os_3(CO)_{10}(\mu\text{-}\eta^2\text{-}C_4H_3O)(\mu\text{-}H)$ was prepared using a modified procedure of Himmelreich and Muller.[34] 2.0 ml of furan was added to a 10 mL high pressure glass vessel with 42.0 mg of $Os_3(CO)_{10}(NCMe)_2$ (0.045 mmol). The mixture was then heated at

80 °C in a sealed high-pressure reactor for 2 hours. The excess furan was removed in vauco, and the orange solid chromatographed on a silica TLC plate. Elution with pure hexane yielded 29.0 mg of $Os_3(CO)_{10}(\mu,\eta^2\text{-}C_4H_3O)(\mu\text{-}H)$, (70 % yield) and 3.7 mg of $Os_3(CO)_9(\mu_3,\eta^2\text{-}C_4H_2O)(\mu\text{-}H)_2$, **5.2** (9 % yield). Compound **5.2** was obtained in a higher yield by a direct conversion from **5.1**. 36.0 mg of $Os_3(CO)_{10}(\mu, \eta^2\text{-}C_4H_3O)(\mu\text{-}H)$ (0.039 mmol) was heated to reflux in 20 mL of octane for 1.5 hours. 34.0 mg of **5.2** was obtained (99 % yield). Spectral data for **5.2**: IR (υ_{CO}, cm^{-1}, in hexane): 2113 (s), 2085 (vs), 2060 (vs), 2036 (vs), 2030 (sh), 2014 (vs), 2002 (vs), 1989 (s), 1960 (w). ^1H NMR (in $CDCl_3$): δ = .7.58 ppm (d, 1H, CH), 6.80 (d, 1H, CH), -19.57 (s, hydride, 2H). EI/MS m/z, 892 = M^+.

Reaction of $Os_3(CO)_{10}(\mu,\text{-}\eta^2\text{-}C_4H_3O)(\mu\text{-}H)$, 5.1 with $Re_2(CO)_8(\mu\text{-}Ph)(\mu\text{-}H)$

14.0 mg (0.015 mmol) of **1** was mixed with 10.0 mg of $Re_2(CO)_8(\mu\text{-}Ph)(\mu\text{-}H)$ (0.015 mmol) in 1 mL of CD_2Cl_2 in an NMR tube. The mixture was heated at 40 °C with intermittent monitoring by NMR for 18 hours. The solvent was then removed and the products isolated by TLC. In order of elution in pure hexane, 3.9 mg of $(\mu\text{-}H)Os_3(CO)_{10}(\mu\text{-}\eta^2\text{-}2,3,\mu\text{-}\eta^2\text{-}4,5\text{-}C_4H_2O)Re_2(CO)_8(\mu\text{-}H)$, **5.3** (59 % yield) and 9.6 mg of **1** (unreacted) were obtained IR (υ_{CO}, cm^{-1}, in hexane): 2119 (vw), 2105 (w), 2093 (m), 2071 (s), 2058 (s), 2024 (vs), 2017 (w) 2010 (m), 2003 (m), 1987 (w), 1980 (s). ^1H NMR (in $CDCl_3$): δ = 5.54 ppm (s, 2H, CH), -13.56 (s hydride, 1H), -15.81 (s, hydride, 1H). EI/MS m/z, 1516 = M^+.

Reaction of $Os_3(CO)_{10}(\mu_3, \eta^2\text{-}C_4H_2O)(\mu\text{-}H)_2$, 5.2 with $Re_2(CO)_8Ph(\mu\text{-}H)$

22.0 mg (0.025 mmol) of **5.2** was mixed with 15.0 mg of $Re_2(CO)_8Ph(\mu\text{-}H)$ (0.022 mmol) in 1 mL of CD_2Cl_2 in an NMR tube. The mixture was heated at 40 °C with

intermittent monitoring by NMR for 17 hours. The solvent was then removed and the products isolated by TLC. In order of elution in pure hexane, 10.3 mg of (μ-H)$_2$Os$_3$(CO)$_9$(μ_3-η^2-2,3-,μ-η^2-4,5-C$_4$HO)Re$_2$(CO)$_8$(μ-H), **5.4** (38 % yield) and 5.8 mg of **5.2** (unreacted) were obtained IR (υ_{CO}, cm^{-1}, in hexane): 2119 (vw), 2110 (m), 2092 (s), 2087 (w), 2064 (vs), 2039 (w), 2034 (s) 2021 (vs), 2011 (w), 2004 (s), 1992 (w), 1974 (s), 1970 (sh).^{1}H NMR (in CDCl$_3$): δ = 6.26 ppm (s, 1H, CH), -13.11 (s hydride, 3H). EI/MS m/z, 1488 = M$^+$.

Reaction of Os$_3$(CO)$_{10}$(μ_3, η^2-C$_4$H$_2$O)(μ-H)$_2$, 5.2 with Os$_3$(CO)$_{10}$(NCMe)$_2$

16.0 mg (0.018 mmol) of **5.2** was added to a solution of 18.11 mg (0.019 mmol) of Os$_3$(CO)$_{10}$(NCMe)$_2$ in cyclohexane. The mixture was heated under reflux for 1 hour with intermittent monitoring by IR. The solvent was then removed in vacuo and the products isolated by TLC. In order of elution in pure hexane, 7.2 mg of (μ-H)$_2$Os$_3$(CO)$_9$(μ_3-η^2-2,3-,μ-η^2-4,5-C$_4$HO)Os$_3$(CO)$_{10}$(μ-H), **5.5** (36 % yield) and 5.3 mg of **5.2** (unreacted) were obtained. IR (υ_{CO}, cm^{-1}, in hexane): 2116 (w), 2103 (m), 2089 (s), 2069 (vs), 2066 (s), 2056 (m), 2040 (m) 2034 (vw), 2023 (sh), 2020 (s), 2009 (vw), 2002 (s), 1983 (vw) ^{1}H NMR (in CDCl$_3$): δ = 7.56 ppm (s, 1H, CH), -15.84 (s hydride, 3H). EI/MS m/z, 1742 = M$^+$.

Crystallographic Analyses

Yellow single crystals of **5.2** and **5.5** were obtained by slow evaporation of solvent from solutions in hexane solvent, while orange crystals of **5.3,** and colorless crystals of **5.4** suitable for x-ray diffraction analyses were obtained by slow evaporation of solvent from solutions in hexane/methylene chloride solvent mixtures. Crystals **5.2**,

5.3 and **5.4** were each glued onto the end of a thin glass fiber and X-ray intensity data measured by using a Bruker SMART APEX CCD-based diffractometer by using Mo Kα radiation (λ = 0.71073 Å). The raw data frames were integrated with the SAINT$^+$ program by using a narrow-frame integration algorithm.[38] Correction for Lorentz and polarization effects were also applied with SAINT$^+$. An empirical absorption correction based on the multiple measurements of equivalent reflections was applied using the program SADABS in each analysis. All structures were solved by a combination of direct methods and difference Fourier syntheses and were refined by full-matrix least-squares on F^2, by using the SHELXTL software package.[39] X-ray intensity data from a yellow block crystal of **5.5** were collected at 100(2) K using a Bruker D8 QUEST diffractometer equipped with a PHOTON-100 CMOS area detector and an Incoatec Microfocus source (Mo Kα radiation, λ = 0.71073 Å).[40] The data collection strategy consisted of five 180° ω-scans at different φ settings, using a scan width per image of 0.5°. The crystal-to-detector distance was 5.0 cm and each image was measured for 6 s with the detector operated in shutterless mode. The average reflection redundancy was 5.5. The raw area detector data frames were reduced, scaled and corrected for absorption effects using the SAINT[40] and SADABS[41] programs. Final unit cell parameters were determined by least-squares refinement of 9796 reflections in the range $4.767° \leq 2\theta \leq 55.228°$ taken from the data set. All non-hydrogen atoms were refined with anisotropic displacement parameters. Hydrogen atoms on the furan ring were placed in geometrically idealized positions and were included as standard riding atoms during the least-squares refinements. Crystal data, data collection parameters, and results of the analyses are listed in Tables 5.1 and 5.2.

Compounds **5.2** and **5.3** and **5.5** crystallized in the triclinic crystal system while **5.4** crystallized in the monoclinic crystal system. The space group *P*-1 was assumed for **5.2**, 5.**3** and **5.5** and confirmed by the successful solution and refinement of the structures. For compound **5.4**, the space group $P2_1/n$ was indicated by the systematic absences in the data and confirmed by the successful solution and refinement of the structure. The bridging Os–H_1 bond distance in compound **5.2** and Os–H_2 and Re–H_5 distances compounds in compounds **5.3** and **5.4** were refined with distance constraints of 1.80 Å. All the bridging hydrides in compound **5.5** were refined with distance constraints of 1.80 Å.

5.3 Results and Discussion

Heating $Os_3(CO)_{10}(\mu,\eta^2\text{-}C_4H_3O)(\mu\text{-}H)$ to reflux in an octane solution resulted in its complete conversion to $Os_3(CO)_9(\mu_3,\eta^2\text{-}C_4H_2O)(\mu\text{-}H)_2$, **5.2**. Compound **5.2** was formed by the elimination of a CO ligand from the Os_3 cluster followed by an oxidative addition one of the β-C-H bonds from the furyl ligand (Scheme 5.3**)**. The ORTEP diagram of the molecular structure of **5.2** is shown in Figure 5.1. The ligand donates a total of four electrons to the cluster from two σ-bonds and one π-bond resulting in a 48-electron saturated cluster. Compound **5.2** was characterized by ^{1}H NMR, IR, single crystal X-ray and mass spec. This compound had been previously observed in solution but no crystal structure was reported.[34] The hydride ligands as expected cause a lengthening of the metal-metal bonds that they bridge, Os(1) – Os(2) = 3.0811(4) and Os(2) – Os(3) = 2.8558(4) compared to the unbridged bond Os(1) – Os(3) = 2.7682(4).[42]The Os(3)/Os(1) – C(2) bonds are longer (Os(1) – C(2) = 2.063(8), Os(3) – C(2) = 2.394(8)) than the corresponding Os(3)/Os(2) - C(3) bonds (Os(2) – C(3) =

2.117(8), Os(3) – C(3) = 2.313(8)) probably because of their proximity electronegative "O" atom in the ring. It's worth noting that the Os(1) and Os(2) bonds to C(2) and C(3) respectively are also shorter than the C(2) or C(3) bonds to Os(3), possibly because the π-bond is delocalized across the 3 metals.[19a]

When $Os_3(CO)_{10}(\mu, \eta^2\text{-}C_4H_3O)(\mu\text{-}H)$ was allowed to react with $Re_2(CO)_8(\mu\text{-}Ph)(\mu\text{-}H)$ at 40°C for 18 hours, compound **5.3**, $(\mu\text{-}H)Os_3(CO)_{10}(\mu\text{-}\eta^2\text{-}2,3,\mu\text{-}\eta^2\text{-}4,5\text{-}C_4H_2O)Re_2(CO)_8(\mu\text{-}H)$ was obtained in a 59 % yield and was characterized by ^{1}H NMR, IR, single crystal X-ray and mass spec. An ORTEP diagram of the molecular structure of **5.3** is shown in Figure 5.2. Compound **5.3** consists of a furyl ligand sandwiched between an "Os_3" cluster and an "Re_2" cluster. It was formed by an oxidative addition of a furyl C(5)-H bond resulting in a second *ortho*-metallation and a $\mu\text{-}\eta^1\text{:}\eta^2$ coordination of the furyl ligand to the dirhenium cluster (Scheme 5.4**)**. The activated "H" becomes a bridging hydrido (H5) ligand across the Re-Re bond. In this coordination mode the furan moiety contributes three electrons to the "Re_2" cluster yielding a total of 34 and to the "Os_3" cluster 48 valence electrons. This bonding mode is well known for reactions of $H_2Os_3(CO)_{10}$ with alkynes[43] and amine containing diynes.[44] The coordination of the dirhenium cluster results in the elongation of C(4) – C(5), 1.385(13) Å compared to the uncoordinated cluster, 1.32 Å.[34] The metal-metal bonds with bridging hydrido ligands, Os(1) – Os(3) = 2.8716(5) Å and Re(1) – Re(2) = 3.0722(6) Å are elongated as expected compared to those without bridging hydrides Os(1) – Os(2) = 2.8427(5) Å, Os(2) – Os(3) = 2.8478(5) Å and Re(1) – Re(2) = 3.0413(11) Å in $Re_2(CO)_{10}$.[45] The Re(1)-C(5) = 2.150(9) and Os(2) - C(2) = 2.115(9) Å σ-bonds are the shortest of the metal-carbon bonds while the π-bonding of C(4) – C(5) to Re(2) and C(2) – C(3) to Os(1) are

asymmetric due to geometrical constraints of the furan ligand.[44] The asymmetry is, however, higher in the Os_3 cluster probably due to steric reasons as Os(2) – C(2) bond is also shorter.

When compound **5.2** was allowed to react with $Re_2(CO)_8(\mu\text{-Ph})(\mu\text{-H})$ at 40 ^oC for 17 hours, compound **5.4**, was obtained $(\mu\text{-H})_2Os_3(CO)_9(\mu_3\text{-}\eta^2\text{-2,3-},\mu\text{-}\eta^2\text{-4,5-}C_4HO)Re_2(CO)_8(\mu\text{-H})$ in a 38 % yield. The ORTEP diagram of the molecular structure of **5.4** is shown in Figure 5.3. It was characterized by IR, ^1H NMR, single crystal X-ray and mass spec. Compound **5.4** like compound **5.3** consists of a furan ligand sandwiched between an "Os_3" and a "Re_2" metal cluster. It also formed by the loss of a benzene ligand from the rhenium cluster followed by an oxidative addition of a C-H bond at C(5) to the dirhenium cluster resulting in *ortho*-metallation, see Scheme 5.5. The activated "H" atom became the bridging hydrido ligand H(5). The difference between **5.3** and **5.4** is in the coordination of the furan ligand to the Os_3 cluster; in **5.4** the cluster is coordinated in a $\mu_3\text{-}\eta^2$ fashion while in **5.3** the coordination is $\mu\text{-}\eta^1\text{:}\eta^2$. As expected, the Os – Os and Re(1) – Re(2) bonds in this cluster remain the same as those in compounds **5.2** and **5.3** respectively. The Re(1) – C(5) and Re(2) – C(4)/C(5) bonds in compound **5.4** are very similar to those in **5.3** as expected because of similar bonding. The dirhenium bonding to the cluster is also asymmetric.

When compound **5.2** was allowed to react with $Os_3(CO)_{10}(NCMe)_2$ at 80^o C in cyclohexane, a new compound $(\mu\text{-H})_2Os_3(CO)_9(\mu_3\text{-}\eta^2\text{-2,3-},\mu\text{-}\eta^2\text{-4,5-}C_4HO)Os_3(CO)_{10}(\mu\text{-H})$, **5.5** was obtained in a 36 % yield. The ORTEP diagram of the molecular structure of **5.4** is shown in Figure 5.4. Compound **5.5** like **5.3** and **5.4** also consists of a furan ligand sandwiched between two clusters. It is formed by the loss of the labile "NCMe" ligands

followed by the oxidative addition of the furyne C(5)-H bond to the triosmium cluster (Scheme 5.6). The activated "H" then becomes the bridging ligand H(5). The π-bonding of C(4)-C(5) to Os(4) is also asymmetric(Os(4) – C(5) = 2.346(9), Os(4) – C(4) = 2.496(9)) as in compounds **5.3** and **5.4**. Sandwich furan structures formed by multiple C-H bond activations by different transition metals have not yet been reported, but several manganese-chromium trimetallic complexes with σ, σ π-bonded thienylene ligands are known.[46]

5.4 Summary

We report for the first time the crystal structure of an unsubstituted furyne ligand in the triosmium cluster complex $Os_3(CO)_9(\mu_3,\eta^2\text{-}C_4H_2O)(\mu\text{-}H)_2$, **5.2** that was obtained from the decarbonylation of $Os_3(CO)_{10}(\mu,\eta^2\text{-}C_4H_3O)(\mu\text{-}H)$, **5.1** followed by an oxidative addition of a C-H bond to the triosmium cluster. A new compound, $(\mu\text{-}H)Os_3(CO)_{10}(\mu\text{-}\eta^2\text{-}2,3,\mu\text{-}\eta^2\text{-}4,5\text{-}C_4H_2O)Re_2(CO)_8(\mu\text{-}H)$, **5.3** was also obtained from the reaction of $Os_3(CO)_{10}(\mu,\eta^2\text{-}C_4H_3O)(\mu\text{-}H)$ and $Re_2(CO)_8(\mu\text{-}Ph)(\mu\text{-}H)$ via an oxidative addition of a C-H bond to the dirhenium cluster complex. We have used **5.2** to prepare a new rhenium-osmium furyne cluster complex **5.4**, $(\mu\text{-}H)_2Os_3(CO)_9(\mu_3\text{-}\eta^2\text{-}2,3\text{-},\mu\text{-}\eta^2\text{-}4,5\text{-}C_4HO)Re_2(CO)_8(\mu\text{-}H)$ and a new "Os_6" furyne cluster $(\mu\text{-}H)_2Os_3(CO)_9(\mu_3\text{-}\eta^2\text{-}2,3\text{-},\mu\text{-}\eta^2\text{-}4,5\text{-}C_4HO)Os_3(CO)_{10}(\mu\text{-}H)$, **5.5** via an oxidative addition of a furyne C-H bond to $Re_2(CO)_8(\mu\text{-}Ph)(\mu\text{-}H)$ and $Os_3(CO)_{10}(NCMe)_2$ respectively. Compounds **5.3**, **5.4** and **5.5** are to the best of my knowledge the first examples of furyl or furyne ligand metallated at both *ortho* positions to two different metal clusters.

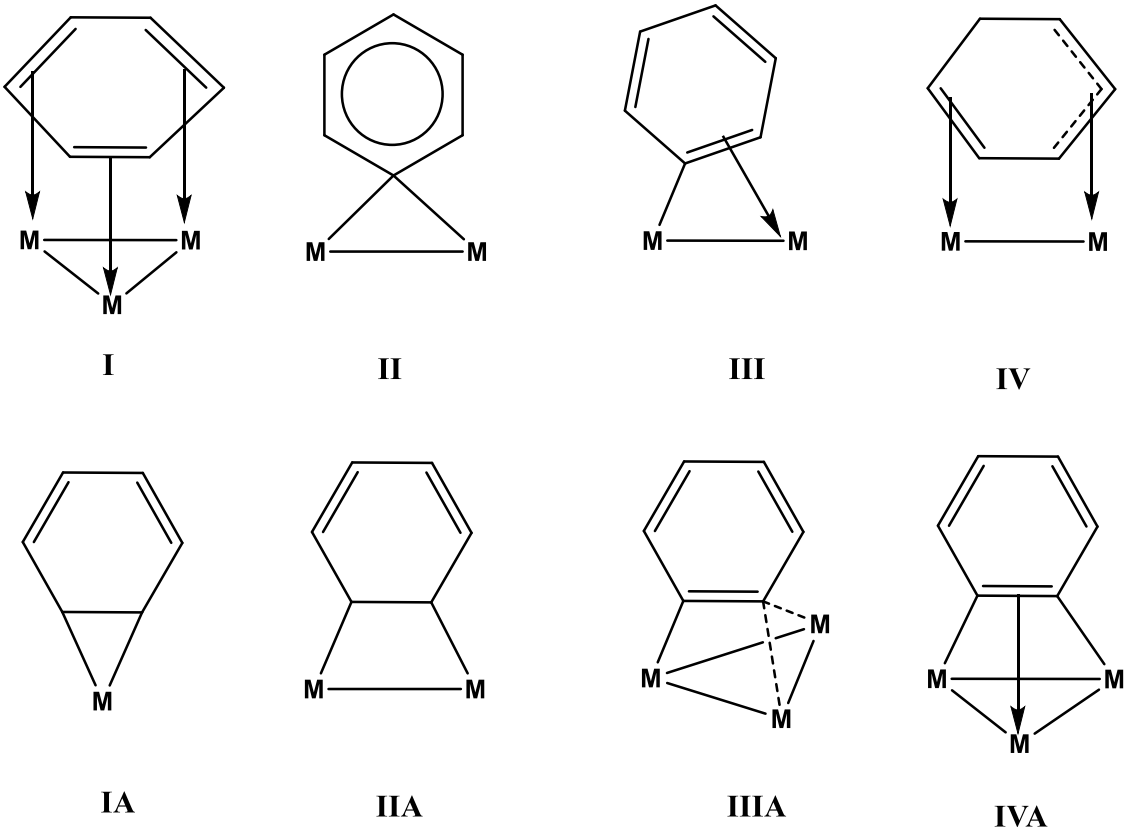

Scheme 5.1: Some of the bonding modes of a benzene and benzyne ligands to metal center(s).

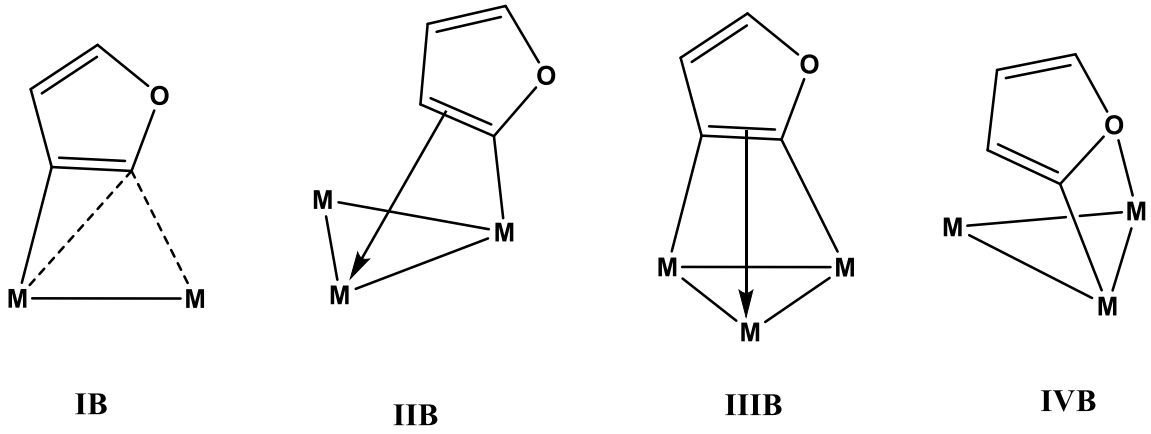

Scheme 5.2: Some of the bonding modes of a furan ligand to metal centers.

Table 5.1. Crystallographic Data for Compounds **5.2, 5.3** and **5.4**

Compound	**5.2**	**5.3**	**5.4**
Empirical formula	$Os_3O_{10}C_{13}H_4$	$Os_3Re_2O_{19}C_{24}H_4$	$Os_3Re_2O_{18}C_{21}H_4$
Formula weight	890.76	1515.36	1487.34
Crystal system	Triclinic	Triclinic	Monoclinic
Lattice parameters			
a (Å)	8.6127(4)	9.1814(6)	9.5548(5)
b (Å)	9.0730(4)	12.9531(6)	15.9881(8)
c (Å)	12.9331(6)	13.5257(7)	20.2486(10)
α (deg)	79.0150(10)	95.3820(10)	90
β (deg)	79.9380(10)	94.2350(10)	101.8440(10)
γ (deg)	63.3600(10)	101.8240(10)	90
V (Å3)	2403.4(5)	1560.34(15)	3027.4(3)
Space group	P-1	P-1	P2(1)/n
Z value	2	2	4
ρ_{calc} (g/cm^3)	3.229	3.225	3.263
μ (Mo Kα) (mm−1)	20.800	19.979	20.589
Temperature (K)	294(2)	294(2)	294(2)
2Θmax (°)	56.56	56.50	56.56
No. Obs. (I > 2σ(I))	3982	4926	4977
No. Parameters	242	432	409
Goodness of fit (GOF)	1.035	1.069	1.081
Max. shift in cycle	0.001	0.001	0.006
Residuals*: R1; wR2	0.0386; 0.1073	0.0394; 0.0891	0.0394; 0.1024
Absorption Correction,	Multi-scan	Multi-scan	Multi-scan
Max/min	1.00/0.164	1.00/0.475	0.1506/0.0844
Largest peak in Final Diff. Map (e$^-$/Å^3)	1.855	2.569	2.678

*$R1 = \Sigma_{hkl}(\,|\,|F_{obs}| - |F_{calc}|\,|)/\Sigma_{hkl}|F_{obs}|$; $wR2 = [\Sigma_{hkl}w(|F_{obs}| - |F_{calc}|)^2/\Sigma_{hkl}wF^2_{obs}]^{1/2}$; $w = 1/\sigma^2(F_{obs})$; $GOF = [\Sigma_{hkl}w(|F_{obs}| - |F_{calc}|)^2/(n_{data} - n_{vari})]^{1/2}$.

Table 5.2. Crystallographic Data for Compound **5.5**

Compound	**5.5**
Empirical formula	$Os_6O_{20}C_{23}H_4$
Formula weight	1741.46
Crystal system	Triclinic
Lattice parameters	
a (Å)	11.3105(5)
b (Å)	16.1718(8)
c (Å)	18.3462(8)
α (deg)	87.0138(14)
β (deg)	89.5808(15)
γ (deg)	81.0114(15)
V (Å3)	3310.0(3)
Space group	P-1
Z value	4
ρcalc (g/cm3)	3.495
μ (Mo Kα) (mm−1)	23.023
Temperature (K)	100(2)
2Θmax (°)	55.26
No. Obs. (I > 2σ(I))	12620
No. Parameters	899
Goodness of fit (GOF)	1.064
Max. shift in cycle	0.001
Residuals*: R1; wR2	0.0316; 0.0599
Absorption Correction,	Semi-empirical from equivalents
Max/min	0.6560/0.1687
Largest peak in Final Diff. Map ($e^-/Å^3$)	2.483

*$R1 = \Sigma_{hkl}(\,|\,|F_{obs}| - |F_{calc}|\,|)/\Sigma_{hkl}|F_{obs}|$; $wR2 = [\Sigma_{hkl}w(|F_{obs}| - |F_{calc}|)^2/\Sigma_{hkl}wF^2_{obs}]^{1/2}$; $w = 1/\sigma^2(F_{obs})$; $GOF = [\Sigma_{hkl}w(|F_{obs}| - |F_{calc}|)^2/(n_{data} - n_{vari})]^{1/2}$.

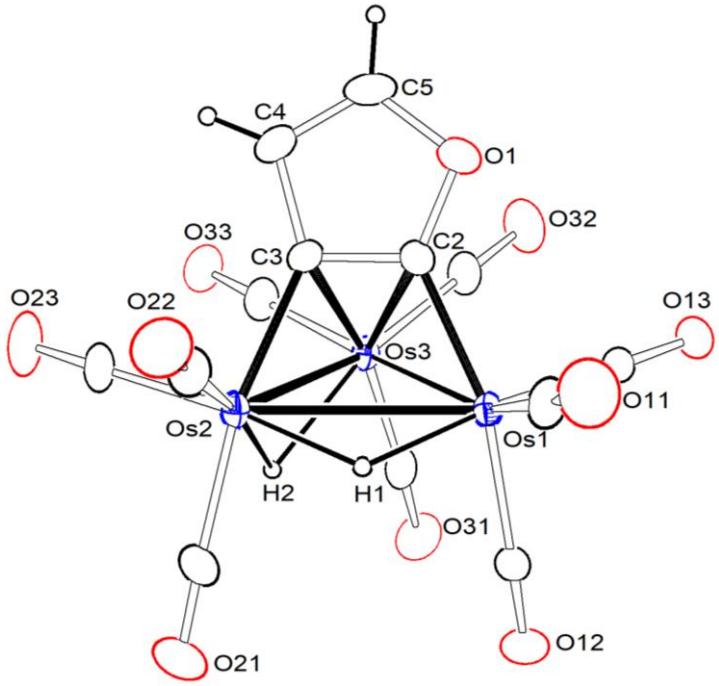

Figure 5.1. An ORTEP diagram of the molecular structure $Os_3(CO)_9(\mu_3, \eta^2\text{-}C_4H_2O)$ $(\mu\text{-}H)_2$, **5.2** showing 20% thermal ellipsoid probability. Selected interatomic bond distances (Å) are as follows: Os(1) – Os(2) = 3.0811(4), Os(1) – Os(3) = 2.7682(4), Os(2) – Os(3) = 2.8558(4), Os(1) – C(2) = 2.063(8), Os(2) – C(3) = 2.117(8), Os(3) – C(3) = 2.313(8),. Os(3) – C(2) = 2.394(8)

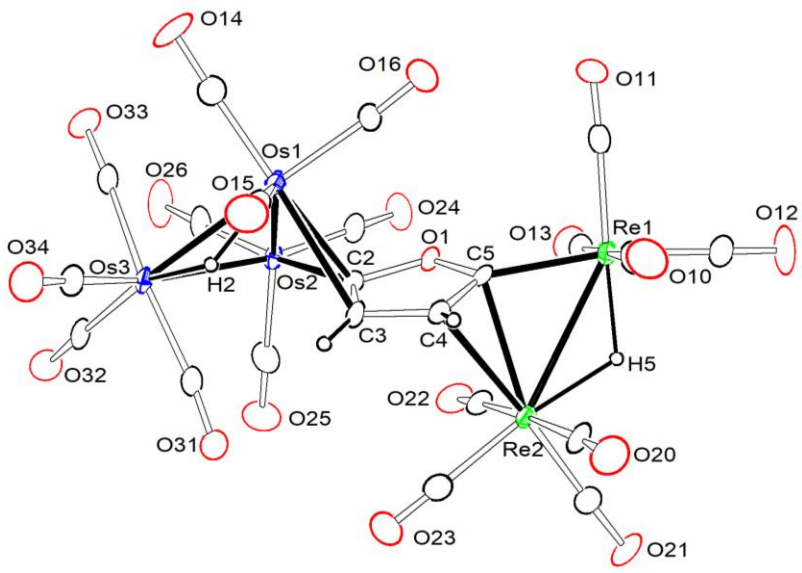

Figure 5.2. An ORTEP diagram of the molecular structure of (μ-H)$Os_3(CO)_{10}$(μ-η^2-2,3,μ-η^2-4,5-C_4H_2O)$Re_2(CO)_8$(μ-H), **5.3** showing 20% thermal ellipsoid probability. Selected interatomic bond distances (Å) are as follows: Os(1) – Os(2) = 2.8427(5), Os(1) – Os(3) = 2.8716(5), Os(2) – Os(3) = 2.8478(5), Os(1) – C(2) = 2.342(8), Os(2) – C(2) = 2.115(9), Os(1) – C(3) = 2.561(9), Re(1) – C(5) = 2.150(9), Re(2) – C(4) = 2.501(8), Re(2) – C(5) = 2.469(8)

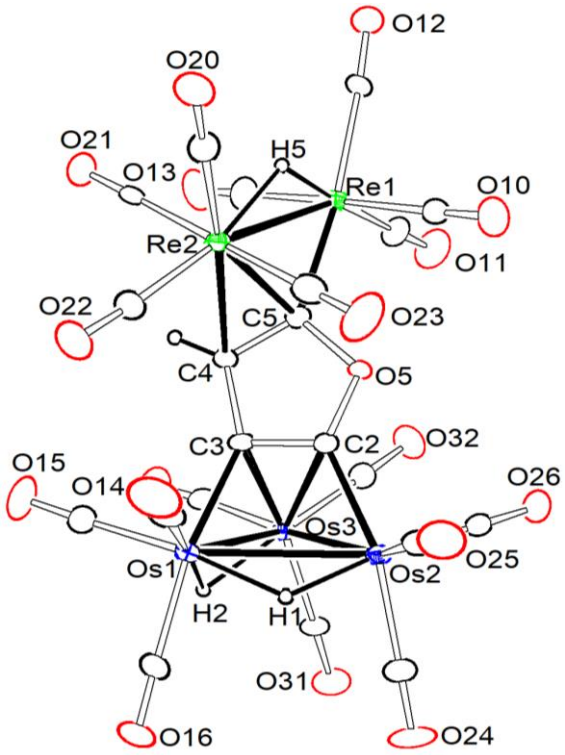

Figure 5.3.. An ORTEP diagram of the molecular structure of $(\mu\text{-H})_2Os_3(CO)_9(\mu_3\text{-}\eta^2\text{-2,3-},\mu\text{-}\eta^2\text{-4,5-}C_4HO)Re_2(CO)_8(\mu\text{-H})$, **5.4** showing 20% thermal ellipsoid probability. Selected interatomic bond distances (Å) are as follows: Os(1) – Os(2) = 3.0804(5), Os(1) – Os(3) = 2.8526(5), Os(2) – Os(3) = 2.7830(5), Os(1) – C(3) = 2.136(8), Os(2) – C(2) = 2.053(8), Os(3) – C(2) = 2.421(8), Os(3) – C(3) = 2.268(8), Re(1) – C(5) = 2.142(9), Re(2) – C(5) = 2.451(8), Re(2) – C(4) = 2.484(8)

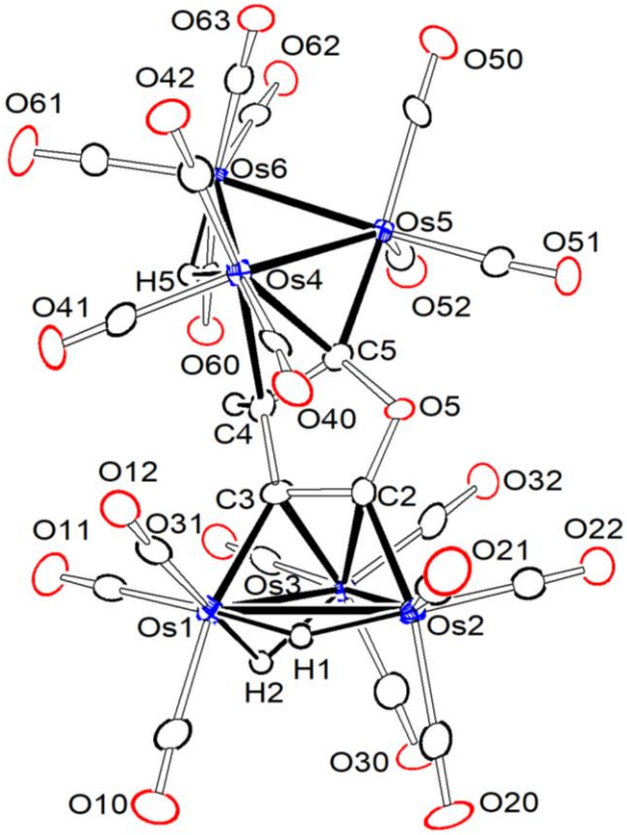

Figure 5.4.. An ORTEP diagram of the molecular structure of $(\mu\text{-H})_2Os_3(CO)_9(\mu_3\text{-}\eta^2\text{-2,3-},\mu\text{-}\eta^2\text{-4,5-}C_4HO)Os_3(CO)_{10}(\mu\text{-H})$, **5.5** showing 50% thermal ellipsoid probability. Selected interatomic bond distances (Å) are as follows: Os(1) – Os(2) = 3.0814(5), Os(1) – Os(3) = 2.8512(5), Os(2) – Os(3) = 2.7811(5), Os(1) – C(3) = 2.141(9), Os(2) – C(2) = 2.031(9), Os(3) – C(2) = 2.397(8), Os(3) – C(3) = 2.245(8), Os(5) – C(5) = 2.101(9), Os(4) – C(5) = 2.346(9), Os(4) – C(4) = 2.496(9)

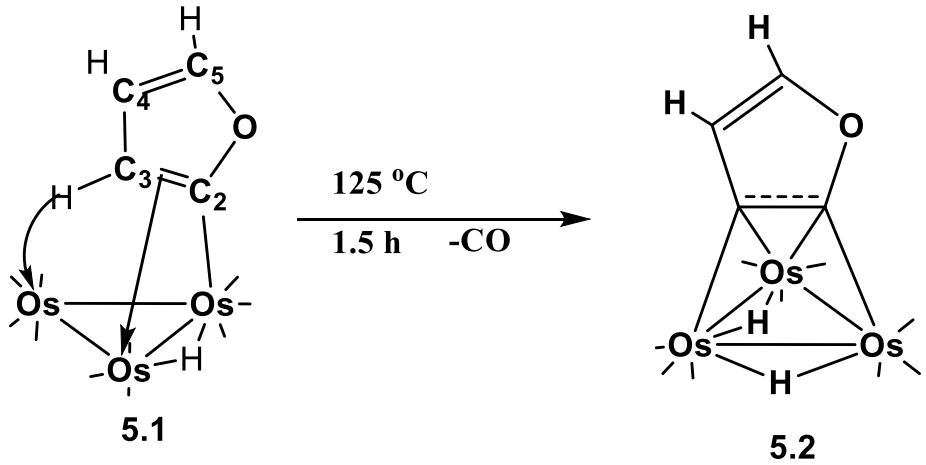

Scheme 5.3: A schematic of the oxidative addition of the C(3)-H bond on an Os_3 cluster

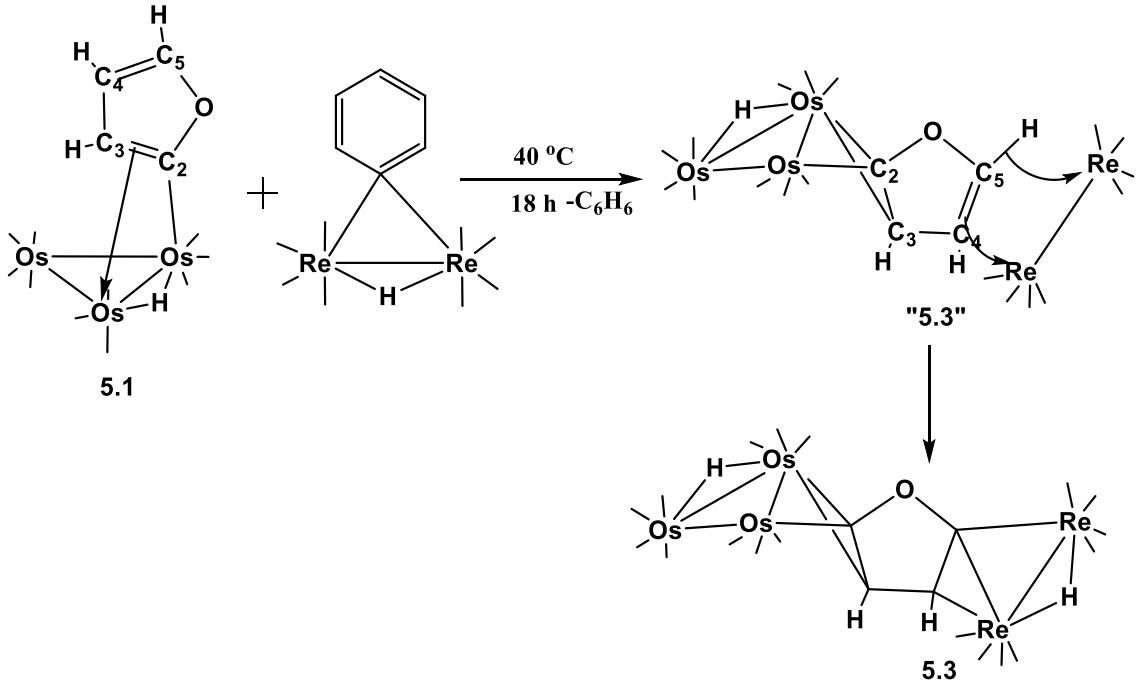

Scheme 5.4: A schematic of the oxidative addition of the C(5)-H bond on an Re_2 cluster followed by π-coordination

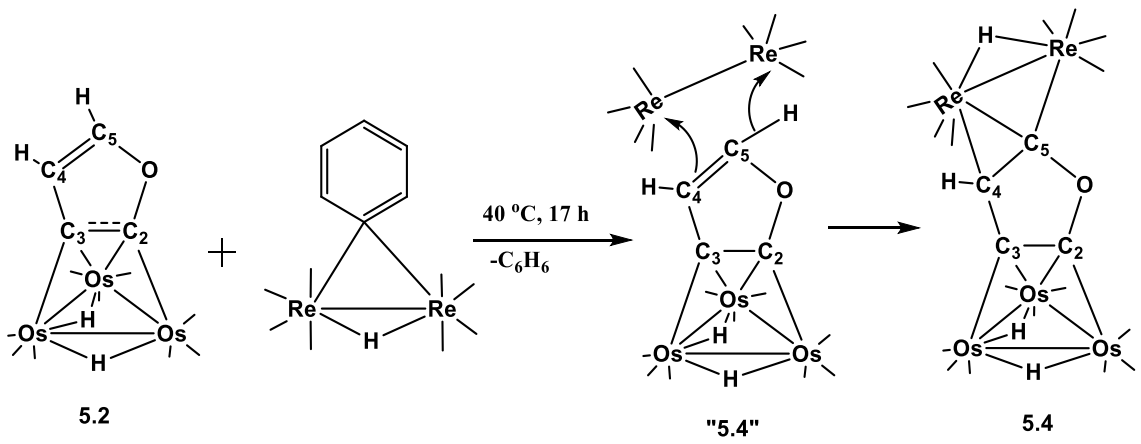

Scheme 5.5: A schematic of the oxidative addition of the C(5)-H bond on an Re_2 cluster followed by π-coordination

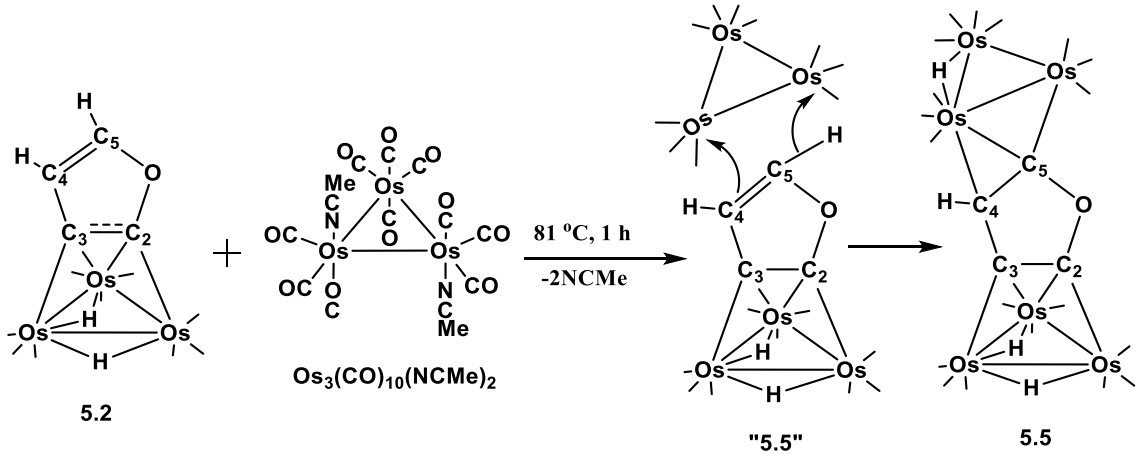

Scheme 5.6: A schematic of the oxidative addition of the C(5)-H bond on an Os_3 cluster followed by π-coordination

5.5 References

1. (a)Anbarasan, P.; Baer, Z. C.; Sreekumar, S.; Gross, E.; Binder, J. B.; Blanch, H. W.; Clark, D. S.; Toste, F. D. *Nature* **2012,** 491, (7423), 235-239; (b)Lanzafame, P.; Centi, G.; Perathoner, S. *Chem. Soc. Rev.* **2014,** 43, (22), 7562-7580; (c)Liu, B.; Zhang, Z. *Chemsuschem* **2016,** 9, (16), 2015-2036.

2. (a)Huber, G. W.; Iborra, S.; Corma, A. *Chem. Rev.* **2006,** 106, (9), 4044-4098; (b)Dawes, G. J. S.; Scott, E. L.; Le Notre, J.; Sanders, J. P. M.; Bitter, J. H. *Green Chem.* **2015,** 17, (6), 3231-3250; (c)Reichert, J.; Brunner, B.; Jess, A.; Wasserscheid, P.; Albert, J. *Energy Environ. Sci* **2015,** 8, (10), 2985-2990.

3. Carpenter, D.; Westover, T. L.; Czernik, S.; Jablonski, W. *Green Chem.* **2014,** 16, (2), 384-406.

4. Kumar, G.; Shobana, S.; Chen, W.-H.; Bach, Q.-V.; Kim, S.-H.; Atabani, A. E.; Chang, J.-S. *Green Chem.* **2017,** 19, (1), 44-67.

5. Monlau, F.; Sambusiti, C.; Ficara, E.; Aboulkas, A.; Barakat, A.; Carrere, H. *Energy Environ. Sci* **2015,** 8, (9), 2600-2621.

6. Besson, M.; Gallezot, P.; Pinel, C. *Chem. Rev.* **2014,** 114, (3), 1827-1870.

7. Kaur, N. *Inorganic and Nano-Metal Chemistry* **2017,** 47, (2), 163-187.

8. Agirrezabal-Telleria, I.; Gandarias, I.; Arias, P. L. *Catal. Today* **2014,** 234, 42-58.

9. A. Aden, J. B., J. Holladay and J. White, A. Manheim, D. Elliot, L. Lasure, S. Jones, M. Gerber, K. Ibsen, L. Lumberg, S. Kelley, Top Value Added Chemicals from Biomass: Volume I--Results of Screening for Potential Candidates from Sugars and Synthesis Gas T. Werpy, G. P., Ed. Pacific Northwest National Laboratory/U.S. Department of Energy Oak Ridge, TN, 2004; Vol. 2017, pp 1-76.

10. Davis, M. E. *Top. Catal.* **2015,** 58, (7-9), 405-409.

11. Lessard, J.; Morin, J.-F.; Wehrung, J.-F.; Magnin, D.; Chornet, E. *Top. Catal.* **2010,** 53, (15-18), 1231-1234.

12. Wang, D.; Osmundsen, C. M.; Taarning, E.; Dumesic, J. A. *Chemcatchem* **2013,** 5, (7), 2044-2050.

13. Dutta, S.; De, S.; Saha, B.; Alam, M. I. *Catal. Sci. Technol.* **2012,** 2, (10), 2025-2036.

14. Kulinna, H.; Spaniol, T. P.; Maron, L.; Okuda, J. *Chem. Eur. J.* **2013,** 19, (29), 9468-9471.

15. Kalman, S. E.; Petit, A.; Gunnoe, T. B.; Ess, D. H.; Cundari, T. R.; Sabat, M. *Organometallics* **2013,** 32, (6), 1797-1806.

16. (a)Shilov, A. E.; Shul'pin, G. B. *Chem. Rev.* **1997,** 97, (8), 2879-2932; (b)Gunay, A.; Theopold, K. H. *Chem. Rev.* **2010,** 110, (2), 1060-1081; (c)Sun, M.; Zhang, J. Z.; Putaj, P.; Caps, V.; Lefebvre, F.; Pelletier, J.; Basset, J. M. *Chem. Rev.* **2014,** 114, (2), 981-1019.

17. Janowicz, A. H.; Bergman, R. G. *J. Am. Chem. Soc.* **1982,** 104, (1), 352-354.

18. Hoyano, J. K.; Graham, W. A. G. *J. Am. Chem. Soc.* **1982,** 104, (13), 3723-3725.

19. (a)Goudsmit, R. J.; Johnson, B. F. G.; Lewis, J.; Raithby, P. R.; Rosales, M. J. *J. Chem. Soc.-Dalton Trans.* **1983**, (10), 2257-2261; (b)McGhee, W. D.; Hollander, F. J.; Bergman, R. G. *J. Am. Chem. Soc.* **1988,** 110, (25), 8428-8443; (c)Fujita, K.; Takahashi, Y.; Nakaguma, H.; Hamada, T.; Yamaguchi, R. *J. Organomet. Chem.* **2008,** 693, (21-22), 3375-3382; (d)Adams, R. D.; Rassolov, V.; Wong, Y. O. *Angew. Chem. Int. Ed.* **2016,** 55, (4), 1324-1327.

20. (a)Suzuki, H. *Eur. J. Inorg. Chem.* **2002**, (5), 1009-1023; (b)Yuan, Y. F.; Jimenez, M. V.; Sola, E.; Lahoz, F. J.; Oro, L. A. *J. Am. Chem. Soc.* **2002,** 124, (5), 752-753.

21. (a)Gainsford, G. J.; Mason, R.; Ireland, P. R.; Guss, J. M.; Bradford, C. W.; Nyholm, R. S. *J. Organomet. Chem.* **1972,** 40, (2), C70-C72; (b)Deeming, A. J.; Underhill, M. *J. Chem. Soc.-Dalton Trans.* **1974**, (13), 1415-1419; (c)McLain, S. J.; Schrock, R. R.; Sharp, P. R.; Churchill, M. R.; Youngs, W. J. *J. Am. Chem. Soc.* **1979,** 101, (1), 263-265; (d)Buchwald, S. L.; Watson, B. T.; Huffman, J. C. *J. Am. Chem. Soc.* **1986,** 108, (23), 7411-7413; (e)McGhee, W. D.; Foo, T.; Hollander, F. J.; Bergman, R. G. *J. Am. Chem. Soc.* **1988,** 110, (25), 8543-8545; (f)Tinga, M.; Akkerman, O. S.; Bickelhaupt, F.; Horn, E.; Spek, A. L. *J. Am. Chem. Soc.* **1991,** 113, (9), 3604-3605; (g)Adams, R. D.; Pearl, W. C. *Inorg. Chem.* **2010,** 49, (15), 7170-7175.

22. (a)Brait, S.; Deabate, S.; Knox, S. A. R.; Sappa, E. *J. Cluster Sci.* **2001,** 12, (1), 139-173; (b)Johnson, B. F. G.; Nairn, J. G. M.; Brown, D. B.; Lewis, J.; Gallop, M.; Parker, D. G. *Chem. Eur. J.* **1995,** 1, (4), 252-260.

23. (a)Kabir, S. E.; Rosenberg, E.; Stetson, J.; Yin, M. Z.; Ciurash, J.; Mnatsakanova, K.; Hardcastle, K. I.; Noorani, H.; Movsesian, N. *Organometallics* **1996,** 15, (21), 4473-4479; (b)Adams, R. D.; Rassolov, V.; Wong, Y. O. *Angew. Chem. Int. Ed.* **2014,** 53, (41), 11006-11009.

24. Muna, R. A. A.; Lewis, J.; Raithby, P. R. *J. Organomet. Chem.* **1997,** 530, (1-2), 247-250.

25. Deeming, A. J.; Marshall, J. E.; Nuel, D.; Obrien, G.; Powell, N. I. *J. Organomet. Chem.* **1990,** 384, (3), 347-360.

26. (a)Leong, W. K.; Chen, G. Z. *Organometallics* **2001,** 20, (11), 2280-2287; (b)Chen, G. Z.; Deng, M. L.; Lee, C. K. D.; Leong, W. K.; Tan, J. L.; Tay, C. T. *J. Organomet. Chem.* **2006,** 691, (3), 387-394.

27. (a)Bennett, M. A.; Hambley, T. W.; Roberts, N. K.; Robertson, G. B. *Organometallics* **1985,** 4, (11), 1992-2000; (b)Hartwig, J. F.; Bergman, R. G.; Andersen, R. A. *J. Am. Chem. Soc.* **1991,** 113, (9), 3404-3418.

28. (a)Deng, M. L.; Leong, W. K. *Organometallics* **2002,** 21, (6), 1221-1226; (b)Moriya, M.; Tahara, A.; Takao, T.; Suzuki, H. *Eur. J. Inorg. Chem.* **2009**, (23), 3393-3397.

29. Ohki, Y.; Hatanaka, T.; Tatsumi, K. *J. Am. Chem. Soc.* **2008,** 130, (50), 17174-17186.

30. Petit, A.; Flygare, J.; Miller, A. T.; Winkel, G.; Ess, D. H. *Org. Lett.* **2012,** 14, (14), 3680-3683.

31. R.Hubener, U. A., J.Strahle, Private Communication, 2000; p CSD ref code WOSREB.

32. Arndt, S.; Spaniol, T. P.; Okuda, J. *Eur. J. Inorg. Chem.* **2001**, (1), 73-75.

33. Wong, W. Y.; Ting, F. L.; Lam, W. L. *J. Chem. Soc.-Dalton Trans.* **2001**, (20), 2981-2988.

34. Himmelreich, D.; Muller, G. *J. Organomet. Chem.* **1985,** 297, (3), 341-348.

35. Yin, C. C.; Deeming, A. J. *J. Chem. Soc.-Dalton Trans.* **1982**, (12), 2563-2564.

36. Churchill, M. R.; Missert, J. R. *J. Organomet. Chem.* **1983,** 256, (2), 349-356.

37. Braga, D.; Grepioni, F.; Parisini, E.; Johnson, B. F. G.; Martin, C. M.; Nairn, J. G. M.; Lewis, J.; Martinelli, M. *J. Chem. Soc.-Dalton Trans.* **1993**, (12), 1891-1895.

38. *SAINT+*, Version 6.2a; Bruker Analytical X-ray Systems, Inc.: Madison, WI 2001.

39. Sheldrick, G. M. *SHELXTL*, Version 6.1; Bruker Analytical X-ray Systems, Inc.: Madison, WI, 1997.

40. *APEX3 Version 2016.5-0 and SAINT Version 8.37A.* , Bruker AXS, Inc. : Madison, WI, USA.

41. *SADABS* 2016/2; Bruker Analytical X-ray Systems, Inc.: Madison, WI, USA, 2016.

42. Bau, R.; Drabnis, M. H. *Inorg. Chim. Acta* **1997,** 259, (1-2), 27-50.

43. (a)Orpen, A. G.; Rivera, A. V.; Bryan, E. G.; Pippard, D.; Sheldrick, G. M.; Rouse, K. D. *J. Chem. Soc., Chem. Commun* **1978**, (16), 723-724; (b)Guy, J. J.; Reichert, B. E.; Sheldrick, G. M. *Acta Crystallogr.* **1976,** 32, (DEC15), 3319-3320; (c)Clauss, A. D.; Tachikawa, M.; Shapley, J. R.; Pierpont, C. G. *Inorg. Chem.* **1981,** 20, (5), 1528-1533.

44. Tunik, S. P.; Khripun, V. D.; Balova, I. A.; Nordlander, E.; Haukka, M.; Pakkanen, T. A.; Raithby, P. R. *Organometallics* **2001,** 20, (18), 3854-3863.

45. Churchill, M. R.; Amoh, K. N.; Wasserman, H. J. *Inorg. Chem.* **1981,** 20, (5), 1609-1611.

46. Waldbach, T. A.; Vanrooyen, P. H.; Lotz, S. *Organometallics* **1993,** 12, (10), 4250-4253.

APPENDIX A

^{11}B NMR for Compounds 2.1

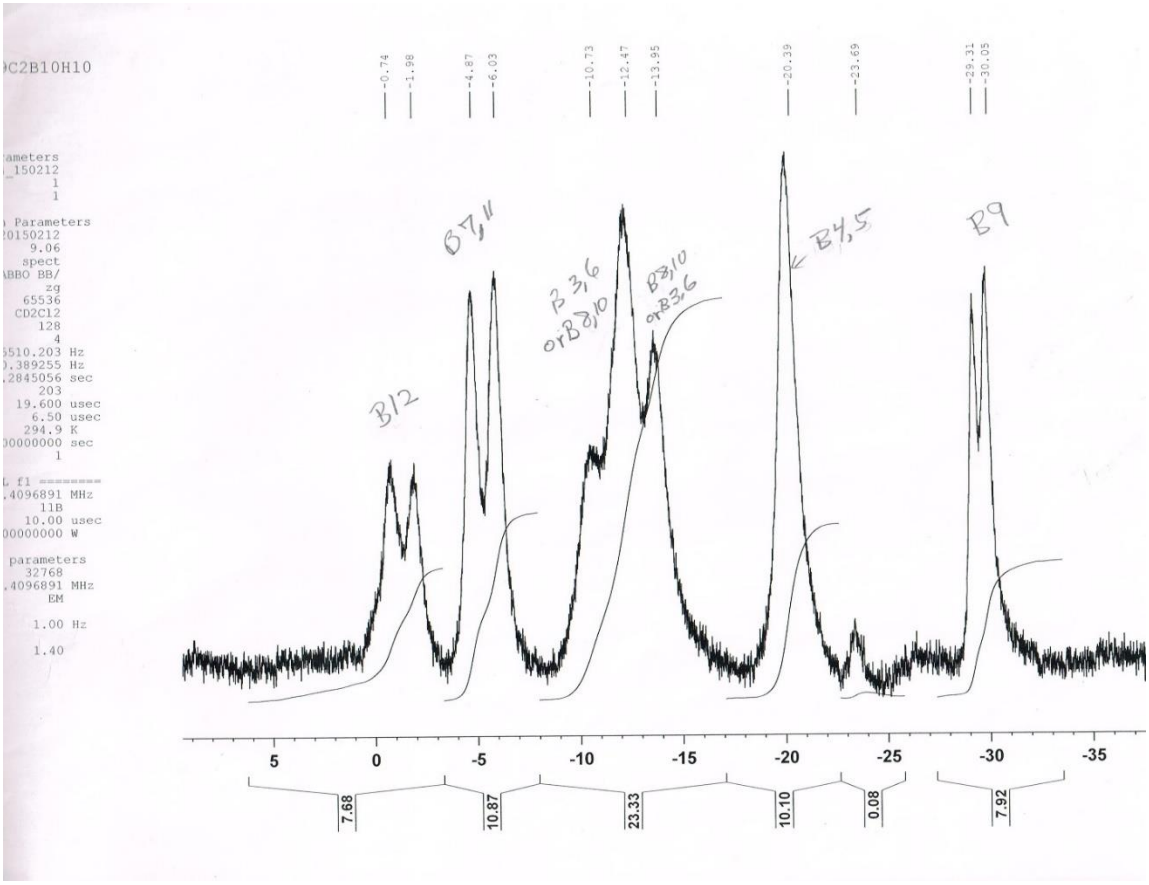

Figure A 1. An ^{1}H-coupled ^{11}B NMR spectrum of **2.1**.

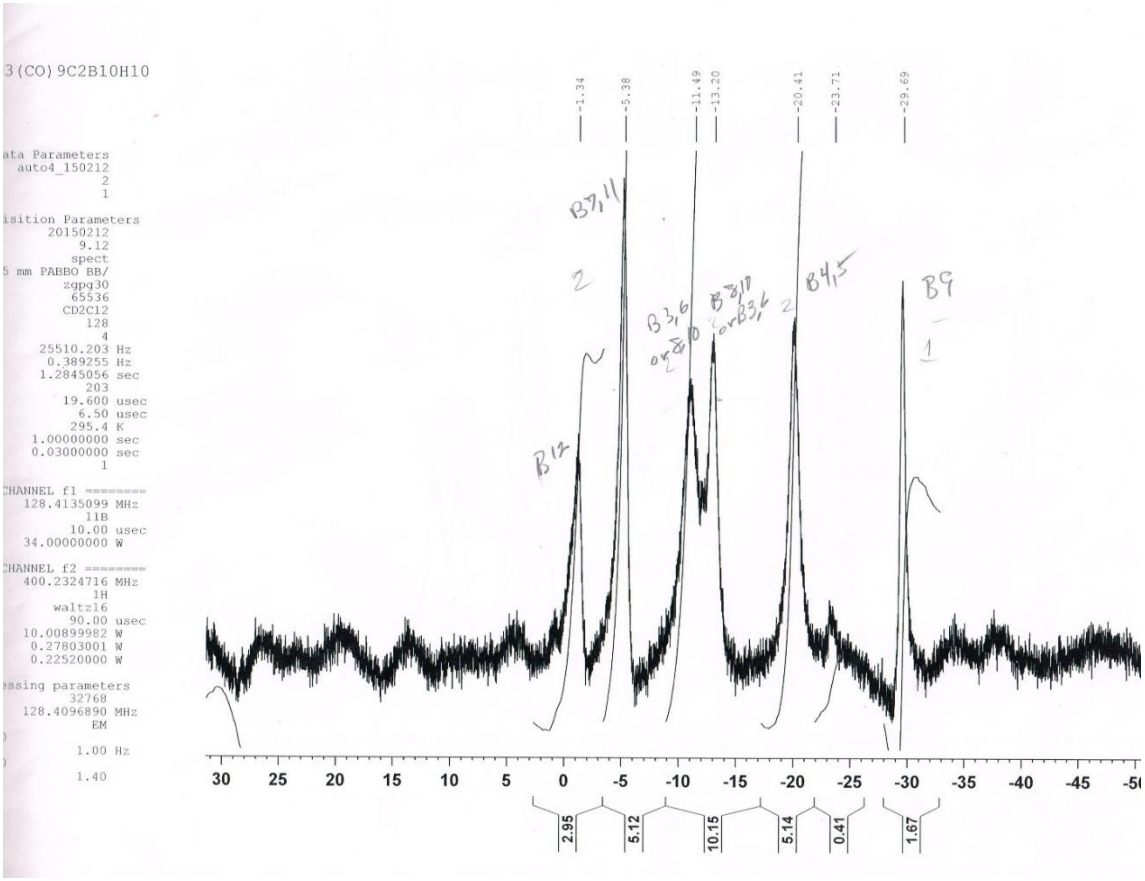

Figure A 2. An ^{1}H-decoupled ^{11}B NMR spectrum of **2.1**

APPENDIX B

^{11}B NMR for Compound 3.1

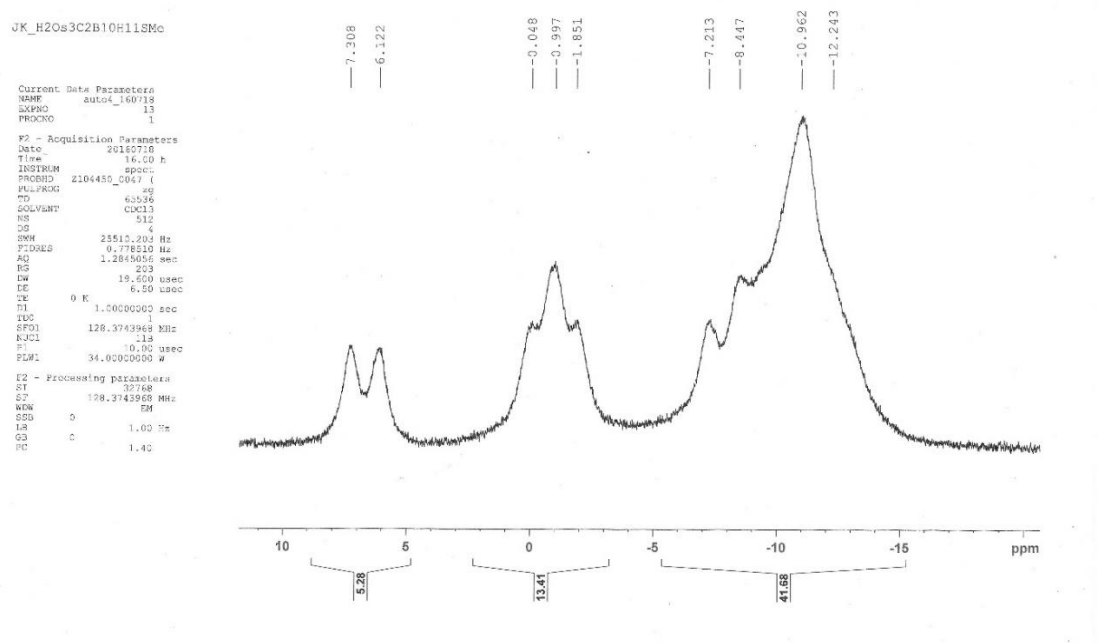

Figure B 1. An ^{1}H-coupled ^{11}B NMR spectrum of **3.1**.

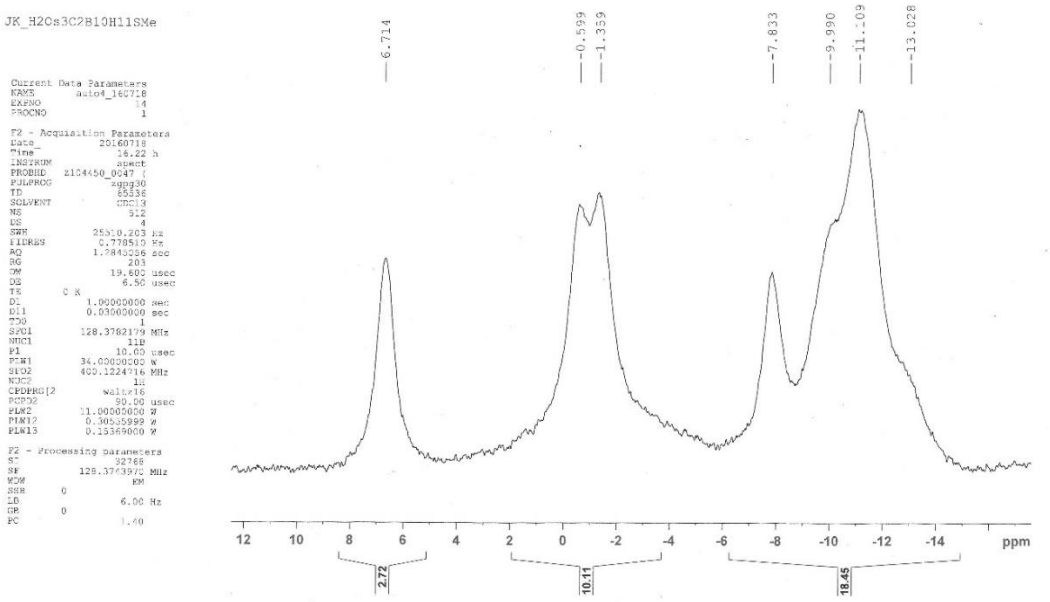

Figure B 2. An ^{1}H-decoupled ^{11}B NMR spectrum of **3.1**

APPENDIX C

Copyright Releases

Title: Cage Opening of a Carborane Ligand by Metal Cluster Complexes

Author: Richard D. Adams,Joseph Kiprotich,Dmitry V. Peryshkov,Yuen Onn Wong

Publication: Chemistry - A European Journal

Publisher: John Wiley and Sons

Date: Mar 23, 2016

Order Completed

Thank you for your order.

This Agreement between University of South Carolina ("You") and John Wiley and Sons ("John Wiley and Sons") consists of your license details and the terms and conditions provided by John Wiley and Sons and Copyright Clearance Center.

Your confirmation email will contain your order number for future reference.

printable details

License Number	4206670127928
License date	Oct 12, 2017
Licensed Content Publisher	John Wiley and Sons
Licensed Content Publication	Chemistry - A European Journal
Licensed Content Title	Cage Opening of a Carborane Ligand by Metal Cluster Complexes
Licensed Content Author	Richard D. Adams,Joseph Kiprotich,Dmitry V. Peryshkov,Yuen Onn Wong
Licensed Content Date	Mar 23, 2016
Licensed Content Pages	4
Type of use	Dissertation/Thesis
Requestor type	Author of this Wiley article
Format	Print and electronic
Portion	Full article
Will you be translating?	No
Title of your thesis / dissertation	COORDINATION CHEMISTRY OF CARBORANES AND FURAN LIGANDS ON TRANSITION METAL CLUSTER COMPLEXES
Expected completion date	Dec 2017
Expected size (number of pages)	150
Requestor Location	University of South Carolina 631 Sumter St COLUMBIA, SC 29208 United States Attn: University of South Carolina
Publisher Tax ID	EU826007151
Billing Type	Invoice
Billing address	University of South Carolina 631 Sumter St COLUMBIA, SC 29208